PHASE SHIFT ANALYSIS OF p-p ELASTIC SCATTERING

by

SIM TOO LIM

B.Sc., NanYang University, 1969

A THESIS SUBMITTED IN PARTIAL FULFILLMENT
OF THE REQUIREMENTS FOR THE DEGREE OF
MASTER OF SCIENCE
in the Department
of
Physics

We accept this thesis as conforming
to the required standard

[redacted]

Accepted by the Faculty of Graduate Studies

on 8 May, 1972 by [redacted] Dean of Faculty

UNIVERSITY OF VICTORIA

April, 1972

ABSTRACT

Supervisor: Dr. G.A. Beer

The development of a p-p phase shift analysis program is described. Following an introductory discussion of the mathematical formalism for phase shift analysis of nuclear scattering data, a brief description is given of computer programs which were developed to perform phase shift analyses on p-^{4}He and p-p elastic scattering data. Two examples of phase shift analyses employing these programs are presented. Results of the fits to 10 MeV p-^{4}He data are in good agreement with published data. Analysis of 310 MeV p-p scattering data, including error estimates, are also in good agreement with previous phase shift analyses of similar data. Using the program, error estimates on the phase shifts have been used to determine an accuracy estimate for various typical experiments. Results, tabulated in graphical form, will be useful in planning scattering experiments to be performed using a proton beam from an accelerator such as the variable energy H^- cyclotron at TRIUMF, Vancouver.

[redacted]

ACKNOWLEDGEMENTS

I am very happy to express my gratitude and appreciation to Dr. G.A. Beer, without whose guidance and encouragement this project could not have been completed.

I wish to thank Dr. L.P. Robertson for many helpful discussions, and also Mr. T.A. Hodges for making available the nucleon-helium-4 scattering computing program.

Financial assistance in the form of a University of Victoria Scholarship is gratefully acknowledged.

I wish to thank my wife, who typed the first draft of this thesis, for her great patience.

Finally, I wish to thank many friends for making my stay in Victoria so interesting.

TABLE OF CONTENTS

LIST OF TABLES

LIST OF FIGURES

Page

SYMBOLS

A and A'	Transverse rotation parameters
C_{NN}, C_{KP}	Spin correlation parameters
$C_{\ell s}(J,m_J;m_\ell,m_s)$	Clebsch-Gordon coefficients
D	Depolarization
J	Total angular momentum quantum number
$\overline{J}$	Total angular momentum (vector)
$\mathcal{J}$	Total angular momentum operator
$\overline{k}$	Wave number of the relative motion of a two-body system at large separation.
ℓ	Orbital angular momentum quantum number
$\overline{\ell}$	Orbital angular momentum (vector)
$\mathcal{L}$	Orbital angular momentum operator
M	Spin-scattering matrix, or M-matrix
M^+	Hermitian conjugate of M-matrix
M_{ss}	M-matrix element, operates only on the spin-singlet state
$M_{m_s m'_s}$	M-matrix element. In the case of nucleon-nucleon scattering, operates only on the spin-triplet state
m_J or M_J	Quantum number of the z-component of the total angular momentum
m_ℓ	Quantum number of the z-component of the orbital angular momentum
m_s	Quantum number of the z-component of the spin angular momentum
P	Polarization
R and R'	Transverse rotation parameters
S	Scattering matrix
S_j	Scattering matrix element

s	spin angular momentum quantum number
$\bar{s}$	spin angular momentum (vector)
$\mathcal{S}$	spin angular momentum operator
S^{μ}	Spin component operator
$\langle S^{\mu} \rangle_i$	Expectation value of S^{μ} before collision, where i denotes initial state
$\langle S^{\mu} \rangle_f$	Expectation value of S^{μ} after collision, where f denotes final state
$V_c(r)$	Central potential
$V_{\bar{\ell}\cdot\bar{s}}(r)$	Central part of the spin-orbit interaction
$V_T(r)$	Central part of the tensor potential
X_i	An observable
$Y_{\ell}^{m\ell}$	Normalized spherical harmonic
$\delta_{\ell J}$	Blatt-Biedenharn's eigen phase shifts
$\bar{\delta}_{\ell J}$	Bar phase shift
$\bar{\delta}_{\ell J}^{N}$	Nuclear bar phase shift
$\bar{\delta}_{\ell}$	Bar phase shift for spin-singlet state
$\bar{\delta}_{\ell}^{N}$	Nuclear bar phase shift for the spin-singlet state
ε_J	Blatt-Biedenharn's mixing parameter
$\bar{\varepsilon}_J$	Bar mixing parameter
θ	Scattering angle in the C.M. system
θ_{lab}	Scattering angle in the laboratory system
ρ_f	Spin density matrix for the final state (after collision)
ρ_i	Spin density matrix for the initial state (before collision)
$\chi^{(n)}$	Spin wave function of the two-nucleon system on which a spin matrix operates
$\chi_s^{m_s}$	Components of the spin wave function

Chapter 1

INTRODUCTION

In spite of the considerable experimental and theoretical activity in the past ten years, the nucleon-nucleon interaction still remains as one of the central and the most challenging problems in nuclear physics. Studies of the interaction at intermediate energies shed light upon such important problems as

1) the role of meson exchange in the nucleon-nucleon force (e.g. Bryan, 1970);
2) time reversal in the strong interaction (e.g. Thorndike, 1965);
3) charge independence of the nucleon-nucleon force (e.g. Breit, 1966);
4) charge symmetry of the nucleon-nucleon force.

Nucleon-nucleon scattering measurements are the most straightforward method of studying the interaction. Scattering measurements may be used to determine scattering amplitudes since these are the quantities that can be readily compared with theoretical predictions, while phase-shift analysis is a method of parameterizing the scattering amplitudes.

Due to the difficulties in obtaining a free neutron target, only proton targets have been used. (Although effective neutron targets are available in deuteron quasi free scattering, the measurements as a rule have very poor precision.) Difficulty in obtaining good high energy neutron beams has also been reflected in the collection of n-p and p-p scattering data; there are fewer data for the scattering of neutron beams than proton beams. Proton-proton experiments up to the present include mainly measurements of

1) total cross sections, σ_T;

2) elastic scattering differential cross sections, $\sigma(\theta)$ or $\frac{d\sigma(\theta)}{d\Omega}$, where θ is the angle through which the incident proton is scattered;

3) polarization measurements, $P(\theta)$, which are usually measured by the left-right asymmetries in the differential cross section for the scattering of a polarized beam by a target;

4) triple scattering parameters, $D(\theta)$, $R(\theta)$, $R'(\theta)$, $A(\theta)$ and $A'(\theta)$, which are quantities representing the transfer of a component of polarization of an initially polarized beam to a component of polarization of the outgoing beam scattered at the angle θ (Wolfenstein, 1956);

5) spin correlation parameters, $C_{NN}(\theta)$ and $C_{KP}(\theta)$, which are deduced from measurements of the polarization of the recoiling target in coincidence with the polarization of the outgoing nucleon for an initially unpolarized beam scattered by an unpolarized target.

In order to find out the most sensitive measurements which could be performed to determine unique phase shifts or more precise phase shifts at a fixed incident energy, the present available experimental data have been investigated by several people. For example, the compilation of nucleon-nucleon scattering measurements updated to 1968 (MacGregor *et al.*, 1968, UCRL-50426) shows that there are 519 measurements on p-p scattering for proton laboratory energies from 100 to 400 MeV. Some remarks may be made on the basis of these data.

1) The bulk of the measurements pertained to the determination of differential cross section and polarization, especially those measurements below 300 MeV.
2) Very few data exist on the spin correlation parameters below 300 MeV. Increased precision in these parameters is needed in the 300 to 400 MeV region.
3) Increased precision in triplet scattering parameters $D(\theta)$, $R(\theta)$, and $A(\theta)$ is needed especially at 300 MeV energy. Most of the data at 310 MeV were obtained 14 years ago.
4) Because of the difficulties in the experimental techniques which were available in the past decade, the scarcity of data on measurements using a polarized target and polarized beams remains unchanged.

Phase-shift analyses of these tabulated data at energies below 400 MeV (e.g. MacGregor *et al.*, 1959 to 1968) have resulted in many ambiguous sets of phase shifts. However, recently a University of Chicago group (Wright *et al.*, 1968) has reported one unique set of phase shifts for p-p scattering at around 400 MeV based on additional experimental values for higher order spin parameters. Thus it would appear that unique phase shifts for elastic scattering are well within the capability of present day technology. However, above 400 MeV the increasing importance of inelastic scattering resulting from pion production (which means the phase shifts may have the form of a complex number rather than a real number as in the case of elastic scattering) has frustrated the development of phase-shift analysis of nucleon-nucleon scattering.

In the present work, one energy region of p-p elastic scattering data is comprehensively investigated. It is shown that improvement of p-p elastic phase shifts depends largely on increased precision in and an adequate number of measurements of triplet scattering parameters such as $D(\theta)$, $R(\theta)$, $C_{NN}(\theta)$, and $C_{KP}(\theta)$, and as well on further measurements of differential cross section and polarization. The accuracies required for such measurements have been investigated using a computer program which was written for the more general purpose of performing phase shift analyses on elastic proton-proton scattering data. An extension to investigation of n-p scattering is straightforward but has not been considered here.

In present analyses, different normalization parameters have been applied to data from different laboratories and different experiments. To avoid the discrepancies coming from such analysis procedures, measurements in one laboratory of all quantities over a range of energies would be most helpful. Such a comprehensive set of measurements would also be useful in determining the energy dependence of phase shifts.

Technologically, these measurements depend on the availability of new accelerators such as TRIUMF which have the advantage of

1) high energy resolution in external proton (and neutron) beams,

2) beam energy variability over a wide range, and

3) high intensity polarized beams.

In addition, for measurements of spin correlation parameters, a polarized target would be useful (Lock and Measday, 1970).

At 310 MeV, where inelastic scattering is believed to be insignificant in p-p scattering, several different kinds of measurements are presently available. Thus it seems an ideal point to start such a comprehensive experimental program of measurements of $\sigma(\theta)$, $P(\theta)$, $A(\theta)$, $R(\theta)$, $D(\theta)$, $A'(\theta)$, and $R'(\theta)$, which may later extend to higher and lower energy. Hence, in Chapter 3, a phase-shift analysis of data at this energy has been carried out to check the validity of the computer program and to evaluate the error matrix. The accuracies of different measurements required in order to improve the phase shifts have also been evaluated in Chapter 4. Several experimental measurements which would significantly improve present knowledge of 310 MeV phase shifts are discussed in Chapter 5 and required accuracies are listed. Should these experiments be performed, the p-p elastic scattering phase shift analysis program which has been developed could then be used in their analysis.

Chapter 2

MATHEMATICAL FORMALISM OF PHASE-SHIFT ANALYSIS

2.1 Introduction

The object in this chapter is to develop explicitly a quantum mechanical formalism in which we can treat elastic collisions between two particles in the non-relativistic approximation.

Consider a collision between two particles of masses m_1 and m_2. If the interaction between the two particles can be represented by a potential $V(r)$ which depends only upon their relative position r, then it is convenient to subtract the motion of the center of mass from the relative motion of the two particles. The technique of separating out the center of mass motion as discussed by Messiah (Chapters 9, 19, 11) permits us to treat the collision of the two particles as the scattering of a particle of mass $m = \frac{m_1 m_2}{m_1+m_2}$ by a potential $V(r)$.

In a typical scattering experiment, one bombards a target composed of particles of mass m_2 with a monoenergetic beam of particles of mass m_1. The solution ψ_k of the Schrödinger equation

$$\left\{ -\frac{\hbar^2}{2m} \nabla^2 + V(r) \right\} \psi_k = E \psi_k \qquad (2.1.1)$$

with a well defined energy E is called a stationary wave function. It represents both an incident beam and the beam of scattered particles. Here, if the energy of an incident particle is much less than the rest mass m_1, E is the total energy in the center of mass frame of the

two-body system mentioned above. (Refer to Appendix A.) Also, $\bar{p} = \hbar\bar{k}$ is the initial momentum of the particle of mass m in the center of mass frame, where $\bar{k}$ is the wave vector of the incident beam of monoenergetic particles.

The usual assumptions made in the theoretical analysis of scattering problems (as well as in studies of nuclear interactions) which have been used in the present development are

1) conservation of parity,

2) conservation of total angular momentum,

3) conservation of isotopic spin,

4) invariance under time reversal, and

5) conservation of total energy.

All are, up to the present, believed to be reasonable assumptions in treating scattering problems. Under this set of assumptions, the mathematics involved in the description of the physical phenomena in scattering experiments has been simplified.

The first part of this chapter is devoted to establishing the formalism in the simple case of spinless incident particles in a central potential $V_c(r)$. This is then extended to the case of the scattering of a beam of spin ½ particles by a target nucleus of spin 0. A phase-shift analysis of p-He scattering at 10.0 MeV is shown as an example of such analysis. The computer program can also be used for n-He scattering. The last section is devoted to the case of a nucleon-nucleon scattering formalism in which both particles have spin ½.

2.2 The scattering of a spinless particle by a central potential

First we consider a mathematical description of the scattering of a beam of spinless particles by a central potential $V_c(r)$, and choose the direction of the incident beam $\bar{k}$ as the z-axis, an axis of rotational symmetry of the problem, so that the wave function is independent of the azimuthal angle ϕ. The wave function representing the incident and scattered beam of particles satisfies the Schrödinger equation,

$$H\psi_k = E\psi_k$$

where

$$H \equiv -\frac{\hbar^2}{2m}\nabla^2 + V_c(r) \qquad (2\cdot2\cdot1)$$

Further, the types of potentials $V_c(r)$, $V_{\vec{l}\cdot\vec{s}}(r)$ and $V_T(r)$ we are going to consider in this chapter have to satisfy the following two conditions:

1) the potential must fall sufficiently rapidly so that it may be neglected beyond some radius r=R, and
2) the wave function and its gradient must be finite everywhere, in particular at r=0.

As a matter of fact, most phenomenological nuclear potentials satisfy these conditions. (The exception, the Coulomb potential, will be treated in section 2.4.) For this type of potential, the stationary wave function ψ_k may be shown to have the asymptotic solution (Messiah)

$$\psi_k \xrightarrow[\text{large } r]{} e^{ikz} + \frac{f(\theta,\phi)}{r} e^{ikr} \qquad (2\cdot2\cdot2)$$

The first term, e^{ikz}, represents an incident wave of unit probability density and of current density $\hbar\bar{k}/m$ or flux of v particles per second moving along the positive z-direction. The second term, $f(\theta,\phi)e^{ikr}/r$, represents a beam of particles of probability $|f(\theta,\phi)|^2/r^2$ with current density $(\hbar\bar{k}/m)(|f(\theta,\phi)|)^2/r^2$ outward from the scattering center along

the direction defined by θ, ϕ. If the potential vanished everywhere, then $f(\theta,\phi)=0$ and equation(2·2·2)reduces to e^{ikz}. The term $f(\theta,\phi)$ reflects the effects of the potential on the incident beam.

We know that, for a central force problem, all solutions of the Schrödinger equation are obtained by assuming that ψ_k, which in this case is independent of ϕ, has the form

$$\psi_k = \sum_\ell A_\ell G_\ell(r)\, Y_\ell^0(\theta,\phi) \qquad (2\cdot2\cdot3)$$

where A_ℓ are determined by boundary conditions (References 1, 2 and 3). The radial wave function, $G_\ell(r)$ and the spherical harmonic function $Y_\ell^0(\theta,\phi)$ satisfy separately the following equations

$$\left\{\frac{1}{r^2}\cdot\frac{d}{dr}\left(r^2\frac{d}{dr}\right)+\left[k^2-U_c(r)-\frac{\ell(\ell+1)}{r^2}\right]\right\} G_\ell(r) = 0 \qquad (2\cdot2\cdot4)$$

where $U_c(r) = 2mV_c(r)/\hbar^2$ and $k^2 = 2mE/\hbar^2$,

and $$L^2 Y_\ell^0(\theta,\phi) = \ell(\ell+1)\hbar^2 Y_\ell^0(\theta,\phi) \qquad (2\cdot2\cdot5)$$

where $$L^2 = \hbar^2\left\{\frac{1}{\sin\theta}\cdot\frac{\partial^2}{\partial\phi^2}+\frac{1}{\sin\theta}\cdot\frac{\partial}{\partial\theta}\left(\sin\theta\,\frac{\partial}{\partial\theta}\right)\right\}$$

with $\ell = 1, 2, 3, 4, 5, \ldots$

The solution shown above obviously is a linear combination of the common eigenfunctions of the operator H, L^2, the square of the orbital angular momentum, and L_z the z-component of the orbital angular momentum. Each term in the combination represents a partial wave corresponding to a definite value of angular momentum $\ell\hbar$. If the A_ℓ are determined, the connection between the Schrödinger equation and the partial

waves is then well established through equation(2·2·3), in which the total wave function is expressed as the sum of the partial waves.

Since we are considering only potentials which fall more rapidly than r^{-2}, the term $U_c(r)$ in equation(2·2·4)may be neglected with respect to the centrifugal term $\ell(\ell+1)/r^2$ in the region where r is large, and the equation reduces to

$$\left\{ \frac{1}{r^2} \cdot \frac{d}{dr}\left(r^2 \frac{d}{dr}\right) + \left[k^2 - \frac{\ell(\ell+1)}{r^2} \right] \right\} G_\ell(r) = 0 \qquad (2\cdot2\cdot6)$$

The two linearly independent solutions for equation(2·2·6)are known as spherical Bessel functions, $j_\ell(kr)$, and spherical Neumann functions, $n_\ell(kr)$. The function $j_\ell(kr)$ is regular at the origin while $n_\ell(kr)$ is irregular. By employing the asymptotic forms of $j_\ell(kr)$ and $n_\ell(kr)$,

$$j_\ell(kr) \xrightarrow[kr \text{ large}]{} \frac{1}{kr} \sin\left[kr - \frac{\ell}{2}\pi\right] \qquad (2\cdot2\cdot7)$$

and

$$n_\ell(kr) \xrightarrow[kr \text{ large}]{} -\frac{1}{kr} \cos\left[kr - \frac{\ell}{2}\pi\right] \qquad (2\cdot2\cdot8)$$

the asymptotic radial wave function $G_\ell(r)$ can be written as a linear combination of the regular and irregular solutions

$$G_\ell(r) \xrightarrow[kr \text{ large}]{} a_\ell \frac{\sin\left[kr - \frac{\ell}{2}\pi\right]}{kr} - b_\ell \frac{\cos\left[kr - \frac{\ell}{2}\pi\right]}{kr} \qquad (2\cdot2\cdot9)$$

If the potential $V_c(r)$ vanishes everywhere, the requirement that the wave function ψ_k must be finite implies that $rG_\ell(r) = 0$ at the origin. In this case, the irregular solution $n_\ell(kr)$ must be excluded, and we have that $b_\ell = 0$. The ratio b_ℓ/a_ℓ is a measure of the intensity of scattering.

Further, we define

$$\frac{b_\ell}{a_\ell} = - \tan \delta_\ell \qquad (2\cdot2\cdot10)$$

and the asymptotic radial wave function can be written as

$$G_\ell(r) \xrightarrow[r \text{ large}]{} \frac{1}{kr} \sin \left[kr - \frac{\ell\pi}{2} + \delta_\ell \right] \qquad (2.2.11)$$

Thus the term δ_ℓ is appropriately called the scattering phase shift for the ℓth-partial wave since it vanishes for all ℓ if $V_c(r)=0$ everywhere.

It is clearly desirable to establish the connection between the scattering amplitude $f(\theta,\phi)$ and the partial wave phase shifts δ_ℓ. Substituting $G_\ell(r)$ from equation(2·2·11)into the right-hand side of equation(2·2·3)and equating it to the right-hand side of equation(2·2·2) (which is also an expression for the stationary wave function ψ_k at large r) we have

$$\sum_\ell A_\ell \sin \left[kr - \frac{\ell}{2}\pi + \delta_\ell \right] Y_\ell^0(\theta, \phi) = e^{ikz} + \frac{f(\theta,\phi)}{r} e^{ikr} \qquad (2\cdot2\cdot12)$$

Using the following expansions for the incident plane wave and the sine functions in equation (2·2·12),

$$e^{ikz} \xrightarrow[kr \text{ large}]{} \sum_\ell \frac{i^\ell(2\ell+1)}{2\,ikr} \sqrt{\frac{4\pi}{2\ell+1}}\, Y_\ell^0(2,\phi) \left\{ e^{i\left[kr - \frac{\ell\pi}{2}\right]} - e^{-i\left[kr - \frac{\ell\pi}{2}\right]} \right\} \qquad (2.2.13)$$

$$\sin \left[kr - \frac{\ell\pi}{2} + \delta_\ell \right] = \frac{1}{2i} \left\{ e^{i\left[kr - \frac{\ell}{2}\pi + \delta_\ell\right]} - e^{-i\left[kr - \frac{\ell}{2}\pi + \delta_\ell\right]} \right\} \qquad (2.2.14)$$

and equating the coefficients of e^{-ikr} on the left of equation(2·2·12)to the corresponding coefficients on the right, we obtain

$$A_\ell = i^\ell (2\ell+1) \sqrt{\frac{4\pi}{2\ell+1}}\, e^{i\delta_\ell} \qquad (2\cdot2\cdot15)$$

When this expression is substituted into equation(22.12)we obtain

$$\frac{f(\theta,\phi)}{r} = \sum_{\ell} \frac{1}{2ikr} (2\ell+1)\, P_\ell^0(\cos\theta) \times \left\{ e^{2i\delta_\ell} - 1 \right\} \qquad (22.16)$$

where $P_\ell^0(\cos\theta) = \sqrt{\frac{4\pi}{2\ell+1}}\, Y_\ell^0(\theta,\phi)$ are the Legendre polynomial functions. The connection between $f(\theta,\phi)$ and phase shifts is explicitly obtained as

$$f(\theta,\phi) = \frac{1}{2ik} \sum_{\ell} (2\ell+1)\, P_\ell(\cos\theta) \left\{ e^{2i\delta_\ell} - 1 \right\} \qquad (22.17)$$

If the scattering potential is strongest at the origin, decreases in strength as r increases, and vanishes when r exceeds a certain range, then we may expect the low angular momentum components, which classically correspond to small impact parameters and therefore close collisions, to scatter more intensely than the higher angular momentum components. Thus the summation index ℓ in equation(22.17)includes only the partial waves from $\ell=0$ to $\ell=\ell_{max}$, a certain maximum number. If the impact parameter exceeds the range "a" of the potential, no appreciable scattering occurs. The angular momentum corresponding to the case of impact parameter equal to the range is

$$\ell_{max}\hbar \approx pa$$

or

$$\ell_{max} \approx pa/\hbar \qquad (22.18)$$

where p is the momentum of the particle of mass m, and a the range.

If we substitute equation(22.16) for $f(\theta,\phi)/kr$ in equation(22.2)and use the asymptotic expansion in equation(22.14) for e^{ikz}, the equivalent form of the asymptotic wave function obtained is

$$\psi_k \xrightarrow[\text{large } r]{} -\frac{1}{2ikr}\sum_\ell i^\ell(2\ell+1)\left\{e^{-i(kr-\frac{\ell\pi}{2})} - S_\ell e^{i(kr-\frac{\ell\pi}{2})}\right\}P_\ell^\circ(\cos\theta) \qquad (2.2.19)$$

and $$S_\ell = \exp(2i\delta_\ell) \qquad (2.2.20)$$

This form shows that the radially incoming ℓth-partial wave and the outgoing ℓth-partial wave differ by a factor S_ℓ. The matrix S, in the present case of central field scattering, which has S_ℓ defined by equation(2·2·20)for its diagonal elements and zero for its nondiagonal elements, is called the scattering matrix or simply the S-matrix.

The physically observable differential scattering cross section, which is defined as the ratio of the flux of scattered particles per unit solid angle in the direction (θ,ϕ) to the incident beam flux, can be expressed (Messiah) as

$$\frac{d\sigma(\theta,\phi)}{d\Omega} = \left|f(\theta,\phi)\right|^2 \qquad (2\cdot2\cdot21)$$

The total scattering cross section, obtained by integrating the differential cross section over all angles, is

$$\sigma_T = \int_0^{2\pi}\int_0^{\pi}\left|f(\theta,\phi)\right|^2 \sin\theta\, d\theta\, d\phi \qquad (2\cdot2\cdot22)$$
$$= \frac{4\pi}{k^2}\sum_\ell^{\ell_{max}}(2\ell+1)\sin^2\delta_\ell$$

2.3 The scattering of spinless particles by a Coulomb potential

Consider a beam of charged particles, each carrying a charge Z'e falling on a target composed of particles of charge Ze. Assume that the only interaction between an incident particle and a particle in the target

is the Coulomb interaction, which can be represented by the Coulomb potential $V(r) = ZZ'e^2/r$. In the classical limit, Rutherford showed that, if the incident beam has only one particle crossing unit area per unit time and the target is composed of a single particle, the number of particles $I(\theta)\, d\omega$ scattered per unit time through an angle θ into the solid angle $d\omega$ is given by

$$I(\theta)\, d\omega = \left[\frac{ZZ'e^2}{2mv^2}\right] \operatorname{cosec}^4\left(\frac{\theta}{2}\right) d\omega \qquad (2\cdot3\cdot1)$$

where m, v, θ are the reduced mass, relative velocity and angle of scattering in the center of mass system. This equation is in good agreement with experimental results for the scattering of α-particles at low energies and forward angles by heavy nuclei.

The Schrödinger equation for the scattering of a beam of particles, each of mass m, by a Coulomb potential may be written as

$$-\frac{\hbar}{2m}\nabla^2\psi + V(r)\psi = E\psi \qquad (2\cdot3\cdot2)$$

where $V(r) = ZZ'e^2/r$. Here the subscript k of the wave function is purposely dropped. We choose ψ to have a similar form to that of wave functions for the central potential scattering problem in the preceding section

$$\psi(r,\theta) = \sum_{\ell=0}^{\infty} A_\ell\, G_\ell(r)\, P_\ell(\cos\theta) \qquad (2\cdot3\cdot3)$$

Substitution of this expression into equation (2·3·2) yields the following radial equation

$$\frac{1}{\rho}\frac{d}{d\rho}\left(\rho^2\frac{dG_\ell(r)}{d\rho}\right) + \left\{1 - \frac{2\alpha}{\rho} - \frac{\ell(\ell+1)}{\rho^2}\right\} G_\ell(r) = 0 \qquad (2\cdot3\cdot4)$$

where $k^2 = 2mE/\hbar^2$

$\alpha = ZZ'e^2/\hbar v$

$\ell = 0, 1, 2, 3, \ldots$

and $\rho = kr.$

The solutions of this differential equation have been treated in great detail by many authors (e.g., Mott and Massey). Briefly, we can find two linearly independent solutions, one of which, L_ℓ, is regular at the origin and the other, K_ℓ, is irregular at the origin. These solutions have the asymptotic forms shown below

$$L_\ell \xrightarrow[kr\ large]{} \frac{1}{kr} \sin\left[kr - \frac{\ell\pi}{2} + \eta_\ell - \alpha \log 2kr\right] \qquad (2\cdot3\cdot5)$$

and

$$K_\ell \xrightarrow[kr\ large]{} -\frac{1}{kr} \cos\left[kr - \frac{\ell\pi}{2} + \eta_\ell - \alpha \log 2kr\right] \qquad (2\cdot3\cdot6)$$

where $\eta_\ell = \arg\Gamma(\ell+1+i\alpha)$ with $\alpha = ZZ'e^2/\hbar v$.

The asymptotic wave function for scattering by a pure Coulomb potential then is

$$\sum_{\ell=0}^{\infty} A_\ell L_\ell(r) P_\ell(\cos\theta) \xrightarrow[large\ kr]{} \frac{A_\ell P_\ell(\cos\theta)}{kr} \sin\left[kr - \frac{\ell\pi}{2} + \eta_\ell - \alpha \log 2kr\right] \qquad (2\cdot3\cdot7)$$

This expansion differs from the expansion we had for a more rapidly falling potential in the previous section by the addition of the logarithmic terms. It has been shown (e.g.,Mott and Massey) that the total wave function representing the scattering by a Coulomb potential can be summed in terms of an exact function so that the wave function has the asymptotic form of an incident wave of unit density for negative and large values of z

$$\psi = I + S f(\theta, \phi) \qquad (2.3.8)$$

where

$$I = [1+\alpha^2/ik(r-z)] \exp i[kz+\alpha \log k(r-z)]$$

$$S = \frac{1}{r} \exp i[kr-\alpha \log 2kr]$$

and

$$f(\theta,\phi) = \frac{zz'e^2}{2mv^2} \operatorname{cosec}^2\left(\frac{\theta}{2}\right) e^{-i\alpha\left[\log \frac{1}{2}(1-\cos\theta) - \pi - 2i\eta_0\right]}$$

The square of the amplitude, $f(\theta,\phi)$, is the differential cross section, $I(\theta)$, in the Rutherford formula.

The presence of a Coulomb potential distorts (even at infinity) the incident plane wave to the form described by

$$z + (ZZ'e^2/mv^2) \log k(r-z) = \text{constant} \qquad (2.3.9)$$

When either Z or Z' is zero, equation(2.3.9)reduces to

$$z = \text{constant} \qquad (2.3.10)$$

which is seen to be a plane wave.

From equation(2.3.7)the equivalent form of the asymptotic wave function may be written as

$$\psi \xrightarrow[kr \text{ large}]{} -\sum_{l}^{\infty} \frac{A_l P_l(\cos\theta) e^{-i\eta_l}}{2ikr} \left\{ e^{-i\left(kr - \alpha \log 2kr - \frac{l\pi}{2}\right)} - e^{2i\eta_l} \cdot e^{i\left[kr - \alpha \log 2kr - \frac{l\pi}{2}\right]} \right\} \qquad (2.3.11)$$

Comparing this with the central potential problem solved in the previous section, the submatrix for the state with angular momentum $l\hbar$ is

$$S_\ell = e^{2i\eta_\ell} \qquad (2\cdot3\cdot12)$$

where

$$\eta_\ell = \sum_{x=1}^{\ell} \text{tangent}^{-1}\ (\alpha/x).$$

For real nucleon-nucleon or nucleon-nucleus problems, the interaction differs from a pure Coulomb interaction. In fact, the interaction is of the Coulomb form at large r, and departs from it at small distance. For this type of potential, the asymptotic radial wave function at large r may be written as the linear combination of the regular and irregular solutions of the Coulomb potential, $L_\ell(r)$ and $K_\ell(r)$; i.e.,

$$G_\ell(r) \xrightarrow[kr\ large]{} A_\ell L_\ell(r) + B_\ell K_\ell(r) \qquad (2\cdot3\cdot13)$$

where $K_\ell(r)$ is irregular at origin. Using the asymptotic expressions for $L_\ell(r)$ and $K_\ell(r)$ given in equations (2·3·5) and (2·3·6) we obtain

$$G_\ell(r) \xrightarrow[kr\ large]{} \frac{1}{kr} \sin\left[kr - \frac{\ell}{2}\pi - \alpha \log 2kr + \eta_\ell + \delta_\ell\right] \qquad (2\cdot3\cdot14)$$

Here $\delta_\ell \equiv \tan^{-1}(-B_\ell/A_\ell)$ is the phase shift for the ℓ-partial wave due to the non-coulomb potential. The asymptotic form of the total wave function can then be written as (Mott and Massey)

$$\psi \xrightarrow[kr\ large]{} \exp\left\{ikz + i\alpha \log k(r-z)\right\} + \left\{f(\theta) + f_c(\theta)\right\}\frac{1}{r}\exp\left\{-i\alpha \log \tfrac{1}{2}(1-\cos\theta)\right\} \qquad (2\cdot3\cdot15)$$

where

$$f_c(\theta) = -\frac{\eta_0}{k(1-\cos\theta)} \exp\left\{-i\eta_0 \log \tfrac{1}{2}(1-\cos\theta)\right\} \qquad (2\cdot3\cdot16)$$

an expression which is exactly the same as for pure Coulomb scattering,

and

$$f(\theta)=\frac{1}{2ik}\sum_{\ell}(2\ell+1)e^{2i\eta_\ell}(e^{2i\delta_\ell}-1)P_\ell(\cos\theta) \qquad (2\cdot3\cdot17)$$

These results show that the effects from the Coulomb part and the non-coulomb part may be separated so that in the more complicated case, provided the potential behaves like a Coulomb potential at large r and behaves like a non-coulomb potential only at small r, we may first neglect the Coulomb interaction and then come back to consider its effect later.

2.4 The scattering of spin 1/2 particles by a spinless particle

In this section we are going to treat the scattering of a beam of spin 1/2 particles by target nuclei with spin zero. The interaction is now more complicated than the central potential $V_c(r)$ which depends only on the relative positions of the two interacting particles. The coupling of the spin $\bar{s}$ and the orbital angular momentum $\bar{\ell}$ to the total momentum $\bar{J}$ leads to the well known spin-orbital interaction. The potential takes the familiar form

$$V = V_c(r) + \bar{S}\cdot\bar{\ell}\, V_{\bar{\ell}\cdot\bar{S}}(r) \qquad (2\cdot4\cdot1)$$

Here $V_c(r)$ and $V_{\bar{\ell}\cdot\bar{S}}(r)$ are, respectively, the central potential and the spin-orbit potential, S is the spin operator and ℓ is the orbital angular momentum operator for the two particles in the center of mass frame. We shall also assume that $V_{\bar{\ell}\cdot\bar{S}}(r)$ is a function only of the relative position of the two interacting particles. The solution of the Schrödinger equation

$$\left\{-\frac{\hbar^2}{2m}\nabla^2 + V_c(r) + \vec{S}\cdot\vec{\ell}\; V_{\vec{\ell}\cdot\vec{S}}(r)\right\}\psi = E\psi \tag{2.4.2}$$

may be written as (Messiah, chapter 13)

$$\psi = \sum_{J,m_J,\ell} A_{\ell J}\, G_{\ell J}\, \mathcal{Y}^{m_J}_{J\ell s} \tag{2.4.3}$$

where s = 1/2, and

$$\mathcal{Y}^{m_J}_{J\ell s} = \sum_{m_\ell, m_s} C_{\ell s}(J, m_s; m_\ell, m_s)\, Y_\ell^{m_\ell}(\theta,\phi)\, \chi_s^{m_s} \tag{2.4.4}$$

is an eigenfunction of $\overline{J}^2$, m_J the z-component of total angular momentum, $\overline{\ell}^2$, and $\overline{s}^2$. $C_{\ell s}(J,m_s;m_\ell,m_s)$ is the Clebsch-Gordon angular momentum coupling coefficient (Appendix B). $G_{\ell J}(r)$ is the radial wave function of the state of total angular momentum J, orbital angular momentum ℓ, and spin 1/2. By using the relation

$$\vec{S}\cdot\vec{\ell}\;\mathcal{Y}^{m_J}_{J\ell s} = \frac{1}{2}\left\{\vec{J}^2 - \vec{\ell}^2 - \vec{S}^2\right\}\mathcal{Y}^{m_J}_{J\ell s}$$

$$= \frac{1}{2}\left\{J(J+1) - \ell(\ell+1) - S(S+1)\right\}\mathcal{Y}^{m_J}_{J\ell s} \tag{2.4.5}$$

it follows that for a given ℓ and s = 1/2, we have

$$\left\{\frac{1}{r^2}\cdot\frac{d}{dr}\left(r^2\frac{d}{dr}\right) + \left[k^2 - U_c(r) - \frac{\ell}{2}U_1(r) - \frac{\ell(\ell+1)}{r^2}\right]\right\}G_{\ell J}(r) = 0 \tag{2.4.6}$$

if $J = \ell + \frac{1}{2}$, and

$$\left\{\frac{1}{r^2}\cdot\frac{d}{dr}\left(r^2\frac{d}{dr}\right) + \left[k^2 - U_c(r) + \frac{\ell+1}{2}U_1(r) - \frac{\ell(\ell+1)}{r^2}\right]\right\}G_{\ell J} = 0 \tag{2.4.7}$$

if $J = \ell - \frac{1}{2}$, where

$$U_c(r) = \frac{2mV_c(r)}{\hbar^2}\,, \qquad U_1(r) = \frac{2mV_{\vec{\ell}\cdot\vec{S}}(r)}{\hbar^2}$$

Similar to the case of spinless incident particles, we obtain

$$G_{\ell J}(r) \xrightarrow[kr \text{ large}]{} \frac{1}{kr} \sin\left[kr - \frac{\ell\pi}{2} + \delta_{\ell,J}\right] \qquad (2\cdot4\cdot8)$$

as the general asymptotic solution of equations (2·4·6) and (2·4·7) at large r. Obviously, the two phase shifts $\delta_{\ell,\ell-1/2}$ and $\delta_{\ell,\ell+1/2}$ with the same ℓ are identical if the spin orbit interaction term $U_{\ell\cdot s}(r)$ vanishes everywhere.

Now we consider the alternative asymptotic expression for the beam of incident and scattered particles. Assume that the beam is incident along the z-axis, so that the projection of the orbital angular momentum $\bar{\ell}$ of the incident particle along this direction is $m_\ell = 0$, and the z-component of the spin $\bar{s}$ is either +1/2 or -1/2. Conservation of the total angular momentum $\bar{J}$ and its z-component m_J leads to the conclusion that the z-component m_J must equal 1/2 or -1/2 after the scattering. If we decompose the spin wave function of the incident wave in terms of two basic states specified by m_s either equal to 1/2 or -1/2, the incident wave function may be written as

$$\sum_{m_s} e^{ikz} \chi_s^{m_s}, \qquad m_s = \pm 1/2 \qquad (2\cdot4\cdot9)$$

Using the following matrix representation*

$$\chi_{1/2}^{1/2} = \begin{bmatrix} a_1 \\ 0 \end{bmatrix}, \qquad \chi_{1/2}^{-1/2} = \begin{bmatrix} 0 \\ a_2 \end{bmatrix} \qquad (2\cdot4\cdot10)$$

---

* In comparison with Wolfenstein, $|a_i|^2 = \sum_n |a_i^{(n)}|^2$. It has been tacitly assumed the independence of phases of different particles, which is true for a beam of particles from an accelerator.

where $|a_1|^2$ and $|a_2|^2$ represent the relative densities of the particles in the beam having $m_s = \frac{1}{2}$ and $m_s = -\frac{1}{2}$ respectively, the asymptotic wave function describing the elastic scattering may be written as a spinor with two components (Mott and Massey, 1965)

$$\psi \xrightarrow[kr \text{ large}]{} \sum_{m_s} \left\{ e^{ikz} \chi_s^{m_s} + M \chi_s^{m_s} \frac{e^{ikr}}{r} \right\} \qquad (2\cdot4\cdot11)$$

Here $M(\theta,\phi)$ is a 2 x 2 matrix,

$$M = \begin{bmatrix} M_{\frac{1}{2},\frac{1}{2}} & M_{\frac{1}{2},-\frac{1}{2}} \\ M_{-\frac{1}{2},\frac{1}{2}} & M_{-\frac{1}{2},-\frac{1}{2}} \end{bmatrix} \qquad (2\cdot4\cdot12)$$

which relates the outgoing spinor to the incident spinor. It takes the place of the usual scattering amplitude $f(\theta)$. The total wave function can then be regarded as consisting of two components, one of which has $m_s = +\frac{1}{2}$ and the other $m_s = -\frac{1}{2}$.

The incident beam is completely polarized in the direction of $m_s = m_s'$ if the spin wave function for every incident particle can be represented by a unit spinor $X_s^{m_s'}$. That is, either a_1 or a_2 in equation (2.4.10) vanishes. In this case, the total wave function $\psi_{m_s'}$, including both the incident and the scattered wave, is

$$\psi_{m_s} \xrightarrow[kr \text{ large}]{} e^{ikz} \chi_s^{m_s'} + M \chi_s^{m_s'} \frac{e^{ikr}}{r} \qquad (2\cdot4\cdot13)$$

In order to expand this wave function in terms of the partial waves, with the spherical harmonic functions introduced, we must refer to some properties of the Clebsch-Gordon angular momentum coupling coefficients, listed for convenience in Appendix B. The partial wave expansion of the incident plane wave can then be written as

$$e^{ikz}\chi_s^{m_s'} \xrightarrow[kr \text{ large}]{} \sum_l \frac{i^l(2l+1)}{kr}\sin\left[kr-\frac{l\pi}{2}\right]P_l^0(\cos\theta)\chi_s^{m_s'}$$

$$\longrightarrow \sum_{l,J}\frac{i^l(2l+1)}{kr}\sin\left[kr-\frac{l\pi}{2}\right]\times\sqrt{\frac{4\pi}{2l+1}}$$

$$\times C_{ls}(J,m_s';0,m_s')\times Y_{Jls}^{m_s'} \qquad (2\cdot4\cdot14)$$

As a consequence of equations(2·4·3) and(2·4·8), we also have

$$\psi_{m_s'} \longrightarrow \sum_{l,J}\frac{A_{l,J}}{kr}\sin\left[kr-\frac{l\pi}{2}+\delta_{l,J}\right]Y_{Jls}^{m_s'} \qquad (2\cdot4\cdot15)$$

By substituting equation(2·4·14)for e^{ikr} in equation(2·4·13)and equating to the right-hand-side of equation(2·4·14), we have

$$M\chi_s^{m_s'}\frac{e^{ikr}}{r} = \sum_{l,J}\left\{\frac{A_{l,J}}{kr}\sin\left[kr-\frac{l\pi}{2}+\delta_{l,J}\right]-\frac{i^l(2l+1)}{kr}\frac{4\pi}{2l+1}\times\right.$$

$$\left.\sin\left[kr-\frac{l\pi}{2}\right]\times C_{ls}[J,m_J';0,m_s']\right\}Y_{Jls}^{m_s'} \qquad (2\cdot4\cdot16)$$

which implies

$$A_{l,J} = i^l\sqrt{4\pi(2l+1)} \qquad (2\cdot4\cdot17)$$

When substituted into equation (2·4·16), we obtain

$$M\chi_s^{m_s'}\frac{1}{r} = \sum_{J,\ell}\frac{1}{2ikr}\sqrt{4\pi(2\ell+1)}\;C_{\ell s}(J, m_s'; 0, m_s')$$
$$\times\left\{e^{2i\delta_{\ell,J}}-1\right\}Y_{J\ell s}^{m_s'}$$
$$=\frac{1}{2ikr}\sum_{J,\ell}\sqrt{4\pi(2\ell+1)}\times C_{\ell s}(J, m_s'; 0, m_s')\sum_{m_\ell} C_{\ell s}(J, m_s'; m_\ell, m_s)$$
$$\times\left\{e^{2i\delta_{\ell,J}}-1\right\}Y_\ell^{m_\ell}\chi_s^{m_s} \qquad (2\cdot4\cdot18)$$

The explicit expression for the elements of the M matrix in equation (2·4·12) can be written down as

$$M_{m_s m_s} = \sum_{J,\ell}\frac{1}{2ik}\left\{e^{2i\delta_{\ell,J}}-1\right\}\left[C_{\ell s}(J, m_s; 0, m_s)\right]^2$$
$$\times\left[4\pi(2\ell+1)\right]^{1/2}Y_0^0(\cos\theta) \qquad (2\cdot4\cdot19)$$

if $m_s = m_s'$, and

$$M_{m_s m_s'} = \frac{1}{2ik}\sum_{J,\ell}\left\{e^{2i\delta_{\ell,J}}-1\right\}\times C_{\ell s}(J, m_s'; 0, m_s')$$
$$\times C_{\ell s}(J, m_s'; m_\ell, m_s)\times\sqrt{4\pi(2\ell+1)}\;Y_\ell^{m_\ell}(\theta,\phi) \qquad (2\cdot4\cdot20)$$

if $m_s \neq m_s'$ and $m_\ell = m_s' - m_s$.

Using the Clebsch-Gordon coefficients given in Appendix B to sum over $J = \ell \pm \frac{1}{2}$, the resultant expressions for M are shown in Table 1.

Table 1

M matrix elements for p-He scattering

$$M_{\frac{1}{2},\frac{1}{2}} = \frac{1}{2ik}\sum_{\ell}^{\ell_{max}} \left\{(\ell+1)(e^{2i\delta_{\ell,\ell+\frac{1}{2}}}-1)+\ell(e^{2i\delta_{\ell,\ell-\frac{1}{2}}}-1)\right\}P_\ell(\cos\theta)$$

$$M_{\frac{1}{2},-\frac{1}{2}} = \frac{1}{2ik}\sum_{\ell}^{\ell_{max}} \left\{e^{2i\delta_{\ell,\ell+\frac{1}{2}}} - e^{2i\delta_{\ell,\ell-\frac{1}{2}}}\right\} P_\ell^1(\cos\theta)e^{-i\phi}$$

$$M_{-\frac{1}{2},-\frac{1}{2}} = M_{\frac{1}{2},\frac{1}{2}}$$

$$M_{-\frac{1}{2},\frac{1}{2}}(\theta,\phi) = -M_{\frac{1}{2},-\frac{1}{2}}(\theta,\phi)$$

Note: The contributions from the higher partial waves (i.e. $\ell > \ell_{max}$), are as a rule discarded because the phase shifts are negligibly small for large ℓ.

If we consider only scattering in the XZ-plane (i.e. $\phi=0$), then the M-matrix can be written as

$$M(\theta,\phi=0) = \begin{vmatrix} f(\theta) & g(\theta) \\ -g(\theta) & f(\theta) \end{vmatrix} \qquad (2\cdot4\cdot21)$$

where $f(\theta) = M_{\frac{1}{2},\frac{1}{2}}(\theta,\phi=0)$ and $g(\theta) = M_{\frac{1}{2},-\frac{1}{2}}(\theta,\phi=0)$.

This expression shows that, during the scattering process, changes of the Z-component of the orbital momentum $\bar{\ell}$ are possible. These changes must be compensated for by an inversion of the Z-component of the spin $\bar{s}$, a process which is called "spin-flip". The chance of flipping from m_s to m_s' is the same as for flipping from m_s' to m_s.

From equation (2·3·16), the complete wave function has the general form

$$\psi = \begin{bmatrix} a_1 \\ a_2 \end{bmatrix} e^{ikz} + \begin{bmatrix} a_1 \\ a_2 \end{bmatrix} f(\theta) \frac{e^{ikr}}{r} + \begin{bmatrix} a_2 \\ -a_1 \end{bmatrix} g(\theta) \frac{e^{ikr}}{r} \qquad (2\cdot4\cdot22)$$

where $f(\theta)$ and $g(\theta)$ represent the scattering amplitudes for non-spin-flip and spin-flip scattering respectively.

The inclusion of the Coulomb potential in the problem is simply the addition of another central potential in the radial wave equation (2·4·5) Under the assumption that the Coulomb potential gives rise to the only long range force, so that the scattering potential is of the Coulomb form at large distances, the asymptotic radial wave function, as shown in the previous section, is

$$G_{\ell J}(r) \xrightarrow[kr \text{ large}]{} \frac{1}{kr} \sin\left[kr - \frac{\ell\pi}{2} + \delta_{\ell,J} + \eta_\ell - \alpha \log 2kr\right] \qquad (2\cdot4\cdot23)$$

The total phase shift for the ℓ-partial wave, with total angular momentum J, is the sum of the phase shifts due to the Coulomb potential (i.e. η_ℓ) and the nucleon-nucleon (non-coulomb) potential (i.e. $\delta_{\ell,J}$). As a consequence of the results in the preceding section, the M-matrix becomes

$$M_{\frac{1}{2},\frac{1}{2}} = M_{-\frac{1}{2},-\frac{1}{2}} = \frac{1}{2ik}\sum_{\ell}^{\ell_{max}} \left\{(\ell+1)(e^{2i\delta_{\ell,\ell+\frac{1}{2}}} - 1) + \ell(e^{2i\delta_{\ell,\ell-\frac{1}{2}}} - 1)\right\} \times e^{2i\eta_\ell} P_\ell(\cos\theta) + f_c(\theta) \quad (2\cdot4\cdot24)$$

$$M_{\frac{1}{2},-\frac{1}{2}}(\theta,\phi) = \frac{1}{2ik}\sum_{2ik}^{\ell_{max}} \left\{e^{2i\delta_{\ell,\ell+\frac{1}{2}}} - e^{2i\delta_{\ell-\frac{1}{2}}}\right\} \times e^{2i\eta_\ell} P_\ell^1(\cos\theta) e^{-i\phi} \quad (2\cdot4\cdot25)$$

where $f_c(\theta) = -\frac{\eta_o}{k(1-\cos\theta)} \exp\left\{-i\eta_o \log \tfrac{1}{2}(1-\cos\theta)\right\}$

In the case of an unpolarized incident beam, i.e. equation (2·4·10) $|a_1|^2 = |a_2|^2$, the density matrix formalism (Wolfenstein, 1956) shows that the observable differential cross section, in terms of phase shifts, is

$$\frac{d\sigma}{d\Omega} = \frac{1}{2}\left\{\left|M_{\frac{1}{2},\frac{1}{2}}\right|^2 + \left|M_{\frac{1}{2},-\frac{1}{2}}\right|^2 + \left|M_{-\frac{1}{2},\frac{1}{2}}\right|^2 + \left|M_{-\frac{1}{2},-\frac{1}{2}}\right|^2\right\}$$

$$= \left\{\left|M_{\frac{1}{2},\frac{1}{2}}\right|^2 + \left|M_{\frac{1}{2},-\frac{1}{2}}\right|^2\right\} \quad (2\cdot4\cdot26)$$

Also both x- and z-components of the polarization (for definition refer to section 2.6) of the scattered wave are equal to zero if we define the scattering plane as the xz plane. The polarization along the direction

$$\vec{n} = \frac{\vec{k}_i \times \vec{k}_f}{|\vec{k}_i \times \vec{k}_f|} \quad (2\cdot4\cdot27)$$

defined by the incident wave vector $\bar{k}_i$ and the scattered wave vector $\bar{k}_f$, which must be either parallel or antiparallel to the y-axis (refer to section 2.6) is

$$P = \frac{2\,\mathrm{Re}\; i\left\{M^{*}_{\frac{1}{2},\frac{1}{2}} \cdot M_{\frac{1}{2},-\frac{1}{2}}\right\}}{\left|M_{\frac{1}{2},\frac{1}{2}}\right|^2 + \left|M_{\frac{1}{2},-\frac{1}{2}}\right|^2} \qquad (2.4.28)$$

where $M^{*}_{\frac{1}{2},\frac{1}{2}}$ is the complex conjugate of $M_{\frac{1}{2},\frac{1}{2}}$.

2.5 The construction of the M-matrix for nucleon-nucleon scattering

2.5.1 Tensor-type interactions and nucleon-nucleon scattering

Historically, the first empirical evidence for the existence of a deviation from central symmetry of the interaction between the proton and the neutron came with the discovery of a quadrupole moment in the ground state of the deuteron. This quadrupole moment has since been explained by the presence of a tensor interaction of the form

$$S_{12}\, V_T(r) = \left[\frac{3(\vec{\sigma}_1 \cdot \vec{r})(\vec{\sigma}_2 \cdot \vec{r})}{r^2} - (\vec{\sigma}_1 \cdot \vec{\sigma}_2)\right] V_T(r) \qquad (2.5.1)$$

where $\bar{r} = \bar{r}_2 - \bar{r}_1$ is the vector connecting the two interacting nucleons, with $r = |\bar{r}|$, and $\bar{\sigma}_1$, $\bar{\sigma}_2$ the Pauli matrix operators for the spins of the two particles, $V_T(r)$ the radial part of the tensor interaction. Thus, in the N-N scattering problem, the consideration of a tensor interaction as part of the total interaction between the two nucleons is seen to be necessary.

Since the nucleon is a Fermion, any state of the two-nucleon system is anti-symmetric with respect to the interchange of all coordinates of the nucleons. Hence the following relation always holds:

$$(-1)^{S+1}\,(-1)^{T+1}\,\pi = (-1)^{S+T+\ell} = -1 \qquad (2.5.2)$$

where π, S, T, and ℓ are, respectively, the parity, spin, isospin, and orbital angular momentum of the two-nucleon system. The conservation of isospin T and parity π, the only two possible values for S, 0 and 1, and the relation, equation(2.4.16), imply the conservation of S in the scattering process. Thus, we can classify the states of the two-nucleon system according to the good quantum numbers J, π, T and S of the state, where

$$J = 0, 1, 2, 3, \ldots\ldots$$

$$S = 0, 1$$

$$T = 0, 1$$

$$\pi = 1 \text{ (even } \ell\text{)}, -1 \text{ (odd } \ell\text{)}$$

Note that there is a degeneracy in L, where $L = J \pm 1$, in the triplet-spin state. All allowable states which satisfy equation(2.4.13) are shown up to J = 5 in Table 2.

Table 2

Classification of states of the two-nucleon system

	T=1		T=0	
	singlet (S=0)	triplet (S=1)	singlet (S=0)	triplet (S=1)
J \ π	+1	-1	-1	+1
0	$^1S_0$	$^3P_0$	/	/
1	/	$^3P_1$	$^1P_1$	$^3S_1 + {}^3D_1$
2	$^1D_2$	$^3P_2 + {}^3F_2$	/	$^3D_2$
3	/	$^3F_3$	$^1F_3$	$^3D_3 + {}^3G_3$
4	$^1G_4$	$^3F_4 + {}^3H_4$	/	$^3G_4$
5	/	$^3H_5$	$^1H_5$	$^3G_5 + {}^3I_5$

Notation: S, P, D, F, G, H, I represent ℓ = 0, 1, 2, 3, 4, 5, 6. Superscript indicates singlet or triplet, and subscript stands for J.

Those states corresponding to the eigenvalue T = 0 (hence the z-component m_T = 0), are forbidden for two equivalent nucleons (i.e. p - p with m_T = 1 and n - n with m_T = -1). Hence, the two-proton or two-neutron system must be in the state with either (spin) singlet and (parity) even or triplet and odd. The transitions between two states are allowable only when the two states are in the same block — e.g., the transition $^3S_1 \nrightarrow {}^3D_1$ is allowable. Obviously transitions are allowable only between the two spin triplet states with same total angular momentum J.

For a given value T, the eigenfunctions of total angular momentum J, and its z-component, can be easily constructed from the eigenfunctions of orbital angular momentum $Y_\ell^{m\ell}(\theta,\phi)$, the spherical harmonic function, and the eigenfunctions of the spin angular momentum $\chi_s^{m_s}$. By the vector-addition law:

$$\mathcal{Y}_{J\ell S}^{m_J} = \sum_{m_\ell m_s} C_{\ell s}(J, m_J;\ m_\ell, m_s)\ Y_\ell^{m_\ell}(\theta,\phi)\ \chi_s^{m_s} \qquad (2\cdot5\cdot3)$$

where $C_{\ell s}(J, m_J; m_\ell, m_s)$ is a Clebsch-Gordon coefficient. The elements of the matrix representation of S_{12} can be evaluated by an explicit use of the above spin-angle function, $y_{J\ell s}^{mJ}$, and are shown in Table 3. (Messiah, chapter 13, problem 11)

Table 3

Matrix representation of S_{12}

$$S_{12}\begin{bmatrix} y^{m_J}_{J,J-1,1} \\ y^{m_J}_{J,J,1} \\ y^{m_J}_{J,J+1,1} \\ y^{m_J}_{J,J,0} \end{bmatrix} = \begin{bmatrix} -\frac{2(J-1)}{2J+1} & 0 & \frac{6\sqrt{J(J+1)}}{2J+1} & 0 \\ 0 & 2 & 0 & 0 \\ \frac{6\sqrt{J(J+1)}}{2J+1} & 0 & -\frac{2(J+1)}{2J+1} & 0 \\ 0 & 0 & 0 & 0 \end{bmatrix} \begin{bmatrix} y^{m_J}_{J,J-1,1} \\ y^{m_J}_{J,J,1} \\ y^{m_J}_{J,J+1,1} \\ y^{m_J}_{J,J,0} \end{bmatrix}$$

Note: m_J, the z-component of J, is conserved.

Also the eigenvalues of the operator $\ell \cdot S$ are given by the relation

$$\vec{\ell} \cdot \vec{S} \; \mathcal{Y}^{m_J}_{J\ell s} = \frac{1}{2}\left\{ J(J+1) - \ell(\ell+1) - S(S+1) \right\} \mathcal{Y}^{m_J}_{J\ell S} \qquad (2.5.4)$$

thus in the spin-singlet states the $\overline{\ell \cdot S}$ coupling force vanishes since S = 0 and J = ℓ.

2.5.2 The asymptotic wave function of singlet and triplet states and Blatt-Biedenharn parameterization. Nuclear bar phase shifts.

First, for mathematical simplicity, we neglect the long range Coulomb force. The nucleon-nucleon interaction is taken to be of the form

$$V = V_c(r) + \overline{V}_{\ell \cdot \bar{S}}(r) + S_{12} V_T(r) \qquad (2.5.5)$$

so that the wave function representing a beam of incident and scattered particles satisfies

$$\left\{ -\frac{\hbar^2}{2m} \nabla^2 + V_c(r) + \vec{S} \cdot \vec{\ell} \; V_{\vec{\ell} \cdot \vec{S}}(r) + S_{12} V_T(r) \right\} \psi = E \psi \qquad (2.5.6)$$

Since the nucleon-nucleon system has four basic spin states, which may be denoted by the spin wave function χ_0 (singlet) and $\chi_1^{m_s}$ where m_s = 1, 0, -1 (triplet), the total wave function may then be written as a spinor of four components, and the description of the scattering amplitude as a 4 x 4 m-matrix, operating on the spin space is most convenient in the connection of matrix elements to physical measurement. (Wolfenstein, 1956 and Hoshizaki, 1968)

The formalism of M depends on the representation of $\chi_s^{m_s}$. Let $\begin{bmatrix}1\\0\\0\\0\end{bmatrix}$ be a state representing a unit spin-singlet state (i.e., s = 0, m_s = 0 state) and $\begin{bmatrix}0\\1\\0\\0\end{bmatrix}\begin{bmatrix}0\\0\\1\\0\end{bmatrix}\begin{bmatrix}0\\0\\0\\1\end{bmatrix}$ be the states representing the unit triplet states s = 1, m_s = +1, 0, -1 respectively. If χ represents any prepared initial spin states of the incident beam, then

$$\chi = \begin{bmatrix} a_1 \\ a_2 \\ a_3 \\ a_4 \end{bmatrix} \qquad (2\cdot5\cdot7)$$

may be written as a linear combination of the four basic states mentioned above. The asymptotic total wave function at large r, written as a spinor of four components, is

$$\psi \xrightarrow[kr\ large]{} e^{ikz}\chi + \frac{e^{ikr}}{r} M\chi \qquad (2\cdot5\cdot8)$$

where M is a 4 x 4 matrix and

$$\psi \equiv \begin{bmatrix} {}^1\psi \\ {}^3\psi_{m_s=1} \\ {}^3\psi_{m_s=0} \\ {}^3\psi_{m_s=-1} \end{bmatrix} \qquad (2\cdot5\cdot9)$$

Following the argument in the last section, M must have the form

$$M = \begin{bmatrix} M_{ss} & 0 & 0 & 0 \\ 0 & M_{11} & M_{10} & M_{1-1} \\ 0 & M_{01} & M_{00} & M_{0-1} \\ 0 & M_{-11} & M_{-10} & M_{-1-1} \end{bmatrix} \qquad (2\cdot5\cdot10)$$

since S is conserved during the scattering. The elements in the matrix show the effect of the potential on different spin components. If the incident beam is prepared so that the initial states of the two-body system are always in a spin singlet state, i.e.

$$\chi = \chi_0^0 = \begin{pmatrix} 1 \\ 0 \\ 0 \\ 0 \end{pmatrix} \qquad (2.5.11)$$

the total wave function, from equation (2.5.8), has only one non-vanishing component

$$^1\psi \longrightarrow e^{ikz}\chi_0^0 + M_{ss}\frac{e^{ikz}}{r}\chi_0^0 \qquad (2.5.12)$$

This means that if the incident wave is in the spin singlet state, the scattered wave always remains in the same spin state. The situation is somewhat different if the incident wave is in a specific spin triplet state $\chi_1^{m_s'}$. The scattered wave in this case is not always in this same spin triplet state but may be in another spin triplet state $\chi_1^{m_s}$ (with $m_s \neq m_s'$). The three components of the asymptotic total wave function in the spin triplet states are

$$^3\psi_{m_s} \xrightarrow[kr \text{ large}]{} e^{ikz}\chi_1^{m_s'}\delta_{m_s m_s'} + M_{m_s m_s'}\chi_1^{m_s}\frac{e^{ikr}}{r} \qquad (2.5.13)$$

where $m_s = 1, 0, -1$ and

$$\delta_{m_s m_s'} = \begin{cases} 0 & \text{if } m_s \neq m_s' \\ 1 & \text{if } m_s = m_s' \end{cases}$$

is the delta function. Here $\chi_1^{m_s}$ are unit spinors of the basic states. The total wave function for this specifically prepared initial spin state is the sum of these three non-vanishing components

$$^3\psi \equiv \begin{bmatrix} 0 \\ {}^3\psi_1 \\ {}^3\psi_0 \\ {}^3\psi_{-1} \end{bmatrix} \longrightarrow e^{ikz} \chi_1^{m_s'} + \sum_{m_s} M_{m_s m_s'} \frac{e^{ikr}}{r} \chi_1^{m_s} \qquad (2.5.14)$$

We may write the total wave function as a linear sum of the eigenfunctions of the Hamiltonian

$$\psi = \sum_{J, m_J, \ell, S} A_{\ell J} g_{s\ell J}(r) \; y_{J\ell S}^{m_J} \qquad (2.5.15)$$

where $g_{s\ell J}(r)$ represents the radially dependent part. Since $\vec{S}^2$ is conserved during the scattering, to simplify the notation we define

$$g_{s\ell J}(r) \equiv \begin{cases} g_J(r) & \text{for the spin singlet state} \\ g_{\ell J}(r) & \text{for the spin triplet state} \end{cases}$$

so that, for an initially prepared spin singlet state in which J = L and $m_J = m_S' = 0$ (conservation of m_J), the total wave function is

$$^1\psi = \sum_J g_J(r) \; y_{J,J,0}^{0} \qquad (2.5.16)$$

and for an initially prepared spin triplet state $\chi_1^{m_S'}$,

$$ {}^3\psi = \sum_{J,\ell,m_s'} g_{\ell J}(r)\, y^{m_s'}_{J,\ell,1} \qquad (2.5.17) $$

The summation indices are related in the following way:

J = L+1, L, L-1 for S = 1

J = L for S = 0

with L = 0, 1, 2, 3 .....

The equivalent forms, equation (2.5.12) and equation (2.5.16), may be connected. Substituting equation (2.5.16) for ${}^1\psi$ in the Schrödinger equation

$$ \left\{ -\frac{\chi^2}{2m}\nabla^2 + V_c(r) + \vec{\ell}\cdot\vec{s}\, V_{\vec{\ell}\cdot\vec{s}}(r) + S_{12} V_T(r) \right\} {}^1\psi = E\, {}^1\psi \qquad (2.5.18) $$

and separating out the spin-angular part, $y^0_{J,J,0}$, which is an eigenfunction of $\overline{J}^2$, m_J, $\overline{\ell}^2$, $\overline{S}^2$ we obtain that the radial wave function $g_J(r)$ must satisfy the equation

$$ \left\{ \frac{1}{r^2}\cdot\frac{d}{dr}\left(r^2\frac{d}{dr}\right) + \left[k^2 - \frac{J(J+1)}{r^2} - U_c(r) \right] \right\} g_J(r) = 0 \qquad (2.5.19) $$

where $k^2 = \dfrac{2mE}{\hbar^2}$ and $U_c(r) = \dfrac{2m\,V_c(r)}{\hbar^2}$

The term $S_{12}\, y_{J,J,0}$ from Table 3 vanishes. The asymptotic form of $g_J(r)$ may be written as

$$ g_J(r) \xrightarrow[\text{large } kr]{} \frac{A_J}{kr}\sin\left[kr - \frac{J\pi}{2} + {}^1\delta_{J,J} \right] \qquad (2.5.20) $$

where A_J is a constant to be determined later and ${}^1\delta_{J,J}$ is the phase shift for the partial wave with S = 0 and L = J. Another more simple notation $\delta_\ell \equiv {}^1\delta_{J,J}$ from here on will be used for the spin singlet state.

Since we choose the Z-axis along the incident beam direction, the following expansion may be used in equation (2.5.12):

$$e^{ikz}\chi_0^0 \xrightarrow[\text{large } r]{} \sum_\ell \frac{i^\ell\sqrt{4\pi(2\ell+1)}}{kr}\sin\left[kr-\frac{\ell\pi}{2}\right]y^0_{\ell,\ell,0} \tag{2.5.21}$$

Comparison of equations (2.5.12) and (2.5.16) yields

$$\sum_\ell i^\ell\sqrt{4\pi(2\ell+1)}\,\frac{\sin\left[kr-\frac{\ell\pi}{2}\right]}{kr}y^0_{\ell,\ell,0} + M_{ss}\frac{e^{ikr}}{r}\chi_0^0 = \sum_\ell A_\ell \sin\left[kr-\frac{\ell\pi}{2}+\delta_\ell\right]y^0_{\ell,\ell,0} \tag{2.5.22}$$

which implies

$$A_\ell = i^\ell\sqrt{4\pi(2\ell+1)}\;e^{i\delta_\ell}$$

When substituted into equation (2.5.22) we have

$$M_{ss} = \frac{1}{2ik}\sum_\ell (2\ell+1)\,P_\ell(\cos\theta)\,\alpha_\ell \tag{2.5.23}$$

where

$$\alpha_\ell = \left\{e^{2i\delta_\ell} - 1\right\}$$

Similarly, equations (2.5.12) and (2.5.17), the two equivalent expressions for the spin triplet state, imply

$$e^{ikz}\chi_1^{m_s'} + \sum_{m_s} M_{m_s m_s'}\frac{e^{ikr}}{r}\chi_1^{m_s} = \sum_{J,\ell} g_{\ell J}\,y^{m_s'}_{J\ell s} = \sum_J\left\{g_{JJ}\,y^{m_s'}_{JJJ} + g_{J-1,J}\,y^{m_s'}_{J,J-1,S} + g_{J+1,J}\,y^{m_s'}_{J,J+1,S}\right\} \tag{2.5.24}$$

Here we have summed over L = J, J - 1, J + 1.

By substituting the right-hand side of the above equation into the Schrödinger equation,

$$\left\{ \frac{-\hbar^2}{2m} \nabla^2 + V_c(r) + \vec{l}\cdot\vec{s}\; V_{\vec{l}\cdot\vec{s}}(r) + S_{12} V_T(r) \right\} \sum_{l,J} g_{lJ}\; y^{m_s'}_{JlS}$$

$$= E \sum_{l,J} g_{lJ}\; y^{m_s'}_{JlS} \qquad (2.5.25)$$

and using the matrix elements in Table 3 for the operation of S_{12} on $y^{m_s}_{JlS}$, then separating out the spin-angular part $y^{m_s}_{JlS}$, we obtain three differential equations

$$\left\{ \frac{1}{r^2}\frac{d}{dr}\left(r^2\frac{d}{dr}\right) + k^2 - \frac{J(J-1)}{r^2} - \left[U_c(r) + (J-1)\,U_{\vec{l}\vec{s}}(r) - \frac{2(J-1)}{2J+1} U_T(r) \right] \right\}$$

$$\times\, g_{J-1,J} = \frac{6\sqrt{J(J+1)}}{2J+1}\, U_T(r)\, g_{J+1,J}(r) \qquad (2.5.26)$$

$$\left\{ \frac{1}{r^2}\frac{d}{dr}\left(r^2\frac{d}{dr}\right) + k^2 - \frac{(J+1)(J+2)}{r^2} - \left[U_c(r) - (J+2)\,U_{\vec{l}\vec{s}}(r) - \frac{2(J+2)}{2J+1} U_T(r) \right] \right\}$$

$$\times\, g_{J+1,J} = \frac{6\sqrt{J(J+1)}}{2J+1}\, U_T(r)\, g_{J-1,J} \qquad (2.5.27)$$

$$\left\{ \frac{1}{r^2}\frac{d}{dr}\left(r^2\frac{d}{dr}\right) + k^2 - \frac{J(J+1)}{r^2} - \left[U_c(r) - 2U_{\vec{l}\vec{s}}(r) - 2U_T(r) \right] \right\}$$

$$\times\, g_{J,J}(r) = 0 \qquad (2.5.28)$$

after the separation of $y^{m_J}_{J,J-1,1}$, $y^{m_J}_{J,J+1,1}$ and $y^{m_J}_{J,J,1}$ from the radial wave functions $g_{lJ}(r)$.

The asymptotic solution at large r for $g_{J,J}(r)$ is easily obtained as

$$g_{J,J}(r) \xrightarrow[kr\ large]{} \frac{A_{J,J}}{kr} \sin\left[kr - \frac{J\pi}{2} + \delta_{J,J}\right] \tag{2.5.29}$$

where $\delta_{J,J}$ is defined as the phase shift for the partial wave of total angular momentum J and orbital angular momentum L = J. For the simultaneous differential equantions (2.5.26) and (2.5.27), a set of the possible forms for the asymptotic solutions at large r is

$$g_{J-1,J}(r) \xrightarrow[kr\ large]{} \frac{A}{kr} \cos\epsilon_J \sin\left[kr - \frac{J-1}{2}\pi + \delta_{J-1,J}\right] - \frac{B}{kr} \sin\epsilon_J \sin\left[kr - \frac{J-1}{2}\pi + \delta_{J+1,J}\right] \tag{2.5.30}$$

$$g_{J+1,J}(r) \xrightarrow[kr\ large]{} \frac{A}{kr} \sin\epsilon_J \sin\left[kr - \frac{J+1}{2}\pi + \delta_{J-1,J}\right] + \frac{B}{kr} \cos\epsilon_J \sin\left[kr - \frac{J+1}{2}\pi + \delta_{J+1,J}\right] \tag{2.5.31}$$

(Mott and Massey, chapter 10). A and B are two arbitrary constants. The two independent parameters $\delta_{J-1,J}$ and $\delta_{J+1,J}$ show the effects of the potentials on the partial waves of $\ell = J-1$ and $\ell = J+1$ respectively. The third independent parameter ϵ_J reflects the magnitude of the coupling effect between the two partial waves due to the potential — in our case the tensor potential $S_{12}V_T(r)$. Obviously, the values of the parameters depend on the form of the asymptotic solutions chosen. The set of parameters, defined by equations (2.5.29), (2.5.30) and (2.5.31), $\delta_{J,J}$, $S_{J-1,J}$, $\delta_{J+J,J}$ and ϵ_J are known as Blatt-Biedenharn phase shifts and

coupling constants. In the absence of the tensor potential, ϵ_J is vanishing so that equation (2.5.30) reduces to the form

$$g_{J-1,J}(r) \longrightarrow \frac{A}{kr} \sin\left[kr - \frac{J-1}{2}\pi + \delta_{J-1,J}\right] \tag{2.5.32}$$

and equation (2.5.31) reduces to

$$g_{J+1,J}(r) \longrightarrow \frac{B}{kr} \sin\left[kr - \frac{J+1}{2}\pi + \delta_{J+1,J}\right] \tag{2.5.33}$$

These are similar to the case of the scattering of a spin 1/2 particle by a spin zero particle treated in the previous section, in which only the spin-orbit interaction is considered. The difference is that the total spin S = 1/2 has been replaced by S = 1.

For convenience, we may also write equations (2.5.30) and (2.5.31) as

$$g_{J-1,J}(r) \longrightarrow \frac{D_{J-1,J}}{kr} e^{i\eta_{J-1,J}} \sin\left(kr - \frac{J-1}{2}\pi + \eta_{J-1,J}\right) \tag{2.5.34}'$$

and

$$g_{J+1,J}(r) \longrightarrow \frac{D_{J+1,J}}{kr} e^{i\eta_{J+1,J}} \sin\left[kr - \frac{J+1}{2}\pi + \eta_{J+1,J}\right] \tag{2.5.35}$$

to obtain the implicit relations

$$D_{J-1,J}\, e^{2i\eta_{J-1,J}} = A\cos\epsilon_J e^{i\delta_{J-1,J}} - B\sin\epsilon_J e^{i\delta_{J+1,J}} \tag{2.5.36}$$

$$\mathcal{D}_{J-1,J} = A\cos\epsilon_J\, e^{-i\delta_{J-1,J}} - B\sin\epsilon_J\, e^{-i\delta_{J+1,J}} \tag{2.5.37}$$

$$\mathcal{D}_{J+1,J}\, e^{2i\eta_{J+1,J}} = A\cos\epsilon_J\, e^{i\delta_{J-1,J}} + B\sin\epsilon_J\, e^{i\delta_{J+1,J}} \tag{2.5.38}$$

$$\mathcal{D}_{J+1,J} = A\cos\epsilon_J\, e^{-i\delta_{J-1,J}} + B\sin\epsilon_J\, e^{-i\delta_{J+1,J}} \tag{2.5.39}$$

These relations imply

$$e^{2i\eta_{J-1,J}} = \left\{ e^{2i\delta_{J-1,J}}\cos^2\epsilon_J + e^{2i\delta_{J+1,J}}\sin^2\epsilon_J \right\} + \tfrac{1}{2}\cdot\frac{\mathcal{D}_{J+1,J}}{\mathcal{D}_{J-1,J}}\left\{ e^{2i\delta_{J+1,J}} - e^{2i\delta_{J-1,J}} \right\}\sin 2\epsilon_J \tag{2.5.40}$$

and

$$e^{2i\eta_{J+1,J}} = \left\{ e^{2i\delta_{J+1,J}}\cos^2\epsilon_J + e^{2i\delta_{J-1,J}}\sin^2\epsilon_J \right\} + \tfrac{1}{2}\frac{\mathcal{D}_{J-1,J}}{\mathcal{D}_{J+1,J}}\left\{ e^{2i\delta_{J-1,J}} - e^{2i\delta_{J+1,J}} \right\}\sin 2\epsilon_J \tag{2.5.41}$$

As shown in Appendix C, by substituting equation (2.5.35) for $g_{\ell S}(r)$ in equation (2.5.24) and using equations (2.5.40), (2.5.41), and also the partial wave expansion

$$e^{ikz}\chi_1^{m_s'} \longrightarrow \frac{1}{kr}\sum_{J,\ell}\frac{1}{kr}\sin\left[kr - \frac{\ell\pi}{2}\right] C_{\ell S}(J, m_s'; 0, m_s')\, \mathcal{Y}_{J\ell S}^{m_s'}$$

we find that

$$\mathcal{D}_{\ell,J} = i^{\ell}\left[4\pi(2\ell+1)\right]^{1/2} C_{\ell S}(J, m_s'; 0, m_s') \tag{3.5.42}$$

so that

$$\frac{\mathcal{D}_{J+1,J}}{\mathcal{D}_{J-1,J}} = -\sqrt{\frac{2J+3}{2J-1}} \cdot \frac{C_{J+1,S}(J, m_s'; 0, m_s')}{C_{J-1,J}(J, m_s'; 0, m_s')}$$

or

$$\frac{\mathcal{D}_{l+2,l+1}}{\mathcal{D}_{l,}\mathcal{D}_{l+1}} = -\sqrt{\frac{2l+1}{2J-1}} \cdot \frac{C_{l+2,S}(l+1, m_s'; 0, m_s')}{C_{l,J}(l+1, m_s'; 0, m_s')} \qquad (2.5.43)$$

and

$$\frac{\mathcal{D}_{l-2,l-1}}{\mathcal{D}_{l,l-1}} = -\sqrt{\frac{2l-3}{2l+1}} \cdot \frac{C_{l-2,S}(l-1, m_s'; 0, m_s')}{C_{l,S}(l-1, m_s'; 0, m_s')}$$

When these values are substituted into equations (2.5.34) and (2.5.35) we obtain

$$g_{J-1,J}(r) \longrightarrow \frac{1}{kr}\, i^l [4\pi(2J-1)]^{1/2} \times \left\{ C_{J-1,S}(J, m_s'; 0, m_s')\alpha_{J-1,J} - \sqrt{\frac{2J+3}{2J-1}}\, C_{J+1,S}(J, m_s'; 0, m_s')\alpha^J \right\}$$

$$\times \sin\left[kr - \frac{J-1}{2}\pi + \eta_{J-1,J} \right]$$

and (2.5.44)

$$g_{J+1,J}(r) \longrightarrow \frac{1}{kr}\, i^l [4\pi(2J+3)]^{1/2} \times \left\{ C_{J+1,S}(J, m_s'; 0, m_s')\alpha_{J+1,J} - \sqrt{\frac{2J-1}{2J+3}}\, C_{J+1,S}(J, m_s'; 0, m_s')\alpha^J \right\}$$

$$\times \sin\left[kr - \frac{J+1}{2}\pi + \eta_{J+1,J} \right] \qquad (2.5.45)$$

where

$$\alpha_{J\pm1,J} = \cos^2\epsilon_J\, e^{2i\delta_{J\pm1,J}} + \sin^2\epsilon_J\, e^{2i\delta_{J\mp1,J}} - 1$$

and

$$\alpha^J = \frac{1}{2}\sin 2\epsilon_J \left(e^{2i\delta_{J\pm1,J}} - e^{2i\delta_{J\mp1,J}} \right)$$

for $l = J \pm 1$.

In order to find an expression in terms of the parameters $\alpha_{\ell,J}$ and α^J, we use

$$\sum_{m_s} M_{m_s m_s'} \chi_1^{m_s} = \sum_{J,\ell} q_{\ell J}(r)\, \mathcal{Y}_{J\ell S}^{m_s'} - \sum_{\ell} i^{\ell} \sqrt{4\pi(2\ell+1)} \times \left\{ \sum_{\ell} C_{\ell s}(J, m_s'; 0, m_s')\, \mathcal{Y}_{J\ell s}^{m_s'} \right\} \times \frac{1}{kr} \sin\left[kr - \frac{\ell}{2}\pi\right]$$

and expand J into J = ℓ+1, ℓ, ℓ-1 using $\mathcal{Y}_{J\ s}^{m_s'} = \sum_{m_s} C_{\ell s}(J, m_s'; m_\ell, m_s) Y_\ell^{m_\ell} \chi_s^{m_s}$ to obtain

$$M_{m_s m_s'} = \frac{1}{2ikr} \sum_{\ell} \Big\{ \Big[\sqrt{4\pi(2\ell+1)}\, C_{\ell s}(\ell+1, m_s'; 0, m_s')\, \alpha_{\ell,\ell+1} - \sqrt{4\pi(2\ell+5)}\, C_{\ell+2,s}(\ell+1, m_s'; 0, m_s')\, \alpha^{\ell+1} \Big] C_{\ell s}(\ell+1, m_s'; m_\ell, m_s) + \Big[\sqrt{4\pi(2\ell+1)}\, C_{\ell s}(\ell-1, m_s'; 0, m_s')\, \alpha_{\ell,\ell-1} - \sqrt{4\pi(2\ell+3)}\, C_{\ell-2,s}(\ell-1, m_s'; 0, m_s')\, \alpha^{\ell-1} \Big] C_{\ell s}(\ell-1, m_s'; m_\ell, m_s) + \sqrt{4\pi(2\ell+1)}\, C_{\ell,s}(\ell, m_s'; 0, m_s') \times C_{\ell s}(\ell, m_s'; m_\ell, m_s) \Big\} Y_\ell^{m_\ell}(\theta, \phi) \qquad (2.5.46)$$

In the scattering of identical particles (e.g. p-p scattering), there are two indistinguishable situations for every scattering direction defined by θ and φ. As shown in Fig. 2.1 the incident particle 1 and the scatterer 2 have equal and opposite velocities in the center-of-mass frame of reference, and the particle observed in the detector at D can be either the incident particle 1 or the "recoiling" scatterer 2. The wave function for case (b) may be

obtained from the wave function for case (a) by changing θ into $\pi-\theta$ and ϕ into $\pi+\phi$. The correct wave function for the scattering of identical particles is obtained from the combination of the two wave functions for case (a) and case (b) respectively.

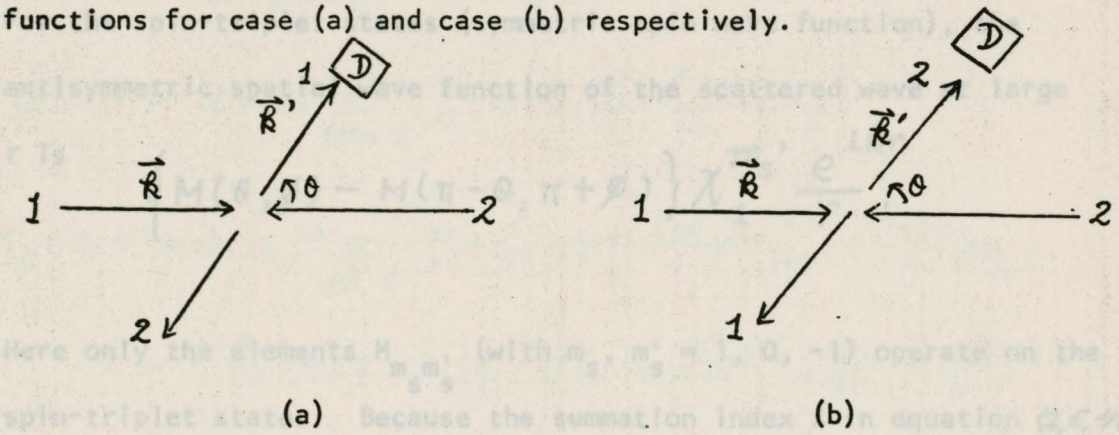

(a) (b)

Fig. 2.1 Scattering of identical particles

In the case of the two-body system in a spin-singlet state (antisymmetric spin wave function), the symmetric spatial wave function of the scattered wave at large separation is

$$\left\{ M_{ss}(\theta,\phi) + M_{ss}(\pi-\theta,\pi+\theta) \right\} \frac{e^{ikr}}{r} \chi_0^0$$

Also in section 2.5.1 it was shown that the assumption of charge independence set different restrictions on the summation index ℓ for T = 0 and T = 1 states. For T = 1 states, ℓ must be an even integer if S = 0 (i.e. ℓ must be even for summing terms of the element M_{ss}) and if S = 1, ℓ must be odd. Thus, with reference to the properties of spherical harmonics (e.g. Messiah), we have

$$M_{ss}(\pi-\theta,\pi+\phi) = M_{ss}(\theta,\phi)$$

and the scattered wave function for the spin-singlet state is

$$2 M_{ss}(\theta,\phi)\chi_0^0 \frac{e^{ikr}}{r}.$$

For the spin-triplet states (symmetric spin wave function), the antisymmetric spatial wave function of the scattered wave at large r is

$$\left\{M(\theta,\phi) - M(\pi-\theta,\pi+\phi)\right\}\chi_1^{m_s'} \frac{e^{ikr}}{r}.$$

Here only the elements $M_{m_s m_s'}$ (with m_s, $m_s' = 1, 0, -1$) operate on the spin-triplet states. Because the summation index ℓ in equation (2.5.46) must be odd for these states, we have (refer to properties of spherical harmonics (Messiah))

$$M_{m_s m_s'}(\theta,\phi) = - M_{m_s m_s'}(\pi-\theta,\pi+\phi)$$

and the scattered wave at large r is

$$2 M(\theta,\phi)\chi_1^{m_s'} \frac{e^{ikr}}{r}$$

Using equation (2.5.46), the Clebsch Gordon coefficients, the relation $Y_\ell^m(\theta,\phi) = (-1)^m Y_\ell^m(\theta,\phi)$ and the principles for indistinguishable particles shown above, the explicit expressions for the M-matrix elements for p-p and n-n scattering are shown in Table 4.

Table 4

M-matrix elements for the T = 1 state

Let $\phi = 0$

$$M_{ss}(\theta,\phi) = 2(ik)^{-1} \sum_{\text{EVEN } \ell} P_\ell(\cos\theta)\left\{\frac{2\ell+1}{2}\right\}\alpha_\ell$$

$$M_{11}(\theta,\phi) = 2(ik)^{-1} \sum_{\text{odd } \ell} P_\ell(\cos\theta)\times\left\{\left(\frac{\ell+2}{4}\right)\alpha_{\ell,\ell+1} + \left(\frac{2\ell+1}{4}\right)\alpha_{\ell,\ell}\right.$$

$$\left. + \left(\frac{\ell-1}{4}\right)\alpha_{\ell,\ell-1} - \frac{1}{4}\left[(\ell+1)(\ell+2)\right]^{1/2}\alpha^{\ell+1} - \frac{1}{4}\left[\ell(\ell-1)\right]^{1/2}\alpha^{\ell-1}\right\}$$

$$= M_{-1,-1}(\theta,-\phi)$$

$$M_{oo}(\theta,\phi) = 2(ik)^{-1} \sum_{\text{odd } \ell} P_\ell(\cos\theta)\times\left\{\frac{\ell+1}{2}\alpha_{\ell,\ell+1} + \frac{\ell}{2}\alpha_{\ell,\ell-1}\right.$$

$$\left. + \frac{1}{2}\left[(\ell+1)(\ell+2)\right]^{1/2}\alpha^{\ell+1} + \frac{1}{2}\left[\ell(\ell-1)\right]^{1/2}\alpha^{\ell-1}\right\}$$

$$M_{o1}(\theta,\phi) = 2(ik)^{-1} e^{i\phi} \sum_{\text{odd } \ell} P_\ell(\cos\theta)\times\left\{-\frac{\sqrt{2}}{4}\cdot\frac{\ell+2}{\ell+1}\alpha_{\ell,\ell+1}\right.$$

$$+ \frac{\sqrt{2}}{4}\cdot\frac{2\ell+1}{\ell(\ell+1)}\alpha_{\ell,\ell} + \frac{\sqrt{2}}{4}\cdot\frac{\ell-1}{\ell}\alpha_{\ell,\ell-1}$$

$$\left. + \frac{\sqrt{2}}{4}\cdot\frac{\ell+2}{\ell+1}\alpha^{\ell+1} - \frac{\sqrt{2}}{4}\cdot\frac{\ell-1}{\ell}\alpha^{\ell-1}\right\}$$

$$= -M_{o,-1}(\theta,\phi)$$

Table 4

(continued)

$$M_{10}(\theta,\phi) = 2(ik)^{-1} e^{-i\phi} \sum_{\text{odd } \ell} P_\ell^1(\cos\theta) \times \left\{ \frac{\sqrt{2}}{4} \alpha_{\ell,\ell+1} - \frac{\sqrt{2}}{4} \alpha_{\ell,\ell-1} + \frac{\sqrt{2}}{4} \cdot \frac{\ell+2}{\ell+1} \alpha^{\ell+1} - \frac{\sqrt{2}}{4} \cdot \frac{\ell-2}{\ell} \alpha^{\ell-1} \right\}$$

$$= -M_{-10}(\theta,\phi)$$

$$M_{1,-1}(\theta,\phi) = 2(ik)^{-1} e^{-2i\phi} \sum_{\text{odd } \ell} P_\ell^2(\cos\theta) \times \left\{ \frac{1}{4(\ell+1)} \alpha_{\ell,\ell+1} - \frac{2\ell+1}{4\ell(\ell+1)} \alpha_{\ell,\ell} + \frac{1}{4\ell} \alpha_{\ell,\ell-1} - \frac{1}{4}\left[(\ell+1)(\ell+2)\right]^{-1/2} \alpha^{\ell+1} - \frac{1}{4}\left[\ell(\ell-1)\right]^{-1/2} \alpha^{\ell-1} \right\}$$

$$= M_{-1,1}(\theta,\phi)$$

For the T = 0 state, the summation index ℓ in the expression for M_{ss} must be odd, while ℓ must be even for the rest of the elements.

The other interesting quantities are the elements of the scattering matrix (S matrix). For the state of orbital angular momentum ℓ and total angular momentum J, it is obvious that

$$S_\ell = e^{2i\delta_\ell} \qquad \text{and} \qquad S_{\ell,\ell} = e^{2i\delta_{\ell,\ell}}$$

if ℓ = J. But for ℓ = J ±1 states, if we let S_J be the submatrix of the S-matrix with a given J, we may write

$$S_J = \begin{bmatrix} 1+\alpha_{J-1,J} & -\alpha^J \\ \alpha^J & 1+\alpha_{J+1,J} \end{bmatrix}$$

$$= \begin{bmatrix} \cos\epsilon_J & -\sin\epsilon_J \\ \sin\epsilon_J & \cos\epsilon_J \end{bmatrix} \begin{bmatrix} e^{2i\delta_{J-1,J}} & 0 \\ 0 & e^{2i\delta_{J+1,J}} \end{bmatrix} \begin{bmatrix} \cos\epsilon_J & \sin\epsilon_J \\ -\sin\epsilon_J & \cos\epsilon_J \end{bmatrix} \tag{2.5.47}$$

Here S_J is symmetric and unitary. Physically, this parameterization considers that the two states are mixed in the asymptotic region.

In p-p scattering, the Coulomb interaction is relatively important for small angle scattering. As has been shown in section 2.3, the inclusion of the Coulomb term in the potential for the radial wave function contributes both a Coulomb scattering amplitude $f_c(\theta)$ as well as additional Coulomb phase shifts to the total phase shifts. Applying the principle of indistinguishable particles, the Coulomb scattering amplitude of p-p scattering for S = 0 state is

$$f_c(\theta) + f_c(\pi-\theta) \tag{2.5.48}$$

and for the S = 1 state is

$$f_c(\theta) - f_c(\pi-\theta) \tag{2.5.49}$$

These Coulomb scattering amplitudes must be added to the diagonal elements of the M-matrix. Also from equation (2.5.46) and equation (2.5.17) in section 2.3, it seems that one may change

$$\alpha_{\ell,\ell\pm1} = \left\{ \cos^2 \epsilon_{\ell+1}\, e^{2i\delta_{\ell,\ell\pm1}} + \sin^2 \epsilon\, e^{2i\delta_{\ell,\ell\pm1}} \right\} - e^{2i\eta_\ell}$$

$$\alpha_{\ell,\ell} = e^{2i\delta_{\ell,\ell}} - e^{2i\eta_\ell}$$

$$\alpha_{\ell} = e^{2i\delta_{\ell}} - e^{2i\eta_\ell}$$

$$\alpha^{\ell\pm1} = \left\{ e^{2i\delta_{\ell,\ell\pm1}} - e^{2i\delta_{\ell,\ell\mp1}} \right\} \frac{1}{2} \sin 2\epsilon_{\ell\pm1} \qquad (2.5.50)$$

Here the phase shifts δ_ℓ and $\delta_{\ell,J}$ are total contributions of nuclear and Coulomb effects.

In an alternative parameterization, we may choose the asymptotic solutions of the coupled equations as

$$g_{J-1,J}(r) \xrightarrow[kr\ large]{} \frac{A}{kr}\left\{ e^{-i\left[kr - \frac{J-1}{2}\pi + \bar{\delta}_{J-1,J}\right]} - \cos 2\epsilon_J\, e^{i\left[kr - \frac{J-1}{2}\pi + \bar{\delta}_{J+1,J}\right]} \right\} - \frac{B}{kr}\left\{ i \sin 2\bar{\epsilon}_J\, e^{i\left[kr - \frac{J-1}{2}\pi + \bar{\delta}_{J+1,J}\right]} \right\} \qquad (2.5.51)$$

and

$$g_{J+1,J}(r) \xrightarrow[kr\ large]{} \frac{A}{kr}\left\{ i \sin 2\bar{\epsilon}_J\, e^{i\left[kr - \frac{J-1}{2}\pi + \bar{\delta}_{J-1,J}\right]} \right\} + \frac{B}{kr}\left\{ e^{-i\left[kr - \frac{J+1}{2}\pi + \bar{\delta}_{J+1,J}\right]} - \cos 2\bar{\epsilon}_J\, e^{i\left[kr - \frac{J+1}{2}\pi + \bar{\delta}_{J+1,J}\right]} \right\} \qquad (2.5.52)$$

The parameters $\bar{\delta}_{\ell,J}$ and $\bar{\epsilon}_J$ so defined are called "bar-phase-shifts" and "bar mixing parameter" respectively. The submatrix S_J in this parameterization is

$$S_J = \begin{bmatrix} \cos 2\bar{\epsilon}_J \, e^{2i\bar{\delta}_{J-1,J}} & i \sin 2\epsilon_J \, e^{i(\bar{\delta}_{J+1,J} + \bar{\delta}_{J-1,J})} \\ i \sin 2\epsilon_J \, e^{i(\bar{\delta}_{J+1,J} + \bar{\delta}_{J-1,J})} & \cos 2\epsilon_J \, e^{2i\bar{\delta}_{J+1,J}} \end{bmatrix}$$

$$= \begin{bmatrix} e^{i\bar{\delta}_{J-1,J}} & 0 \\ 0 & e^{i\bar{\delta}_{J+1,J}} \end{bmatrix} \begin{bmatrix} \cos 2\bar{\epsilon}_J & i \sin 2\bar{\epsilon}_J \\ i \sin 2\bar{\epsilon}_J & \cos 2\bar{\epsilon}_J \end{bmatrix} \begin{bmatrix} e^{i\bar{\delta}_{J-1,J}} & 0 \\ 0 & e^{i\bar{\delta}_{J+1,J}} \end{bmatrix} \tag{2.5.53}$$

Physically, in this parameterization, the mixing of partial waves $\ell = J \pm 1$ occurs in the core part of the interaction. In this core region the nuclear interaction dominates the Coulomb one, and hence the parameter $\bar{\epsilon}_J$ may give a measure of the amount of mixed states due to pure nuclear interaction. The bar-phase shifts are also useful in separating Coulomb effects from total phase shifts. For these reasons, the bar formalism is usually used in nucleon-nucleon scattering analyses. In this formalism, the α's used in Table 4 for p-p scattering are defined as

$$\alpha_\ell = e^{2i\bar{\delta}_\ell} - e^{2i\eta_\ell}$$

$$\alpha_{\ell,\ell} = e^{2i\bar{\delta}_{\ell,\ell}} - e^{2i\eta_\ell} \tag{2.5.54}$$

for the uncoupled states. For the coupled states, we have

$$\alpha_{J\pm1,J} = \cos 2\bar{\epsilon}_J \, e^{2i\bar{\delta}_{J\pm1,J}} - e^{2i\phi_{J\pm1}}$$

$$\alpha^J = i \sin 2\bar{\epsilon}_J \, e^{i[\bar{\delta}_{J+1,J} + \bar{\delta}_{J-1,J}]} \tag{2.5.55}$$

To obtain the relations between the two sets of phase shifts, we simply equate equations (2.5.50) and (2.5.55) to get

$$\begin{aligned}
&\delta_{J-1,J} + \delta_{J+1,J} = \bar{\delta}_{J-1,J} + \bar{\delta}_{J+1,J} \\
&\sin(\delta_{J-1,J} - \delta_{J+1,J}) = \sin 2\bar{\epsilon}_J / \sin 2\epsilon_J \\
&\sin(\bar{\delta}_{J-1,J} - \bar{\delta}_{J+1,J}) = \tan 2\bar{\epsilon}_J / \tan 2\epsilon_J
\end{aligned} \tag{2.5.56}$$

We also have $\bar{\delta}_\ell = \delta_\ell$

and $\bar{\delta}_{\ell,\ell} = \delta_{\ell,\ell}$

for the uncoupled states.

To get information on the pure nuclear interaction, Coulomb effects have to be removed from the total phase shifts. The set of phase shifts defined by

$$\begin{aligned}
\bar{\delta}^N_\ell &= \bar{\delta}_\ell - \eta_\ell \\
\bar{\delta}^N_{\ell,J} &= \bar{\delta}_{\ell,J} - \eta_\ell \\
\bar{\epsilon}^N_J &= \bar{\epsilon}_J
\end{aligned} \tag{2.5.57}$$

are called "nuclear-bar phase shifts". Consequently, the α's in Table 4 have the following expressions

$$\begin{aligned}
\alpha_\ell &= \left[e^{2i\bar{\delta}^N_\ell} - 1\right] e^{2i\eta_\ell} \\
\alpha_{\ell,\ell} &= \left[e^{2i\bar{\delta}^N_{\ell,\ell}} - 1\right] e^{2i\eta_\ell} \\
\alpha_{\ell,J} &= \left[e^{2i\bar{\delta}^N_{\ell,J}} - 1\right] e^{2i\eta_\ell} \\
\alpha^J &= i \sin 2\bar{\epsilon}_J \exp i\left\{\bar{\delta}^N_{J+1,J} + \bar{\delta}^N_{J-1,J}\right\} e^{2i\eta_\ell}
\end{aligned} \tag{2.5.58}$$

and the submatrix of the S-matrix for a given ℓ may be expressed as the following,

$$S_\ell = S_N S_c \,, \tag{2.5.59}$$

which can be regarded as a product of a nuclear scattering matrix and the Coulomb scattering matrix S_c, where

$$S_N = \begin{pmatrix} e^{2i\bar{\delta}^N_\ell} & 0 & 0 & 0 \\ 0 & e^{2i\bar{\delta}^N_{\ell+1,\ell}} & 0 & \alpha^{\ell+1} \\ 0 & 0 & e^{2i\bar{\delta}^N_{\ell,\ell}} & 0 \\ 0 & \alpha^{\ell-1} & 0 & e^{2i\bar{\delta}^N_{\ell-1,\ell}} \end{pmatrix}$$

$$S_\ell = \exp(2i\eta_\ell) \begin{pmatrix} 1 & 0 & 0 & 0 \\ 0 & 1 & 0 & 0 \\ 0 & 0 & 1 & 0 \\ 0 & 0 & 0 & 1 \end{pmatrix} . \tag{2.5.60}$$

2.6 The density matrix formalism and physical observables

A simple way to formulate the dependence of the physical observables on the initial state and the parameters (phase shifts and coupling coefficients) is to use the density matrix method (Wolfenstein, 1956).

For the system of two particles with spins s and s_t, an arbitrary spin state (n) can be written as a linear combination of the $(2s+1)(2s_t+1)$ basic spin state of the composite system and may be represented by a vector with $(2s+1)(2s_t+1)$ components

$$\chi^{(n)} = \begin{pmatrix} a_1^{(n)} \\ a_2^{(n)} \\ \cdot \\ \cdot \\ a_{(2s+1)(2s_t+1)}^{(n)} \end{pmatrix} . \qquad (2.6.1)$$

An arbitrary operator, including the M matrix, operating on the spin space, may be written as a linear combination of hermitian base matrices, S^{μ}, where μ runs from 1 to $(2s+1)^2(2s_t+1)^2$. For these base matrices, we require the orthogonality relations

$$Tr(S^{\mu} S^{\nu}) = \delta_{\mu\nu}(2s+1)(2s_t+1) , \qquad (2.6.2)$$

where $Tr(S^{\mu} S^{\nu})$ is the trace of the matrix, the trace of a matrix being the sum of the diagonal elements in the matrix. For example, in p-He scattering analysis with s = 1/2 and s = 0, the two basic states could be the states of $m_s = 1/2$ and $m_s = -1/2$, where m_s is the z-component of the spin of the two-body system. The four base matrices could be a unit matrix I and the three Pauli matrices σ_x, σ_y, σ_z.

For a pure spin state $\chi^{(n)}$, a state for which the spin is completely specified, the density matrix is defined as

$$\rho_{ij} = a_i^{(n)} \, a_j^{(n)+} \qquad (2.6.3)$$

where $a_i^{(n)}$ is the i^{th} component of the column vector $\chi^{(n)}$; $a_j^{(n)+}$ is the j^{th} component of the adjoint row vector $\chi^{(n)+}$. Actually, for the

case of nucleon beamsfrom an accelerator, we are dealing with an incoherent sum of pure spin states. The density matrix is then defined as

$$\rho_{ij} = \sum_n a_i^{(n)} \, a_j^{(n)+} \qquad (2.6.4)$$

where the sum may be considered as a sum over the states of the individual particles in the beam.

In nucleon-nucleon scattering, $s = s_t = 1/2$, the four basic states may be taken as three triplet states and the singlet state. For convenience we may also use another set of basic states defined by the four possible combinations of the eigenstates of the z-components of the two particles in the two-body system. Let s_{z1}, s_{z2} be the z-component of the spin of the incident particle and the target particle respectively. Each basic state is characterized by a pair of eigenvalues as follows:

$$\begin{aligned}
&1)\ s_{z1} = 1/2, \quad s_{z2} = 1/2, \quad \text{eigenstate} \equiv \begin{bmatrix} 1 \\ 0 \\ 0 \\ 0 \end{bmatrix} \\
&2)\ s_{z1} = 1/2, \quad s_{z2} = -1/2, \quad \text{eigenstate} \equiv \begin{bmatrix} 0 \\ 1 \\ 0 \\ 0 \end{bmatrix} \\
&3)\ s_{z1} = -1/2, \quad s_{z2} = 1/2, \quad \text{eigenstate} \equiv \begin{bmatrix} 0 \\ 0 \\ 1 \\ 0 \end{bmatrix} \\
&4)\ s_{z1} = -1/2, \quad s_{z2} = -1/2, \quad \text{eigenstate} \equiv \begin{bmatrix} 0 \\ 0 \\ 0 \\ 1 \end{bmatrix}
\end{aligned} \qquad (2.6.5)$$

Employing this set as a basis for a matrix representation, the singlet and triplet states may be written as

$$\sqrt{1/2}\begin{bmatrix}0\\1\\-1\\0\end{bmatrix} \quad \text{singlet,}$$

$$\text{and} \quad \begin{bmatrix}1\\0\\0\\0\end{bmatrix}, \quad \sqrt{1/2}\begin{bmatrix}0\\1\\1\\0\end{bmatrix}, \quad \begin{bmatrix}0\\0\\0\\1\end{bmatrix} \quad \text{triplet.} \qquad (2.6.6)$$

The change in the basis states, or a transformation, corresponds, geometrically speaking, to a rotation of the coordinate frame in state vector space. As a consequence of the relation between equations(2.6.5) and(2.6.6), the rotational matrix (or operator) corresponding to the transformation may be written as

$$T = \begin{pmatrix} 0 & \sqrt{\frac{1}{2}} & -\sqrt{\frac{1}{2}} & 0 \\ 1 & 0 & 0 & 0 \\ 0 & \sqrt{\frac{1}{2}} & \sqrt{\frac{1}{2}} & 0 \\ 0 & 0 & 0 & 1 \end{pmatrix},$$

so that the M-matrix in the spin space defined by the set of basis states in equation(2.6.5) becomes

$$M = T^{-1}\begin{pmatrix} M_{ss} & 0 & 0 & 0 \\ 0 & M_{11} & M_{10} & M_{1-1} \\ 0 & M_{01} & M_{00} & M_{0-1} \\ 0 & M_{-11} & M_{-10} & M_{-1-1} \end{pmatrix} T,$$

where T^{-1} is the inverse T-matrix (note T is a unitary matrix).

In particular, for p-p scattering

$$M = \begin{pmatrix} M_{11} & \frac{M_{10}}{\sqrt{2}} & \frac{M_{10}}{\sqrt{2}} & M_{1-1} \\ \frac{M_{01}}{\sqrt{2}} & \frac{M_{00}+M_{SS}}{2} & \frac{M_{00}-M_{SS}}{2} & \frac{-M_{01}}{\sqrt{2}} \\ \frac{M_{01}}{\sqrt{2}} & \frac{M_{00}-M_{SS}}{2} & \frac{M_{00}+M_{SS}}{2} & \frac{-M_{01}}{\sqrt{2}} \\ M_{1-1} & \frac{-M_{10}}{\sqrt{2}} & \frac{-M_{10}}{\sqrt{2}} & M_{11} \end{pmatrix}. \qquad (2.6.7)$$

In a scattering experiment, a beam and a target with specified initial states are prepared and subsequently the states of the outgoing particles after the scattering are measured. Thus, the general scattering problem is that of finding the final spin expectation values of the scattered and recoiled particles

$$\langle \sigma_\alpha^{(1)} \quad \sigma_\beta^{(2)} \rangle_f \qquad \alpha, \beta = 0, 1, 2, 3 \qquad (2.6.8)$$

when a specified initial polarization state is known. Here the subscript f implies the expectation values after scattering; α,β indicate the component of the spin to be measured and $\sigma_0 \equiv I$, a unit operator, implies that the spin is neglected; the superscripts are used to distinguish the operators of the incident particle and the target. The sixteen different basic hermitian matrices S^μ for a nucleon-nucleon system may then be a matrix I, three spin operators for the incident particle, three spin operators for the target, and nine operators from the binary products of the spin operators.

The matrices of the spin operators may be written as (Lawden, 1967)

$$\sigma_1^{(1)} = \sigma_x^{(1)} = \begin{pmatrix} 0 & 0 & 1 & 0 \\ 0 & 0 & 0 & 1 \\ 1 & 0 & 0 & 0 \\ 0 & 1 & 0 & 0 \end{pmatrix}; \quad \sigma_2^{(1)} = \sigma_y^{(1)} = \begin{pmatrix} 0 & 0 & -i & 0 \\ 0 & 0 & 0 & -i \\ i & 0 & 0 & 0 \\ 0 & i & 0 & 0 \end{pmatrix};$$

$$\sigma_3^{(1)} = \sigma_z^{(1)} = \begin{pmatrix} 1 & 0 & 0 & 0 \\ 0 & 1 & 0 & 0 \\ 0 & 0 & -1 & 0 \\ 0 & 0 & 0 & -1 \end{pmatrix}; \quad \sigma_1^{(2)} = \sigma_x^{(2)} = \begin{pmatrix} 0 & 1 & 0 & 0 \\ 1 & 0 & 0 & 0 \\ 0 & 0 & 0 & 1 \\ 0 & 0 & 1 & 0 \end{pmatrix}$$

$$\sigma_2^{(2)} = \sigma_y^{(2)} = \begin{pmatrix} 0 & -i & 0 & 0 \\ i & 0 & 0 & 0 \\ 0 & 0 & 0 & -i \\ 0 & 0 & i & 0 \end{pmatrix}; \quad \sigma_3^{(2)} = \sigma_z^{(2)} = \begin{pmatrix} 1 & 0 & 0 & 0 \\ 0 & -1 & 0 & 0 \\ 0 & 0 & 1 & 0 \\ 0 & 0 & 0 & 1 \end{pmatrix}. \quad (2.6.9)$$

Consequently, the M matrix may be written as a linear combination of the basic matrices and, based on the usual assumptions made in the beginning of the chapter, the M matrix may be written (Plummer, 1968)

$$\begin{aligned} M = {} & a\,I + c(\sigma^{(1)} + \sigma^{(2)}) \cdot \vec{n} + m(\sigma^{(1)} \cdot \vec{n})(\sigma^{(2)} \cdot \vec{n}) \\ & + g\{(\sigma^{(1)} \cdot \vec{P})(\sigma^{(2)} \cdot \vec{P}) + (\sigma^{(1)} \cdot \vec{K})(\sigma^{(1)} \cdot \vec{K}) \\ & + h\{(\sigma^{(1)} \cdot \vec{P})(\sigma^{(2)} \cdot \vec{P}) - (\sigma^{(1)} \cdot \vec{K})(\sigma^{(2)} \cdot \vec{K}), \end{aligned} \quad (2.6.10)$$

where a, c, m, g and h are functions of θ and ϕ only. The directions $\bar{n}$, $\bar{P}$ and $\bar{K}$ are defined as

$$\vec{n} = \frac{\vec{P}_i \times \vec{P}_f}{|\vec{P}_i \times \vec{P}_f|}, \qquad \vec{P} = \frac{\vec{P}_i + \vec{P}_f}{|\vec{P}_i + \vec{P}_f|}, \qquad \vec{K} = \frac{\vec{P}_f - \vec{P}_i}{|\vec{P}_f - \vec{P}_i|},$$

where $\bar{p}_i$ and $\bar{p}_f$ are the incoming and outgoing momenta of the particles in the beam in the center-of-mass system. If we choose the incident beam direction along the z-axis and the outgoing beam in the x-z plane,

as shown in Fig.2.2, we have

$$M = aI + C\begin{pmatrix} 0 & -i & -i & 0 \\ i & 0 & 0 & -i \\ i & 0 & 0 & -i \\ 0 & i & i & 0 \end{pmatrix} + m\begin{pmatrix} 0 & 0 & 0 & -1 \\ 0 & 0 & 1 & 0 \\ 0 & 1 & 0 & 0 \\ -1 & 0 & 0 & 0 \end{pmatrix}$$

$$+ g\begin{pmatrix} 1 & 0 & 0 & 1 \\ 0 & -1 & 1 & 0 \\ 0 & 1 & -1 & 0 \\ 1 & 0 & 0 & 1 \end{pmatrix} + h\begin{pmatrix} \cos\theta & \sin\theta & \sin\theta & -\cos\theta \\ \sin\theta & -\cos\theta & -\cos\theta & -\sin\theta \\ \sin\theta & -\cos\theta & -\cos\theta & -\sin\theta \\ -\cos\theta & -\sin\theta & -\sin\theta & \cos\theta \end{pmatrix}.$$

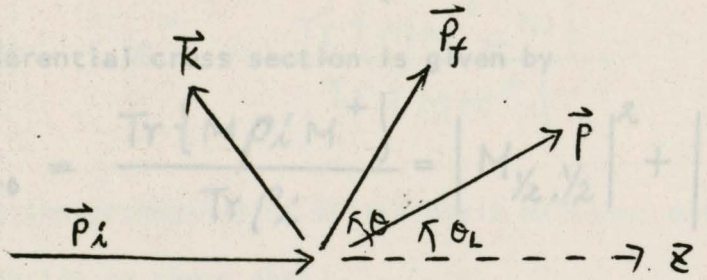

Figure 2.2 Definitions of $\overline{n}$, $\overline{P}$, $\overline{K}$

By comparing with the expression in equation (2.6.7), we further obtain

$$a = \frac{1}{4}\{2M_{11} + M_{00} - M_{ss}\}$$

$$c = \frac{2i}{4}\{M_{10} - M_{01}\}$$

$$m = \frac{1}{4}\{M_{00} - M_{ss} - 2M_{1-1}\}$$

$$g = \frac{1}{4}\{M_{11} + M_{1-1} - M_{ss}\}$$

$$h = \frac{1}{4\cos\theta}\{M_{11} - M_{1-1} - M_{00}\}$$

for p-p scattering.

The average value $\langle S^u \rangle$ of any operator S^u is then given by

$$\langle S^u \rangle = \frac{Tr(M\rho_i M^+ S^u)}{Tr(M\rho_i M)}, \qquad (2\cdot6\cdot11)$$

where ρ_i is the density matrix of the initially prepared state and is a linear combination of the basic matrices (Hoshizaki, 1968).

For example, consider the scattering of an unpolarized proton beam on a helium target. The density matrix of the incident beam is

$$\rho_i = \begin{pmatrix} 1 & 0 \\ 0 & 1 \end{pmatrix}.$$

The differential cross section is given by

$$I_0 = \frac{Tr\{M\rho_i M^+\}}{Tr\rho_i} = \left| M_{1/2,1/2} \right|^2 + \left| M_{1/2,-1/2} \right|^2,$$

and the polarization of the scattered proton beam produced by the scattering is

$$P = \langle \sigma \rangle = \frac{Tr\{MM^+\sigma\}}{Tr\{MM^+\}}$$

since $\langle \sigma_x \rangle = \langle \sigma_z \rangle = 0$,

$$P = \frac{2\,Re\; i\{M^+_{1/2,1/2}\, M_{1/2,-1/2}\}}{\left| M_{1/2,1/2} \right|^2 + \left| M_{1/2,-1/2} \right|^2}.$$

Consider the scattering of an unpolarized nucleon beam on a nucleon target. The density matrix of the incident beam is

$$\rho_i = \begin{bmatrix} 1 & 0 & 0 & 0 \\ 0 & 1 & 0 & 0 \\ 0 & 0 & 1 & 0 \\ 0 & 0 & 0 & 1 \end{bmatrix}.$$

The differential cross section is given by

$$I_0 = \frac{1}{4} Tr(MM^+) = |a|^2 + |m|^2 + 2|c|^2 + 2|g|^2 + 2|h|^2$$

and the polarization of the scattered nucleon beam produced by the scattering is

$$P = \langle \sigma^{(1)} \rangle = \frac{Tr\{MM^+ \sigma^{(1)}\}}{Tr\{MM^+\}}.$$

By using the orthogonality of the basic matrices and equation (2.6.12) it can easily be shown that

$$Tr\{MM^+ \sigma_x^{(1)}\} = 0$$

and

$$Tr\{MM^+ \sigma_z^{(1)}\} = 0.$$

Thus,

$$I_0 P = \frac{1}{4} Tr\{MM^+ \sigma_n^{(1)}\} = 2 Re\{(a+m) C^*\}.$$

Different types of scattering experiments have been discussed in detail by Wolfenstein (1956) and Hoshizaki (1968). Among all observables and parameters associated with such experiments, we are interested in

i) differential cross section, I_0

ii) polarization, P

iii) depolarization D, which is defined as

$$I_0 D = \frac{1}{4} Tr\left(M \sigma_n^{(1)} M^+ \sigma_n^{(1)} \right)$$

iv) the parameter R, which is defined as

$$I_0 R = \frac{1}{4} Tr\left(M \sigma_{s_i}^{(1)} M^+ \sigma_{s_f}^{(1)} \right)$$

v) the parameter A, which is defined as

$$I_0 A = \frac{1}{4} Tr\left(M \sigma_{p_i}^{(1)} M^+ \sigma_{s_f}^{(1)} \right)$$

vi) C_{nn}, the spin-correlation parameter,

$$I_0 C_{nn} = \frac{1}{4} Tr\left(M M^+ \sigma_n^{(1)} \sigma_n^{(2)} \right)$$

vii) C_{KP}, a second spin-correlation parameter,

$$I_0 C_{kp} = \frac{1}{4} Tr\left(M M^+ \sigma_{s_f}^{(1)} \sigma_{s_f}^{(2)} \right)$$

viii) spin rotational parameter R',

$$I_0 R' = \frac{1}{4} Tr\left(M \sigma_{s_i}^{(1)} M^+ \sigma_{s_f}^{(1)} \right)$$

ix) spin rotational parameter A',

$$I_0 A' = \frac{1}{4} Tr\left(M \sigma_{p_i}^{(1)} M^+ \sigma_{p_f}^{(1)} \right).$$

The directions $\bar{s}_i$, $\bar{s}_f$, $\bar{s}_r$, $\bar{p}_i$, $\bar{p}_f$, $\bar{p}_r$ are defined in Fig. 2·3 $\bar{p}_i^{\,L}$, $\bar{p}_f^{\,L}$ and $\bar{p}_r^{\,L}$ are incident, outgoing and recoil momenta in the laboratory system. We define the following three sets of orthogonal unit vectors

$$\vec{p}_i = \frac{\vec{p}_i^{\,L}}{|\vec{p}_i^{\,L}|},$$

$$\vec{n} = \frac{\vec{p}_i^{\,L} \times \vec{p}_f^{\,L}}{|\vec{p}_i^{\,L} \times \vec{p}_f^{\,L}|},$$

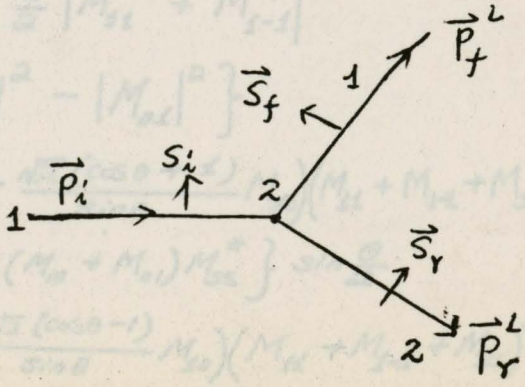

Fig. 2·3 Definition of $\vec{s}_i$, $\vec{s}_r$, $\vec{s}_f$ etc.

$$\vec{S}_i = \vec{n} \times \vec{P}_i \,, \qquad \vec{P}_f = \frac{\vec{P}_f^{\perp}}{|\vec{P}_f^{\perp}|} \,,$$

$$\vec{S}_f = \vec{n} \times \vec{P}_f \,, \qquad \vec{P}_r = \frac{\vec{P}_r^{\perp}}{|\vec{P}_r^{\perp}|} \,,$$

$$\vec{S}_r = \vec{n} \times \vec{P}_r \,.$$

In terms of the elements of the M-matrix, the observables and parameters may be written as

$$I_0 = \frac{1}{4}\left\{ |M_{ss}|^2 + |M_{00}|^2 + 2|M_{11}|^2 + 2|M_{10}|^2 + 2|M_{01}|^2 + 2|M_{1-1}|^2 \right\}$$

$$I_0 P = \frac{\sqrt{2}}{4} Re\left\{ i(M_{10} - M_{01})(M_{11} - M_{1-1} + M_{00})^* \right\}$$

$$I_0(1-D) = \frac{1}{4}\left| M_{11} + M_{1-1} - M_{ss} \right|^2 + \frac{1}{4}\left| M_{11} - M_{1-1} - M_{00} \right|^2 + \frac{1}{2}\left| M_{10} + M_{01} \right|^2$$

$$I_0 R = \frac{1}{2} Re\left\{ \left(M_{00} + \frac{\sqrt{2}(\cos\theta - 1)}{\sin\theta} M_{10} \right)(M_{11} + M_{1-1} + M_{ss})^* + \frac{\sqrt{2}}{\sin\theta}(M_{10} + M_{01}) M_{ss}^* \right\} \cos\frac{\theta}{2}$$

$$I_0 A = -\frac{1}{4} Re\left\{ \left(M_{00} + \frac{\sqrt{2}(\cos\theta + 1)}{\sin\theta} M_{10} \right)\left(M_{11} + M_{1-1} + M_{ss} \right)^* - \frac{\sqrt{2}}{\sin\theta}\left(M_{10} + M_{01} \right)\left(M_{11} + M_{1-1} \right)^* \right\} \sin\frac{\theta}{2}$$

$$I_0(1 - C_{NN}) = \frac{1}{2}|M_{ss}|^2 + \frac{1}{2}|M_{11} + M_{1-1}|^2$$

$$I_0 C_{KP} = \frac{1}{2\sin\theta}\left\{ |M_{01}|^2 - |M_{01}|^2 \right\}$$

$$I_0 R' = \frac{1}{2} Re\left\{ \left(M_{00} + \frac{\sqrt{2}(\cos\theta + 1)}{\sin\theta} M_{10} \right)(M_{11} + M_{1-1} + M_{ss})^* - \frac{\sqrt{2}}{\sin\theta}(M_{10} + M_{01}) M_{ss}^* \right\} \sin\frac{\theta}{2}$$

$$I_0 A' = \frac{1}{2} Re\left\{ \left(M_{00} + \frac{\sqrt{2}(\cos\theta - 1)}{\sin\theta} M_{10} \right)(M_{11} + M_{1-1} + M_{ss})^* + \frac{\sqrt{2}}{\sin\theta}(-M_{10} + M_{01})(M_{11} + M_{1-1})^* \right\} \cos\frac{\theta}{2}$$

In theory, once one has phase shifts, it is trivial to calculate the observables. Conversely, given the experimental quantities, it is possible to obtain from them the phase shifts. In practice, there is in general no feasible analytical procedure to obtain from a given set of experimental quantities the phase shifts. In general, however, one can guess the phase shifts, then calculate the observables and compare with the experimental quantities. Usually, one has to improve the fitting by stepwise alteration of the phase shifts. Some of the difficulties of the procedure to obtain phase shifts from experimental data will be shown in the following chapter.

Chapter 3
TWO EXAMPLES OF PHASE-SHIFT ANALYSIS

3.1 Introduction

We now consider the techniques used in determining phase shifts from experimental data. Generally speaking, the starting phase shifts used for a completed phase-shift analysis must be generated randomly and cover the whole possible range, which means from $-\pi$ to $+\pi$ (in radians) for every phase shift. The number of sets of starting phase shifts is expected to be as large as possible — in some analyses perhaps hundreds or thousands of different starting phase shifts have been used (e.g., Stapp *et al.*, and Plummer *et al.*, 1968).

The goodness of fit of phase shifts to experimental quantities is measured by the quantity

$$\chi^2 = \sum_j \left\{ \sum_i \left[\frac{N_j (X_i)_{\text{calc.}} - (X_i)_{\text{expt.}}}{(\Delta X_i)_{\text{expt.}}} \right]^2 + \left(\frac{1-N_j}{\Delta N_j} \right)^2 \right\} \qquad (3.1)$$

The better the fit, the smaller the value of χ^2. In this equation, $(X_i)_{\text{expt.}}$ is the experimentally measured value of a quantity X_i and $(\Delta X_i)_{\text{expt.}}$ is the experimental error attributed to the measurement of X_i; $(X_i)_{\text{calc.}}$ is the value of the quantity calculated from the fitted phase shifts. The outer summation is over all experimentally measured quantities with the same normalization factor N_j. Here we treat N_j as a fixed quantity for all data obtained from the same experiment. In fitting data, N_j may be a variable for different sets of experimental

data, in which case it contributes to the χ^2 in the form of the second term in equation (3.1). In the case where ΔN_j, the quoted normalization error, is uncertain, N_j is usually fixed at unity.

The expected value of χ^2 for a good fit is equal to the number of pieces of data minus the number of variables. The procedure for finding a set of better phase shifts from an arbitrary set of starting phase shifts is to minimize χ^2 by varying the phase shifts. The set of phase shifts with χ^2 having a reasonable value is said to be the "best fitted" set of phase shifts to the given experimental data. If more than one set of best fitted phase shifts exists, criteria such as the requirement of smooth energy dependence of every phase shift may be used to obtain a unique solution. This smooth energy dependence may be established by the existing solutions at nearby energies.

The complexity and laboriousness of performing a phase-shift analysis is obvious. Computer programs for phase-shift analysis of p-He scattering data and p-p scattering data have been completed and are described in VPN-71-27. The iterative procedure developed by Powell (1964) and extensively used in the p-He scattering analyses (e.g. Plummer, 1967 and Plummer *et al.*, 1968) has been chosen to minimize the χ^2 value in the analyses. This mimimization process does not require the evaluation of derivatives of the function χ^2 with respect to the variables. Instead, the first iteration minimizes χ^2 with respect to all N variables by changing every variable in a linearly independent direction. A new direction is then defined in the hyperspace of variables by the starting and end points of the first iteration and this new direction replaces the

first of the originally independent directions. After each successive iteration a new direction is defined and thus, after N interactions, N new directions have been defined. This iteration procedure is followed until either an iteration causes the change in each variable to be less than one tenth the accuracy required in the variable or the change of χ^2 after a specified number of iterations is less than 0.5%.

A routine for the evaluation of the error matrix associated with the resultant phase shifts has also been completed and is incorporated in the computer program. A treatment of the error matrix was described by Anderson, Davidon, Glicksman and Kruse (1955). In this treatment, the square root of the diagonal elements is the root-mean-square of the error in phase shifts and normalization parameters. In the case where phase shifts resulting from a phase-shift analysis are not determined accurately enough, negative diagonal elements in the error matrix are obtained. In such cases the minimization routine is called to perform another phase-shift analysis. The programme will recall the minimization routine up to four times if negative diagonal terms are obtained in the error matrix.

3.2 Phase-shift analysis of p-^{4}He scattering at 10.0 MeV

Historically, a programme was available for the phase-shift analysis of experimental data on the scattering of a nucleon by a Helium-4 target. In order to illustrate the efficiency of the minimizing procedure which will be used in the computation of proton-proton scattering and also to check the computer programme with the published literature, a phase-shift analysis of experimental data on the scattering of protons at a laboratory kinetic energy of 10 MeV by a He target has been carried out.

Phase shifts with orbital angular momentum greater than 2 are not required at this low energy since it has been found that the D-wave phase shift (ℓ=3) is only of the order of 0.1 radian at a proton energy of 11.2 MeV, whereas the S- and P-waves phase shifts are of the order of 1.0 radian. A total of 43 experimental data points, of which 24 are differential cross-sections and 18 are polarization measurements, had previously been fitted by Plummer (1968). The normalization parameters were fixed at unity in our early analysis.

The starting phase shifts for the present analysis were generated quite randomly in the range from 0 to π radians. The 40 sets of random starting phase shifts so derived were reduced to 7 different solutions, only 4 of which had χ^2 less than 1000. These solutions were used as starting phase shifts for a further analysis in which the normalization parameter for the last 9 polarization measurements (refer to Table 3.3) was left free. The required accuracies of the phase shifts were set equal to 0.002 radians during the search for minimum χ^2. This procedure resulted in only 3 solutions with χ^2 values near the expected value of 38. These 3 solutions are shown below. Only solution 1 has been shown to be consistent with the requirement of smooth energy dependence of the phase shifts (Plummer *et al.*, 1968). In addition, solutions 2 and 3 have a value of $\delta_{1,1/2}$ of almost zero, hence are considered unphysical.

Table 3.1

The 3 "best fitted" solutions out of the 40 sets of random starting phase-shifts

	Solution 1 (χ^2= 28.5)	Solution 2 (χ^2= 89.4)	Solution 3 (χ^2=273.6)
$\delta_{0,0}$	2.086 ± 0.012	2.344	1.691
$\delta_{1,1/2}$	1.978 ± 0.016	0.073	0.079
$\delta_{1,3/2}$	1.152 ± 0.022	1.315	1.810
$\delta_{2,5/2}$	0.094 ± 0.010	0.026	0.027
$\delta_{2,3/2}$	0.066 ± 0.010	1.319	1.043
N (DCS)	1.000	1.000	1.000
N_1(POL)	1.000	1.000	1.000
N_2(POL)	0.999 ± 0.006	0.996	1.161

The error matrix for solution 1 has been evaluated and is shown below.

Table 3.2

p-He scattering at 10 MeV

Error matrix for solution 1 phase shifts (elements are in units of 10^{-4} radian^2)

$\delta_{0,0}$	1.358					
$\delta_{1,3/2}$	1.477	2.495				
$\delta_{1,1/2}$	1.749	3.207	4.804			
$\delta_{2,5/2}$	0.506	1.135	1.970	1.087		
$\delta_{2,3/2}$	0.656	1.011	1.720	0.937	1.011	
N (POL)	0.301	0.228	0.388	0.142	0.242	0.411

Table 3.3

A comparision of calculated quantities from solution 1 and measured quantities used in the analysis,

	CALCULATED	MEASURED	ERROR	C.M. ANGLE	DATA PT.	F-VALUE	TOTAL F.
DCS=	367.896	371.000	7.420	21.10	1	0.18	0.18
	332.160	339.000	6.780	30.89	2	1.02	1.19
	308.881	305.000	6.100	35.07	3	0.41	1.60
	230.877	232.000	9.280	49.03	4	0.02	1.61
	199.338	205.000	3.200	54.70	5	3.13	4.74
	170.775	176.000	7.040	60.00	6	0.55	5.29
	120.792	124.000	2.480	70.10	7	1.67	6.96
	79.965	82.000	1.640	80.00	8	1.54	8.50
	48.985	49.200	0.980	90.00	9	0.05	8.56
	39.585	39.100	0.780	94.07	10	0.39	8.94
	26.492	26.200	0.520	102.17	11	0.32	9.26
	22.227	22.000	0.440	106.90	12	0.27	9.53
	20.754	21.000	0.420	109.90	13	0.34	9.87
	22.578	23.000	0.460	120.60	14	0.84	10.71
	24.168	24.500	0.490	122.80	15	0.46	11.17
	31.857	31.900	0.638	130.13	16	0.01	11.17
	32.847	33.200	0.660	130.90	17	0.29	11.46
	38.381	37.800	0.760	134.87	18	0.58	12.04
	47.641	47.700	0.960	140.80	19	0.00	12.05
	54.573	54.000	1.080	145.00	20	0.28	12.33
	61.851	61.600	1.240	149.40	21	0.04	12.37
	70.529	70.400	1.400	154.90	22	0.01	12.38
	77.727	78.400	1.560	160.00	23	0.19	12.56
	82.979	84.900	1.700	164.40	24	1.28	13.84
POL=	-0.332	-0.323	0.021	46.50	25	0.19	14.03
	-0.426	-0.413	0.022	55.90	26	0.37	14.40
	-0.631	-0.626	0.030	73.50	27	0.02	14.43
	-0.766	-0.761	0.036	89.70	28	0.02	14.45
	-0.591	-0.593	0.025	99.80	29	0.01	14.46
	0.504	0.482	0.032	114.30	30	0.47	14.93
	-0.430	-0.444	0.009	56.20	31	2.57	17.51
	-0.630	-0.648	0.019	73.50	32	0.84	18.35
	-0.767	-0.755	0.024	89.70	33	0.23	18.58
	0.978	0.994	0.033	128.30	34	0.25	18.84
	0.954	0.962	0.017	123.30	35	0.20	19.04
	0.973	0.954	0.018	124.70	36	1.15	20.19
	0.982	0.992	0.016	126.90	37	0.39	20.58
	0.981	0.98	0.018	127.40	38	0.00	20.58
	0.973	0.968	0.015	128.70	39	0.14	20.73
	0.965	0.972	0.016	129.60	40	0.18	20.90
	0.961	0.943	0.015	130.00	41	1.41	22.31
	0.942	0.923	0.016	131.40	42	1.41	23.73
	0.906	0.937	0.014	133.50	43	4.75	28.48
NORM=	0.999	1.000	0.020		46	0.00	28.48

Both the calculated and measured quantities are shown in Table 3.3. The F-values assigned to every data point in the table are defined as

$$F_i = \left(\frac{(X_i)_{calc.} - (X_i)_{expt.}}{(\Delta X_i)_{expt.}} \right)^2 \qquad (3.2)$$

Although a unique solution, with reasonable accuracy in comparison with solutions near 10 MeV, has been determined (Plummer *et al.*, 1968), the distribution of F-values among the data points shows that there are relatively large deviations between a calculated and a measured differential cross section at 54.7° and a polarization at 133.5° indicating that these measurements may be suspect.

3.3 Phase-shift analysis of p-p scattering at 310 MeV

The computer program which has been developed for p-p elastic scattering has been used to obtain a comparison with the phase shift analysis of Stapp (1957). Because of the scarcity of experimental p-p scattering data and the computational problems connected with a large number of free parameters, only tentative analyses of p-p data were carried out at energies higher than 100 MeV before 1956. These were based mostly on measurements of differential cross section and polarization. These early tentative analyses, which usually did not give satisfactory solutions, have been of considerable value in checking the compatibility of data and helping to determine the number of phase shifts needed for a complete and unique analysis at a given energy. These early sets of phase shifts also served very well as starting points for later analyses using an enlarged set of data.

The first satisfactory analysis was carried out after a series of measurements on p-p scattering at 310 MeV had been completed at Berkeley (Stapp *et al.*, 1957). These experiments were carried out to measure five different quantities, and yielded a total of 36 pieces of data consisting of one total cross section, 14 differential cross sections, 6 polarization, 6 depolarization, 6 R-parameter, and 3 A-parameter measurements. Eight significantly better solutions were determined from the analysis.

A re-analysis of the same set of experimental data but omitting the total cross section has been carried out using the techniques outlined in the introduction. The lowest-order field-theoretical relativistic Coulomb interaction correction calculated by Garren (1956) has also been added to the M-matrix. S, P, D, F, G and H waves have been included in this analysis. The required accuracies for the phase shifts needed in the minimizing process were set not greater than 0.01 radian ($\sim$0.6 degree) and the change in individual phase shifts was restricted to less than 0.1 radian per iteration. The 8 resultant sets of fitted phase-shifts so obtained are in agreement with those quoted by Stapp *et al.* (1957) except for solution 2. If we assume that δ_o has a negative value at 310 MeV (Stapp *et al.*, 1960), then solutions 5, 7 and 8 can be eliminated leaving only solutions 1, 2, 3, 4 and 6 which are shown in Table 3.4. For comparison, Stapp's phase shift solutions are shown in Table 3.4b.

3.1.1 Rationale for choice of one of the solutions at 310 MeV

We now give a summary of the arguments used in selecting solution 1. On the basis of the data used, it was not possible to choose the correct solution from the five best solutions listed. This problem was not solved until the so-called modified analysis (MacGregor *et al.*, 1959) based on

the idea of including the one-pion exchange contribution in the higher-angular-momentum states (also Grashin, 1959) showed that solutions 3 and 4 were local minima near the deeper minima of solutions 1 and 2. The inclusion of the one-pion exchange contribution did not improve much on the fitting of solution 6 to the data points and solution 6 was excluded. If we believe that C_{NN} at 90° changes very slowly and smoothly with energy in the 300 MeV region, then an experimental measurement of spin correlation C_{NN} in p-p scattering at an energy of 382 MeV and angle of 90° may be used to verify the rejection of solution 6. The result of such a C_{NN} measurement was 0.63 ± 0.1 while the calculated value from solution 6 was -0.3 (Allaby *et al.*, 1961). More recent measurements on C_{NN} in the 300 MeV region have confirmed that the values of C_{NN} at 90° must be positive (MacGregor *et al.*, UCRL-50426).

Table 3.4 Nuclear-bar phase shifts in degrees for 310 MeV p-p scattering

	Solution 1	2	3	4	6
δ_0	-10.48 ± 2.14	-24.91	-10.81	-26.31	-0.82
$\delta_{1,0}$	-13.66 ± 3.24	-28.98	-5.59	-21.51	-66.03
$\delta_{1,1}$	-26 58 ± 1.74	-11.13	-20.04	-7.64	-14.43
$\delta_{1,2}$	16.09 ± 0.78	19.60	21.95	23.43	8.80
δ_2	12.62 ± 1.20	4.22	13.61	4.71	12.43
$\delta_{3,2}$	1.58 ± 0.91	2.63	-1.55	-0.46	-0.88
$\delta_{3,3}$	-4.77 ± 0.82	-2.38	-2.39	-0.59	1.41
$\delta_{3,4}$	3.49 ± 0.53	4.69	0.79	2.93	3.00
δ_4	0.84 ± 0.36	0.94	0.98	1.46	-0.64
$\delta_{5,4}$	1.70 ± 0.57	1.84	-0.90	-0.35	1.83
$\delta_{5,5}$	-0 20 ± 0.70	-1.21	0.64	-0.96	-0.89
$\delta_{5,6}$	1.43 ± 0.41	1.31	-0.73	-0.39	0.25
ε_2	-1.11 ± 0.94	-10.16	1.82	-8.85	-0.52
ε_4	-1.16 ± 0.56	-1.28	-1.18	0.73	0.69
χ^2	18.5	19.9	23.5	19.1	37.5

Table 3.4b. Nuclear-bar phase shifts in degrees for 310 MeV p-p scattering from Stapp *et al.* (1957)

	Solution 1	2	3	4	6
δ_0	-10.1 ± 2.5	-19.5	-11.0	-26.9	-0.3
$\delta_{1,0}$	-14.3 ± 2.2	-36.1	-4.1	-25.4	-64.7
$\delta_{1,1}$	-26.5 ± 1.3	-16.7	-19.8	-7.3	-13.7
$\delta_{1,2}$	16.1 ± 1.9	18.8	22.6	23.1	8.2
$\delta_{2,}$	12.9 ± 0.7	4.4	13.3	4.9	12.9
$\delta_{3,2}$	0.8 ± 1.0	-0.5	-2.0	-1.4	-2.1
$\delta_{3,3}$	-4.4 ± 1.1	0.3	-2.6	1.6	3.1
$\delta_{3,4}$	3.2 ± 0.5	2.5	0.5	2.6	3.3
δ_4	1.0	1.3	1.1	-1.1	-1.1
$\delta_{5,4}$	1.5	2.1	-1.1	-0.7	2.2
$\delta_{5,5}$	0.1	-1.4	0.9	-0.9	-2.0
$\delta_{5,6}$	1.3	1.4	-0.6	-0.8	0.3
ε_2	-1.0 ± 0.6	-9.3	1.8	-7.5	-0.2
ε_4	-1.2	-1.5	-0.9	-0.9	1.3
χ^2	17.9	21.7	23.8	24.5	34.6

In order to choose the correct solution from solutions 2 and 1, spin correlation coefficients were measured in p-p scattering at an energy of 310 MeV and angle of 45° in the center-of-mass system (Kazarinov *et al.*, 1965). The results were $C_{NN}(45°) = 0.9 \pm 0.51$ and $C_{KP}(45°) = 0.75 \pm 0.51$. Calculated values for solution 1 were $C_{NN}(45°) = 0.8$ and $C_{KP}(45°) = 0.75$ for solution 1, and $C_{NN}(45°) = 0.31$ and $C_{KP}(45°) = 0.05$ for solution 2. Solution 1 was thus chosen as the "most reasonable" correct solution, although after the inclusion of these further measurements into the phase-shift analysis, the χ^2 criterion did not show solution 1 was much more preferable than solution 2 (Kazarinov *et al.*, 1965).

3.3.2 Compatibility of experimental data with phase shifts and the error matrix

In the following discussion, compatibility means the ability of various experimental data at a given energy to be described by the set of phase shifts.

A comparison of the calculated and measured quantities is shown in Table 3.5. Although the distribution of F-values among the data points shows that two measurements, R at 70.9° and 41.8° out of the total of 35 data points, lie beyond two standard deviations from calculations based on the phase shifts, from a statistical point of view the compatibility of all data points with the set of phase shifts is obvious. Error matrix elements for solution 1 phase shifts were then evaluated and are shown in Table 3.6. For example, to provide stronger evidence for the correctness of the choice of solution 1, it is necessary to obtain considerably more accurate values of the coefficients C_{NN} and C_{KP}. The diagonal elements are relatively large in comparison with the p-He scattering treated in the previous section. Of course, we are now treating a problem of 14 variables and only 35 data points; the present 35 data points are not as statistically accurate as the case of p-He scattering in the previous section. Perhaps introduction of more measurements may improve the present status of phase-shift analysis.

The predicted physical quantities calculated from solution 1 are shown in the following figures (Fig. 3.1 to Fig. 3.7) along with the experimental data points. Evidently a requirement for more accurately determining the 310 MeV phase shifts is to extend the range of experimental

Table 3.5. Quantities calculated from solution 1 in p-p scattering at 310 MeV and experimental measurements

	Calculated	Measured	C M Angle	F-value	Accumulation
DCS=	3.7300 mb	3.720 mb	90.00	0.0017	0.0017
DCS=	3.7300	3.887	80.20	1.1479	1.1514
DCS=	3.7000	3.610	71.40	0.5274	1.6788
DCS=	3.6700	3.560	64.00	0.7732	2.4520
DCS=	3.6600	3.770	60.80	0.5322	2.9843
DCS=	3.6900	3.710	52.40	0.0162	3.0005
DCS=	3.7600	3.750	44.80	0.0142	3.0146
DCS=	3.8400	3.995	36.00	1.0904	4.1050
DCS=	3.8800	3.840	31.90	0.1186	4.2236
DCS=	4.0200	4.090	23.40	0.3673	4.5909
DCS=	4.0700	3.810	18.64	0.8292	5.4201
DCS=	4.0200	3.860	14.80	0.2539	5.6740
DCS=	3.8500	3.480	11.30	0.8496	6.5235
DCS=	0.0039	4.010	9.10	0.1490	6.6725
POL=	0.1433	0.142	76.20	0.0027	6.6752
POL=	0.2480	0.250	63.90	0.0055	6.6807
POL=	0.3173	0.303	53.40	0.3303	7.0110
POL=	0.3660	0.379	42.90	0.4268	7.4378
POL=	0.3834	0.378	32.30	0.0389	7.4767
POL=	0.3318	0.305	21.60	1.3657	8.8424
D=	0.4861	0.472	80.50	0.0502	8.8927
D=	0.4742	0.503	65.20	0.3601	9.2528
D=	0.5318	0.533	52.00	0.0004	9.2532
D=	0.4719	0.456	36.50	0.0383	9.2915
D=	0.2945	0.291	25.80	0.0040	9.2955
D=	0.2399	0.245	23.00	0.0042	9.2997
R=	0.4760	0.476	80.10	1.3026	10.6024
R=	0.4372	0.310	70.90	3.1284	13.7308
R=	0.2822	0.287	54.10	0.0079	13.7387
R=	-0.0116	0.104	41.80	2.6353	16.3740
R=	-0.1754	-0.167	34.40	0.0105	16.3846
R=	-0.2409	-0.324	22.30	0.3543	16.7389
A=	0.2689	0.236	76.30	0.4670	17.2058
A=	0.0026	0.005	51.40	0.0041	17.2099
A=	-0.2477	-0.339	25.40	1.3091	18.5190

The χ^2 value for 35, data points is 18.519.

The units for differential cross section are 10^{-27} cm^2.

Table 3.6. Error matrix in degree^2 for solution 1 in p-p scattering at 310 MeV

4.57													
-1.22	1.44												
0.21	-0.14	0.13											
1.87	-2.54	-0.01	10.52										
-2.58	1.66	-0.08	-3.42	3.03									
0.01	-0.33	0.04	1.66	0.00	0.61								
0.65	-0.53	0.11	0.63	-0.38	0.27	0.82							
0.93	-0.49	0.01	2.03	-0.98	0.25	0.17	0.68						
0.10	-0.21	0.00	0.75	-0.15	0.18	0.33	0.20	0.28					
-0.22	-0.18	0.03	0.75	0.03	0.24	0.06	0.08	0.06	0.32				
-0.27	0.57	-0.01	-1.69	0.68	-0.25	-0.18	-0.30	-0.12	-0.14	0.49			
-0.06	-0.20	0.06	0.34	-0.04	0.14	0.10	0.02	0.02	0.18	-0.05	0.17		
-1.32	0.83	-0.09	-1.96	1.36	-0.12	-0.23	-0.44	-0.12	-0.08	0.41	-0.07	0.89	
0.35	-0.50	0.01	1.26	-0.63	0.16	0.16	0.26	0.16	0.13	-0.21	0.08	-0.36	0.32
δ_0	δ_2	δ_4	$\delta_{1,0}$	$\delta_{1,1}$	$\delta_{1,2}$	$\delta_{3,2}$	$\delta_{3,3}$	$\delta_{3,4}$	$\delta_{5,4}$	$\delta_{5,5}$	$\delta_{5,6}$	ε_2	ε_4

measurements of more scattering parameters and to improve considerably the accuracy of the experimental data entering into the phase-shift analysis. The measurements of the coefficients R, D and A at angles greater than 90° in the center-of-mass system would be both helpful and desirable.

At energies between 100 MeV and 300 MeV the phase shifts are better defined due to more recent measurements, although the minimization of χ^2 usually gives several possible solutions rather than a unique solution. As a matter of fact, precise measurements of differential cross section and polarization only are insufficient for the unique determination of phase shifts in p-p scattering.

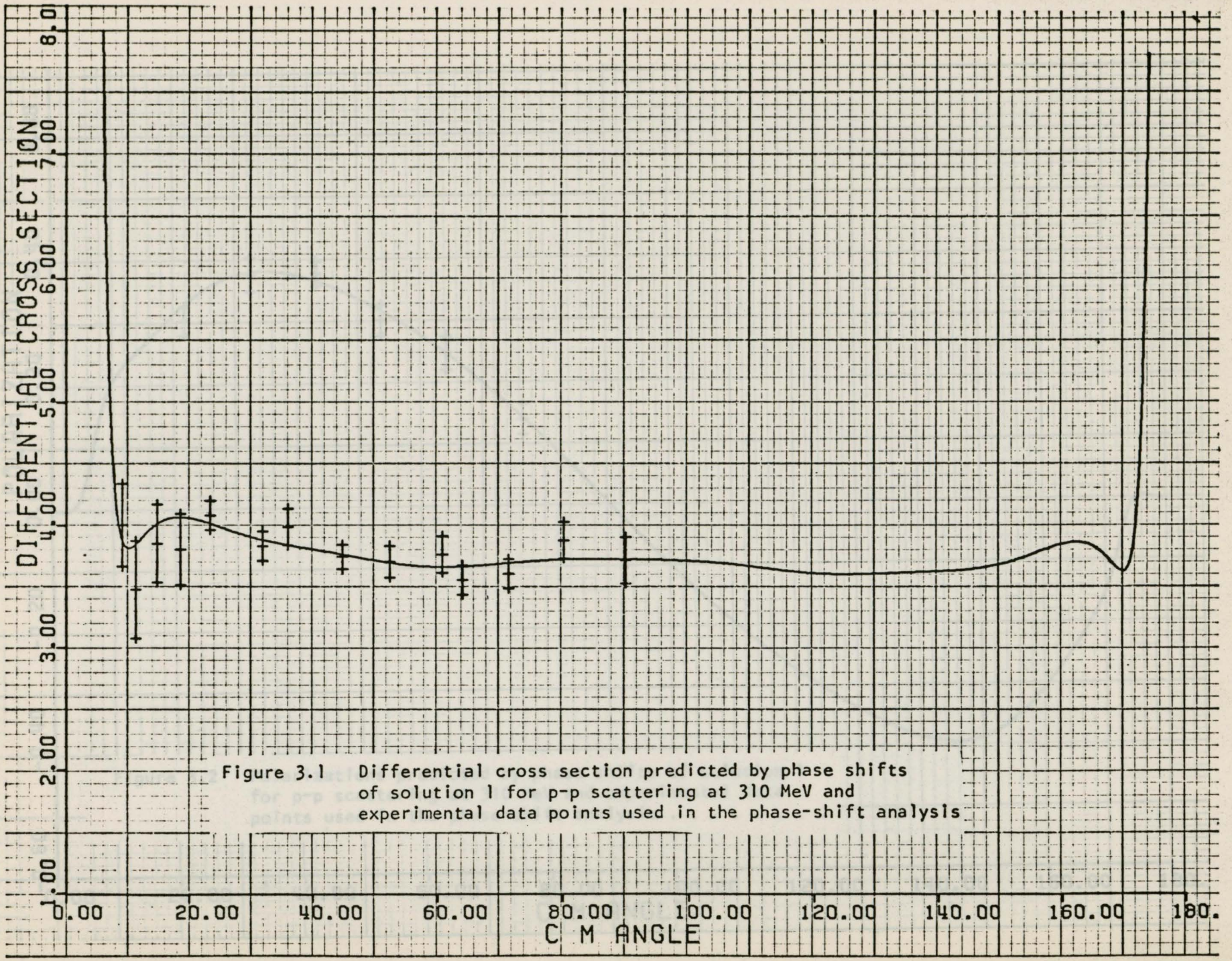

Figure 3.1 Differential cross section predicted by phase shifts of solution 1 for p-p scattering at 310 MeV and experimental data points used in the phase-shift analysis

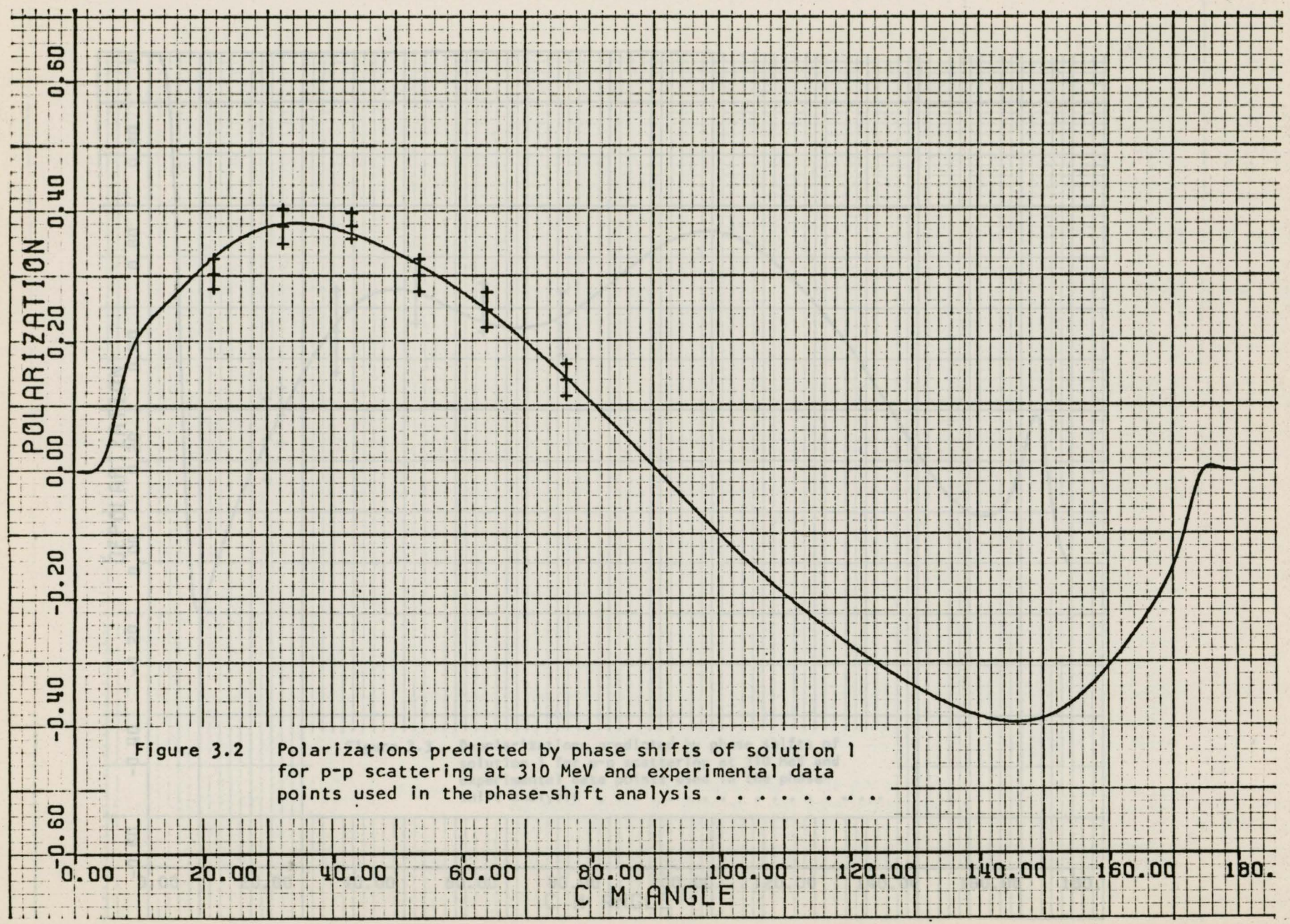

Figure 3.2 Polarizations predicted by phase shifts of solution 1 for p-p scattering at 310 MeV and experimental data points used in the phase-shift analysis . . . . . .

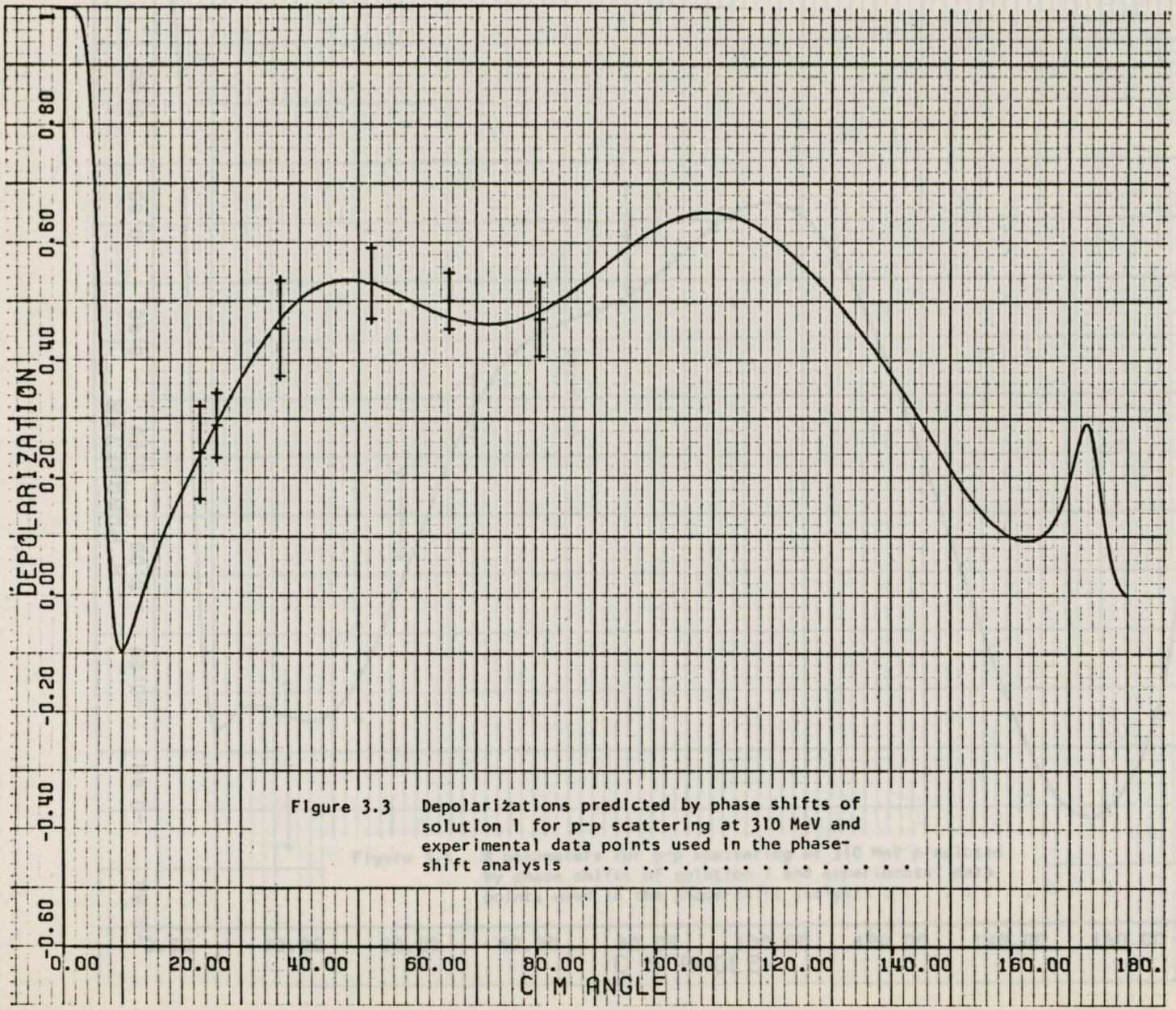

Figure 3.3 Depolarizations predicted by phase shifts of solution 1 for p-p scattering at 310 MeV and experimental data points used in the phase-shift analysis . . . . . .

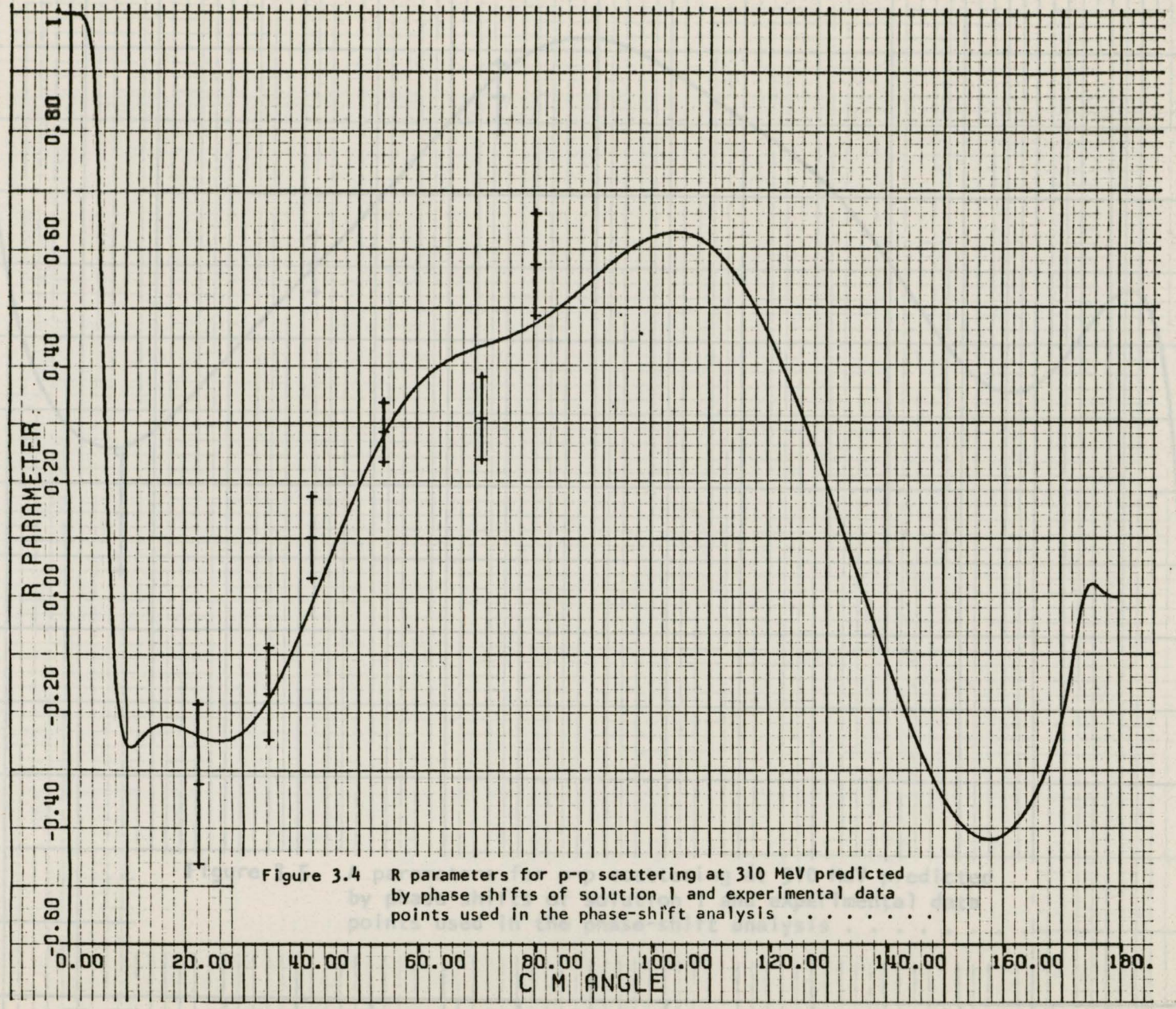

Figure 3.4 R parameters for p-p scattering at 310 MeV predicted by phase shifts of solution 1 and experimental data points used in the phase-shift analysis . . . . . .

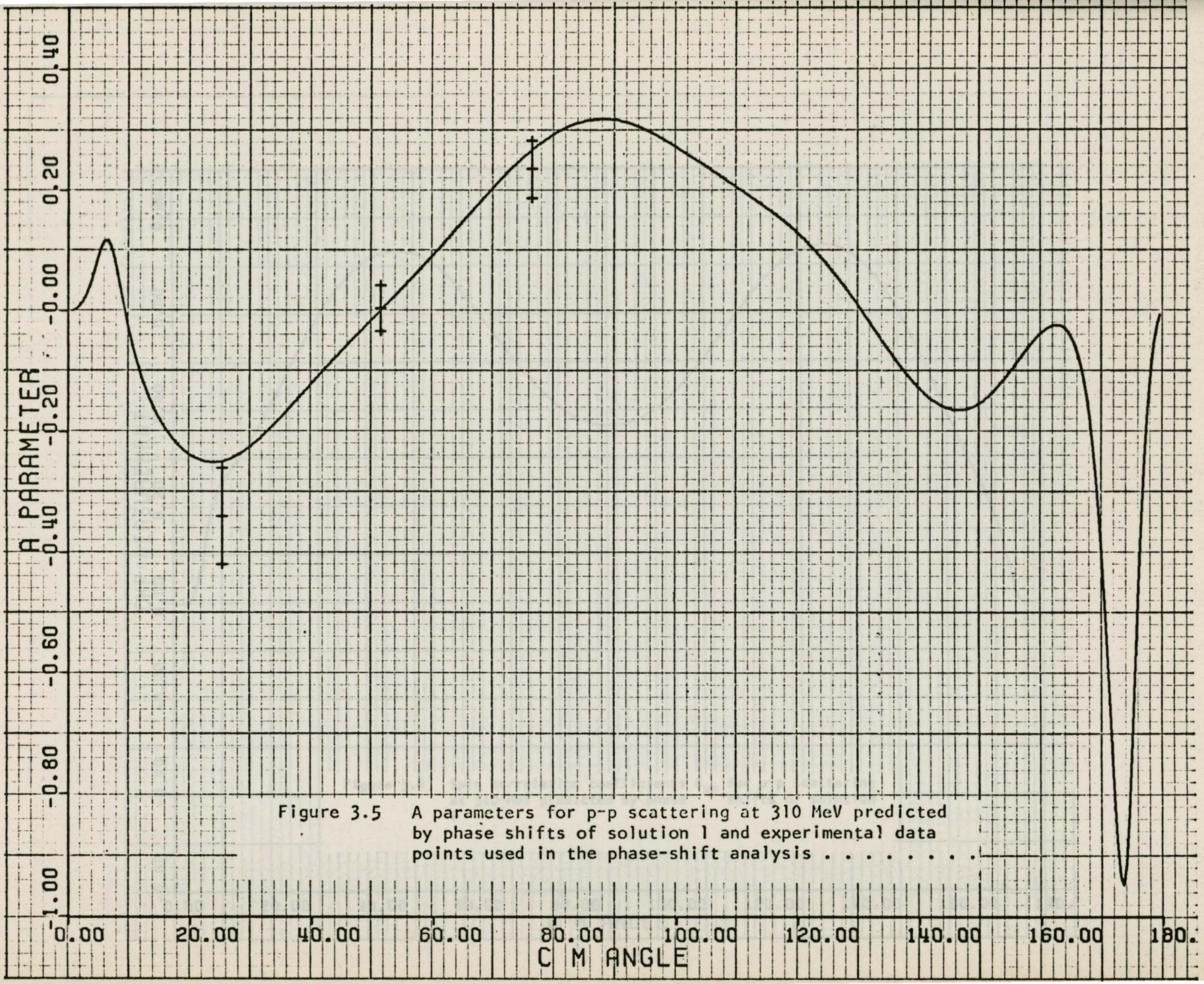

Figure 3.5 A parameters for p-p scattering at 310 MeV predicted by phase shifts of solution 1 and experimental data points used in the phase-shift analysis . . . . . .

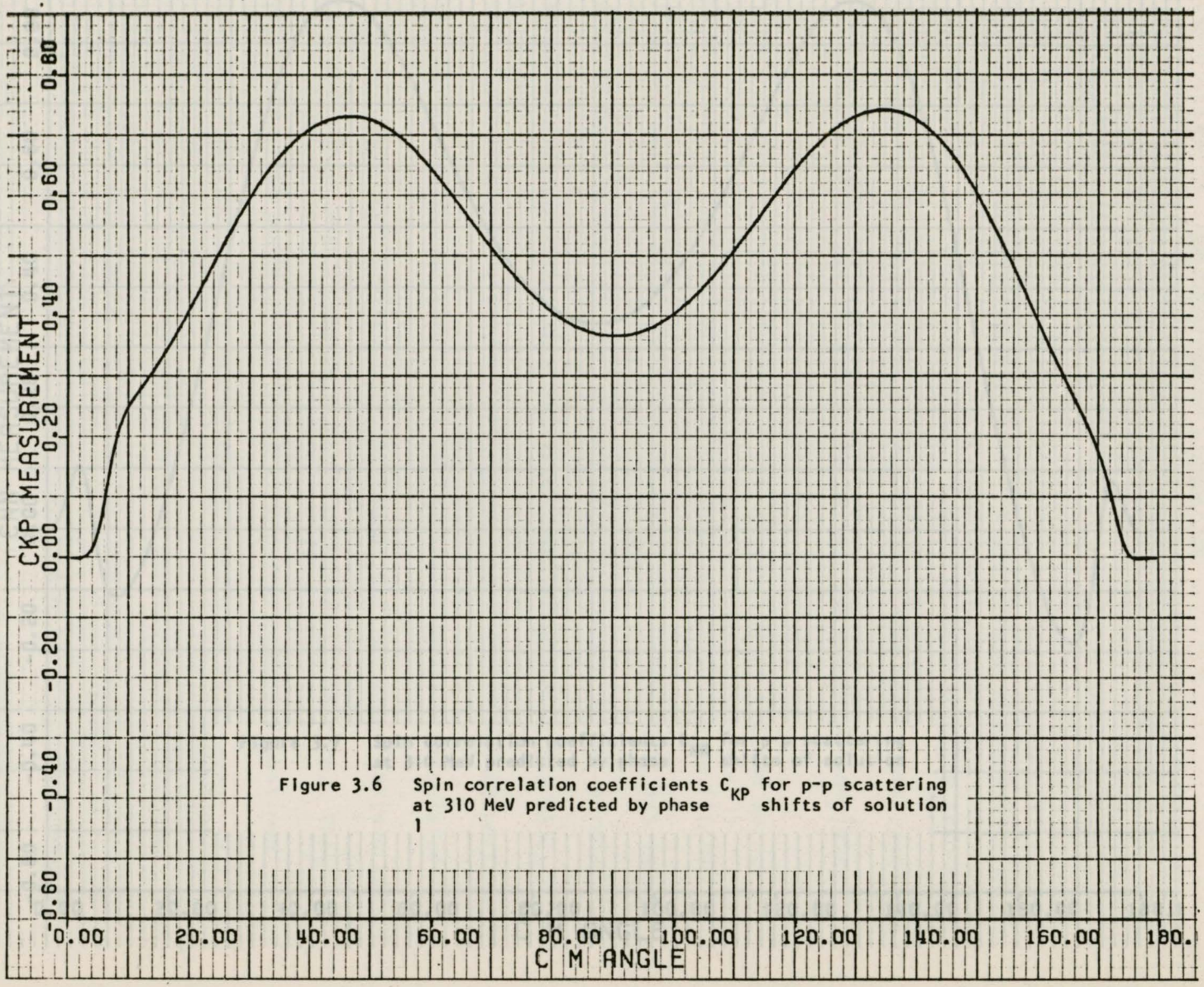

Figure 3.6 Spin correlation coefficients C_{KP} for p-p scattering at 310 MeV predicted by phase shifts of solution 1

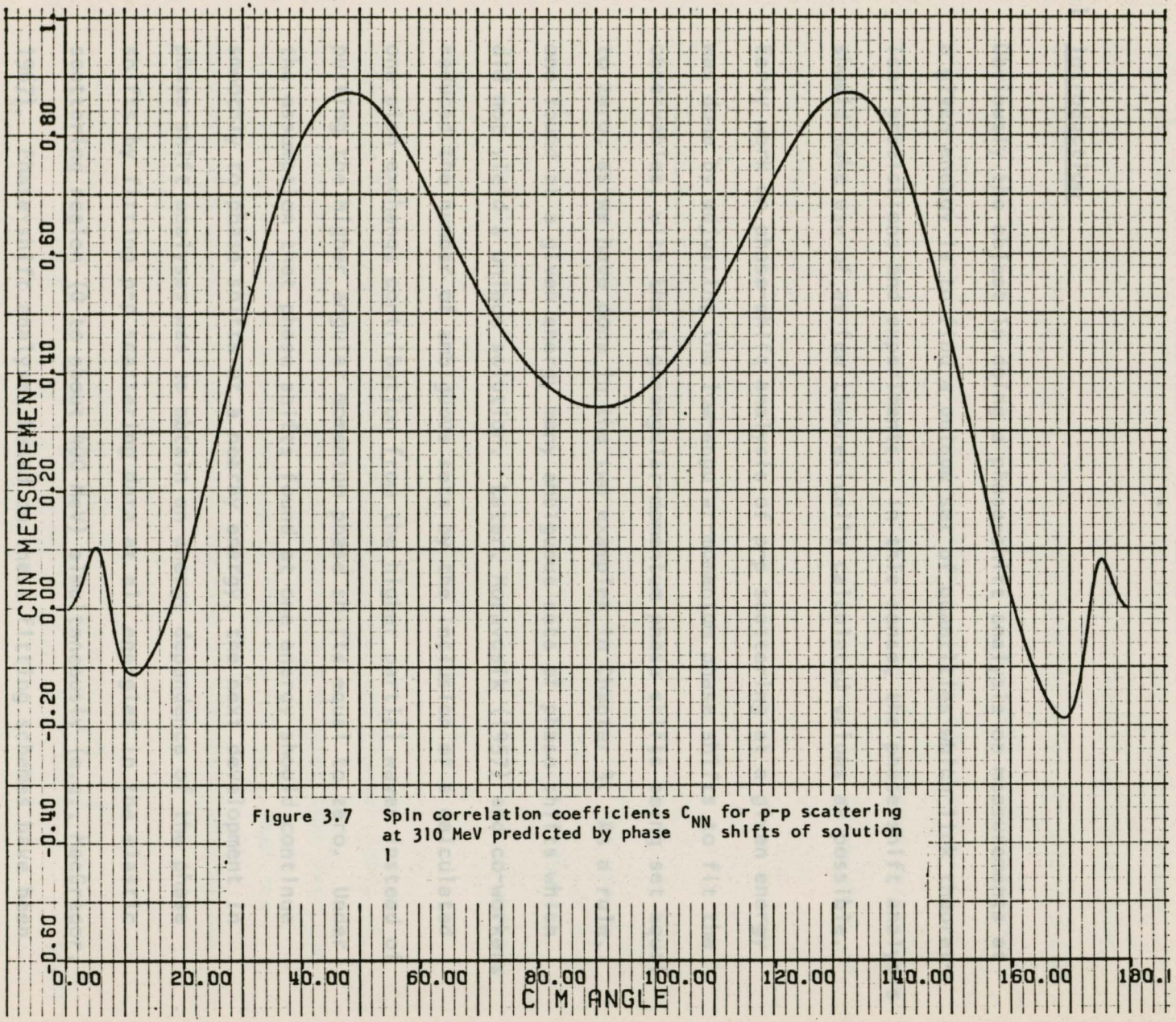

Figure 3.7 Spin correlation coefficients C_{NN} for p-p scattering at 310 MeV predicted by phase shifts of solution 1

Chapter 4
CALCULATION OF ACCURACIES

4.1 Introduction

Obviously the object in doing a phase-shift analysis on measurements at a given energy is to find a unique set of quantities which link theoretical predictions and experiments. In this sense, the phase-shift analysis should make use of as few theoretically calculated values as possible.

Early work on phase-shift analysis of p-p scattering at a given energy was done by adjusting the low-angular-momentum phase shifts to fit the observables, with the high-angular-momentum phase shifts being set equal to zero, as we have done in the two examples in Chapter 3. As a rule, one found at a given energy many ambiguous sets of phase shifts which did not yield a unique solution. Later, Moravcsik (1957) and co-workers reduced the number of ambiguous sets by the inclusion of a calculated one-pion-exchange contribution from the higher partial waves instead of putting the higher angular momentum phase shifts equal to zero. Under the assumption that phase shifts found at one energy should continue smoothly to phase shifts at a nearby energy, the next development in phase-shift analyses was to obtain an energy dependence of the phase shifts by fitting p-p scattering data at all energies in the elastic scattering region (0 to about 400 MeV) simultaneously (e.g., MacGregor, 1967). Phase-shift analyses based on these fitting schemes have been carried out extensively in the past fourteen years.

This considerable activity in the past decade may lead to the conclusion that the data are now complete enough to definitely choose a unique solution and to define quite accurately the scattering amplitudes over the whole elastic energy range. But the presently existing unique phase-shift solutions at various energies are really a result of both theory and experimental measurements, rather than a result of experimental measurements alone. It seems more likely that detailed elastic scattering experiments at various energies will be necessary for the improvement of present phase shifts.

4.2 Studies of p-p scattering at 310 MeV

In an attempt to choose the more sensitive experiments for the determination of a more precise set of phase shifts for p-p scattering at 310 MeV, the effects of the uncertainties in the present "unique" phase shifts on the physical quantities have been investigated.

According to statistical theory (MacGregor, 1968 and Plummer 1967) if all the diagonal elements of the error matrix are greater than zero (in fact, the error matrix is not defined if they are not so), then the accuracy of a quantity A, which is a function of the phase shifts, can be calculated from

$$(\Delta A)_{RMS} = \left| \sum_{i}^{N} \sum_{j}^{N} \frac{\partial A}{\partial a_i} \cdot \frac{\partial A}{\partial a_j} (G^{-1})_{ij} \right| \qquad (4.1)$$

where $a_1, a_2, a_3 \ldots\ldots a_N$ are the N phase shifts and G^{-1} is the error matrix. Using this result, the accuracies of the seven different

measurements predicted by the type 1 solution obtained in the previous chapter are evaluated for every 0.5° between 6° and 174° for differential cross section results and between 0° and 180° for the rest. All angles are in the center-of-mass system. These accuracies and calculated values for the physical quantities are shown in figures 4.1 to 4.7 along with the experimental data used in the fits of chapter 3.

These accuracies were then compared with accuracies obtained from a comparable 330 MeV fit as discussed below.

In Chapter 3, the 35 p-p scattering measurements used in the analysis did show some incompleteness through the existence of 5 ambiguous solutions. The type 1 solution is believed to be the correct solution. However, in order to avoid the possibility that the result corresponds to a solution ending in an incorrect local minimum on the χ^2 (δ) surface, the error matrix for the solution at 330 MeV (Table 4.1) given by MacGregor *et al.* (1968), after their analysis of 122 data points at energies centered on 330 MeV, has also been used to predict the accuracies. Results of these evaluations are shown in figures 4.8 to 4.14 along with the experimental errors of the measurements used. The experimental errors shown in the figures had been renormalized as suggested (MacGregor, 1968). Both exact energies and "year of measurement" are also shown on the figures.

In the total of 122 data points there are combinations of several selected sets of measurements from different sources. These sets were selected because they were shown to be more compatible with each other. In the selected sets, only data points within three standard deviations

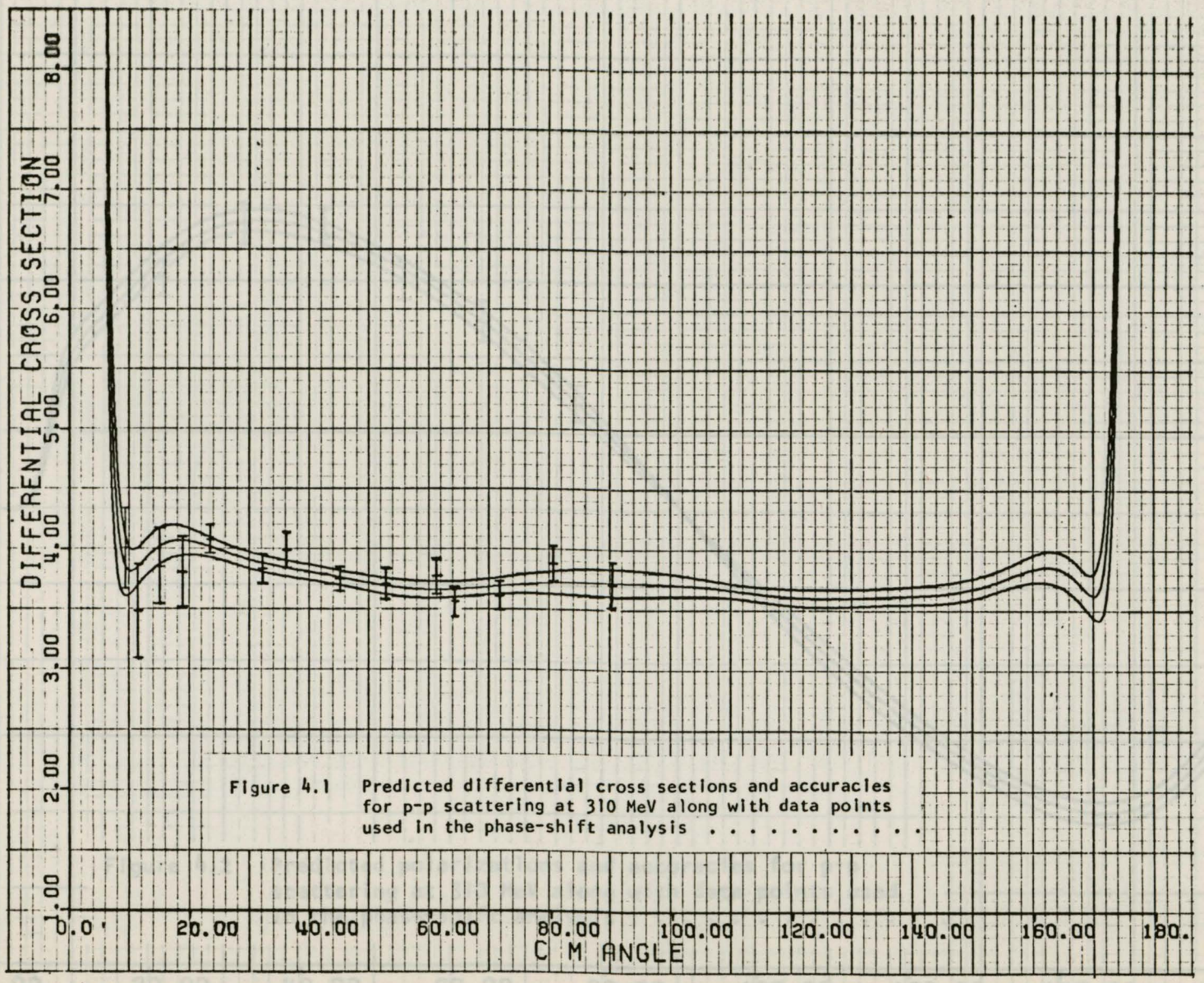

Figure 4.1 Predicted differential cross sections and accuracies for p-p scattering at 310 MeV along with data points used in the phase-shift analysis . . . . . .

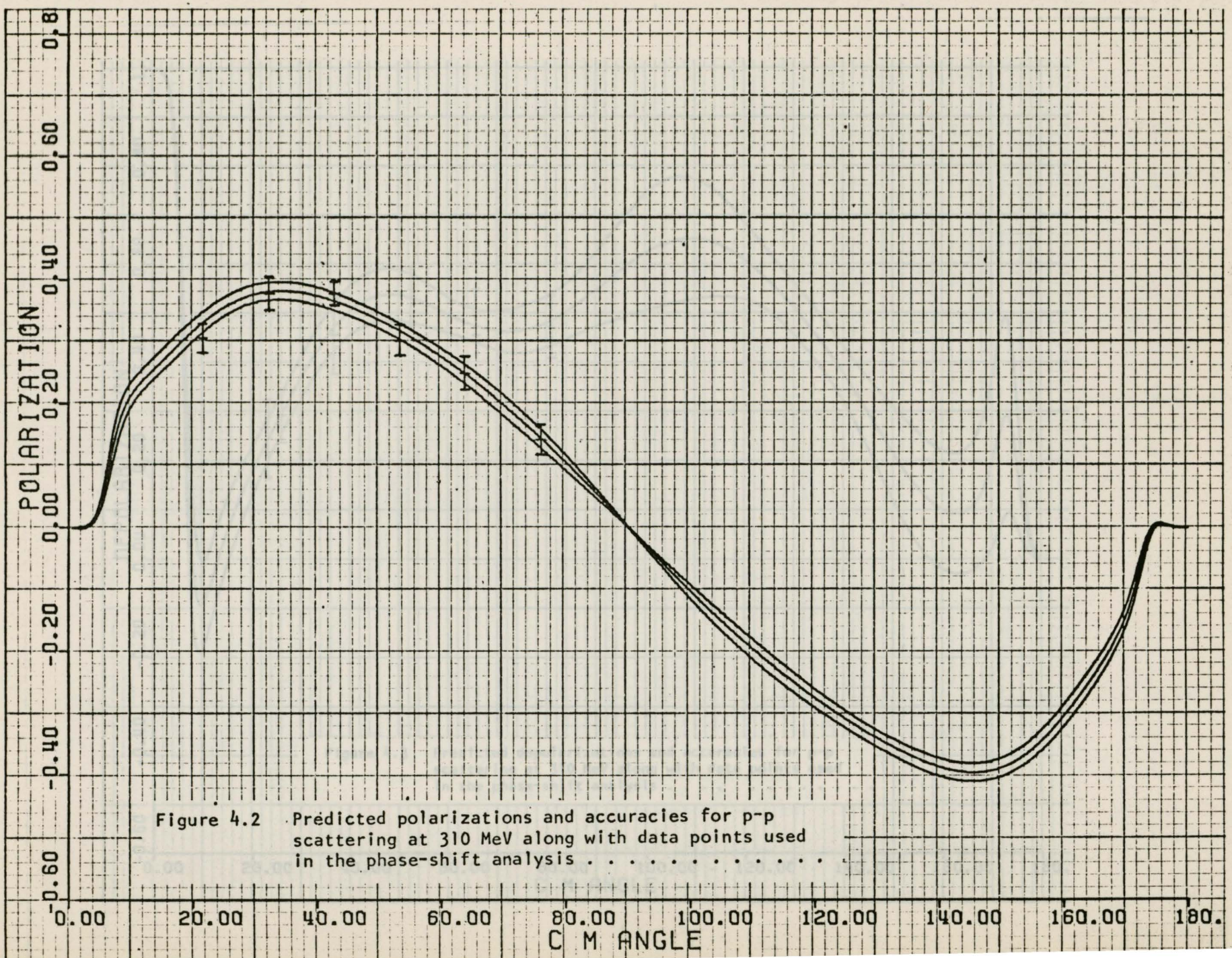

Figure 4.2 Predicted polarizations and accuracies for p-p scattering at 310 MeV along with data points used in the phase-shift analysis . . . . . .

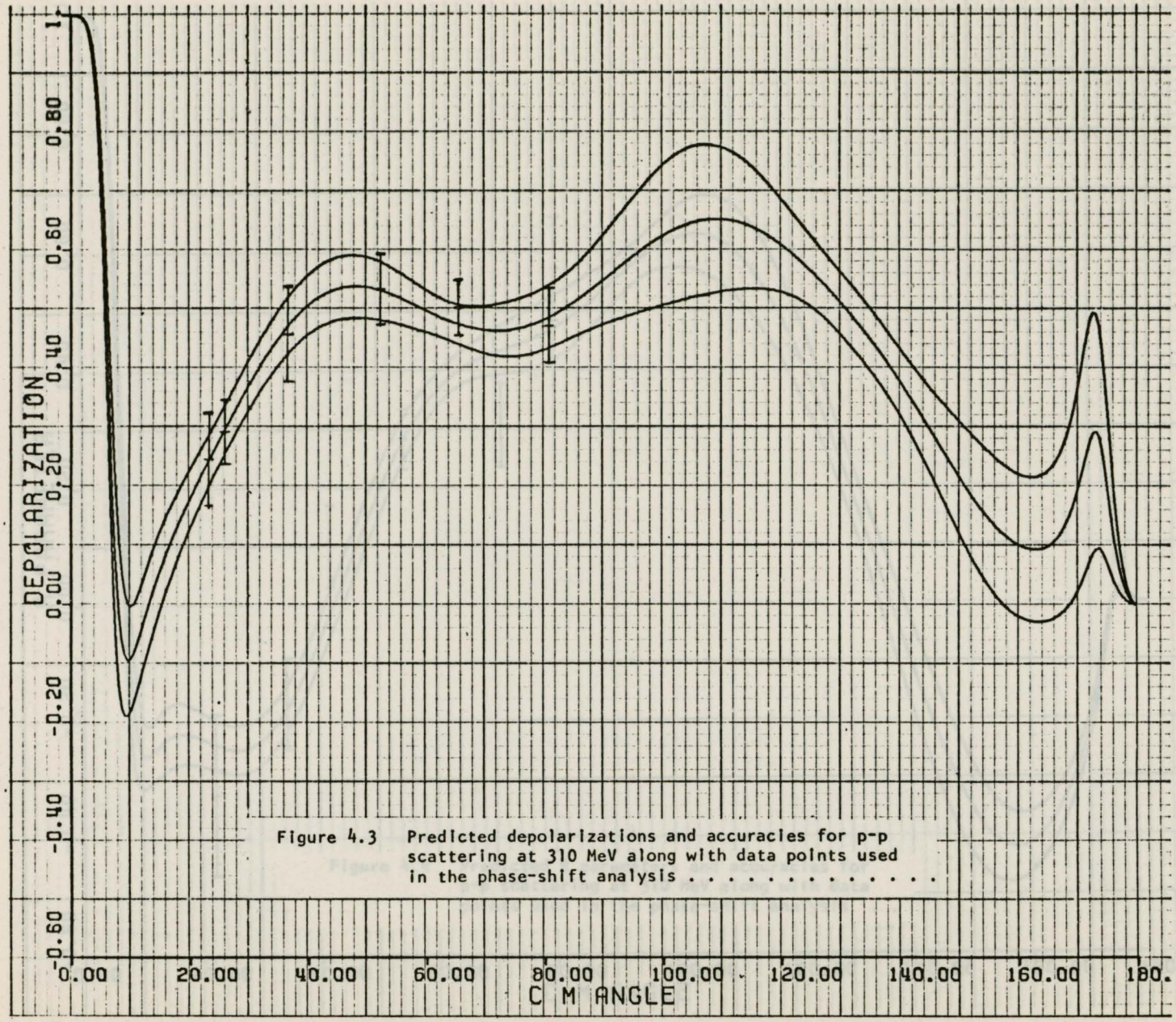

Figure 4.3 Predicted depolarizations and accuracies for p-p scattering at 310 MeV along with data points used in the phase-shift analysis . . . . . .

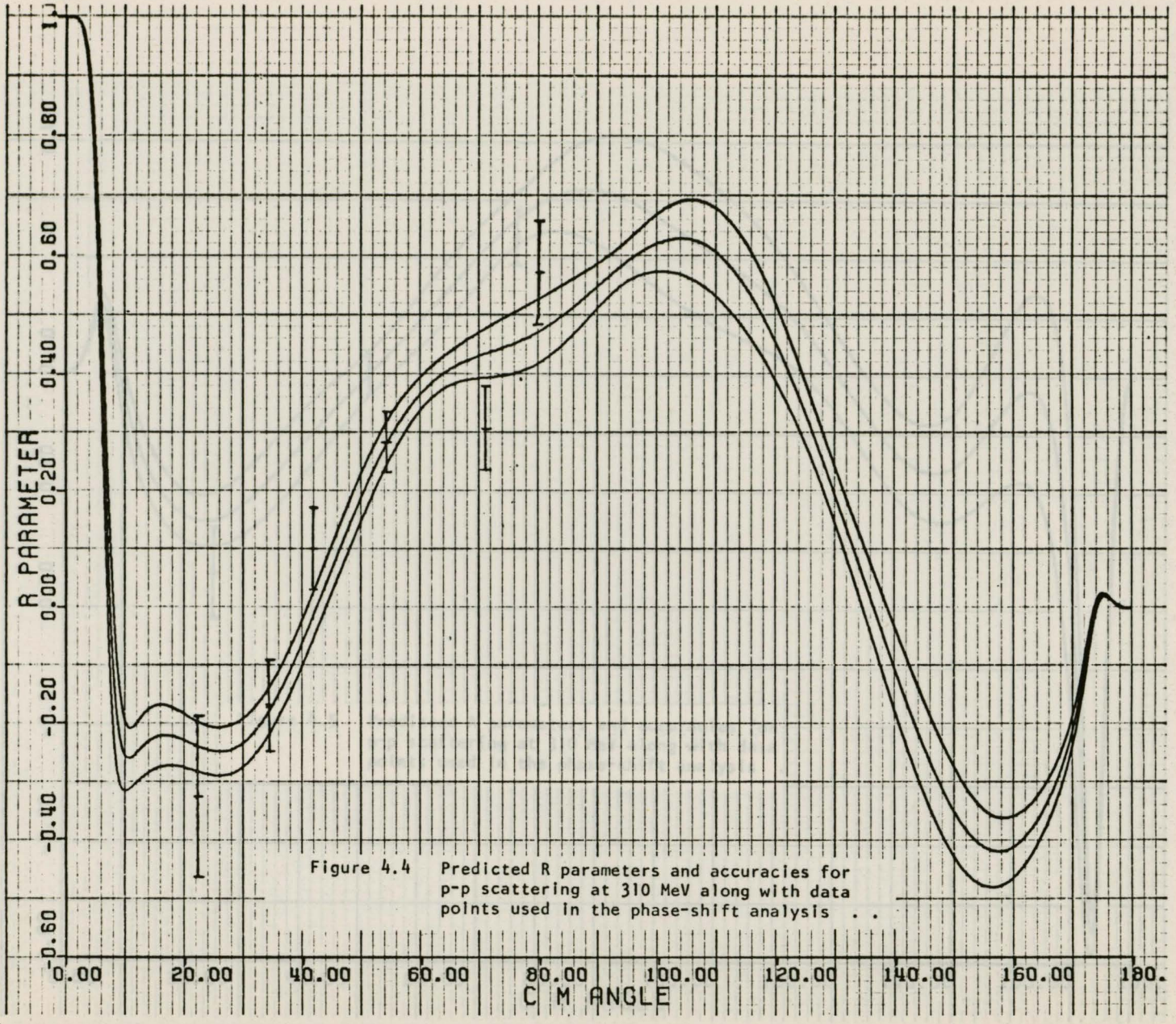

Figure 4.4 Predicted R parameters and accuracies for p-p scattering at 310 MeV along with data points used in the phase-shift analysis . .

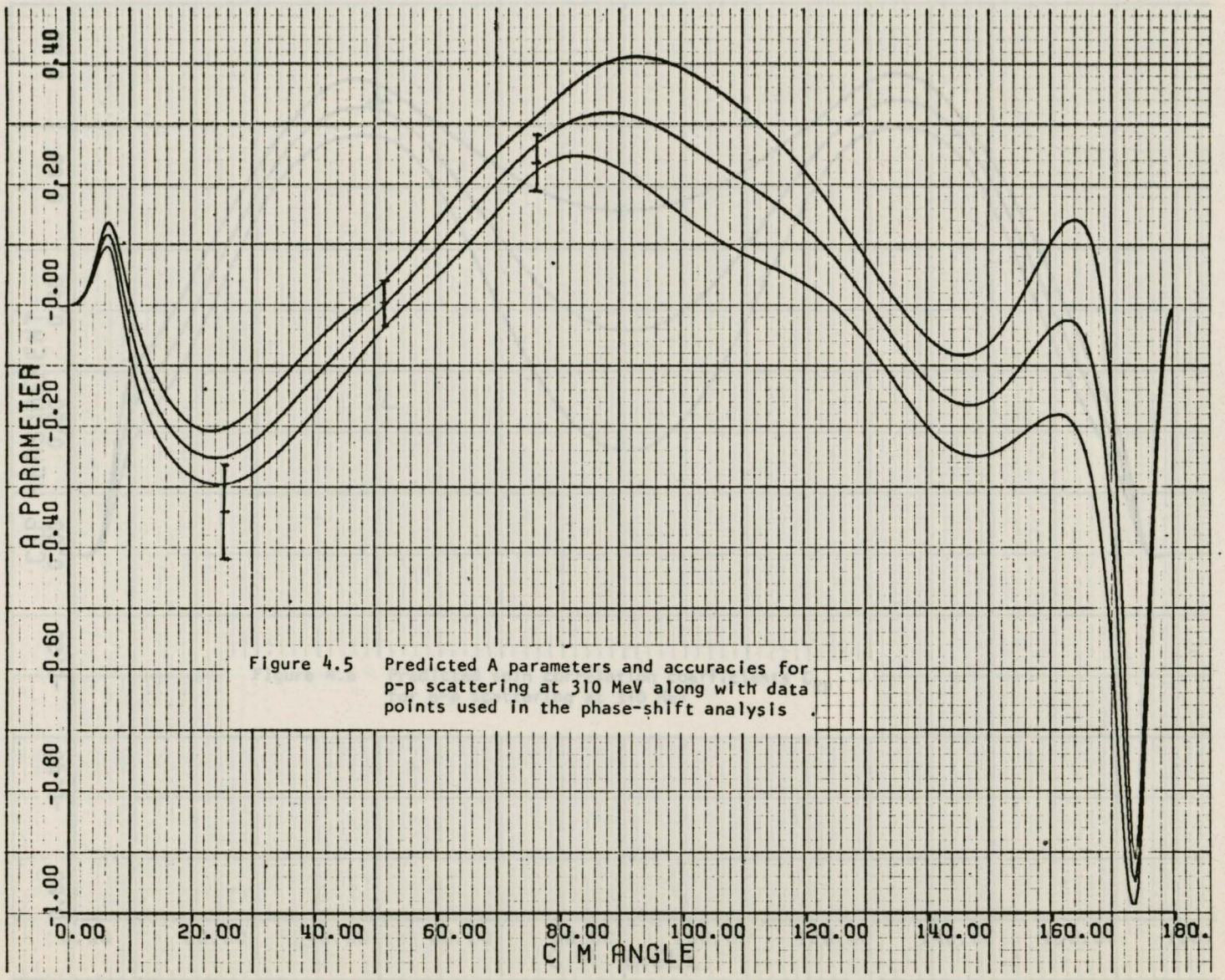

Figure 4.5 Predicted A parameters and accuracies for p-p scattering at 310 MeV along with data points used in the phase-shift analysis .

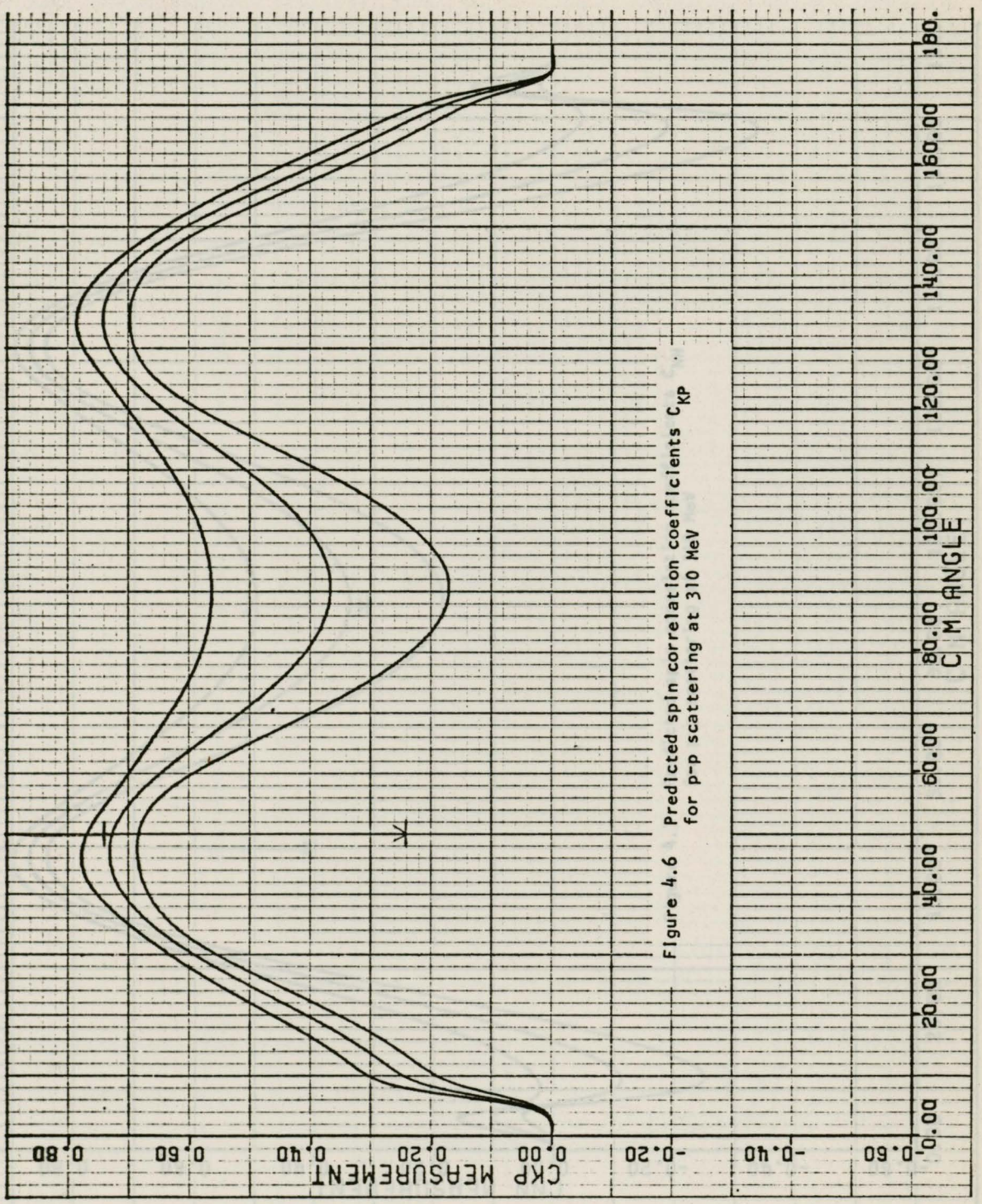

Figure 4.6 Predicted spin correlation coefficients C_{KP} for p-p scattering at 310 MeV

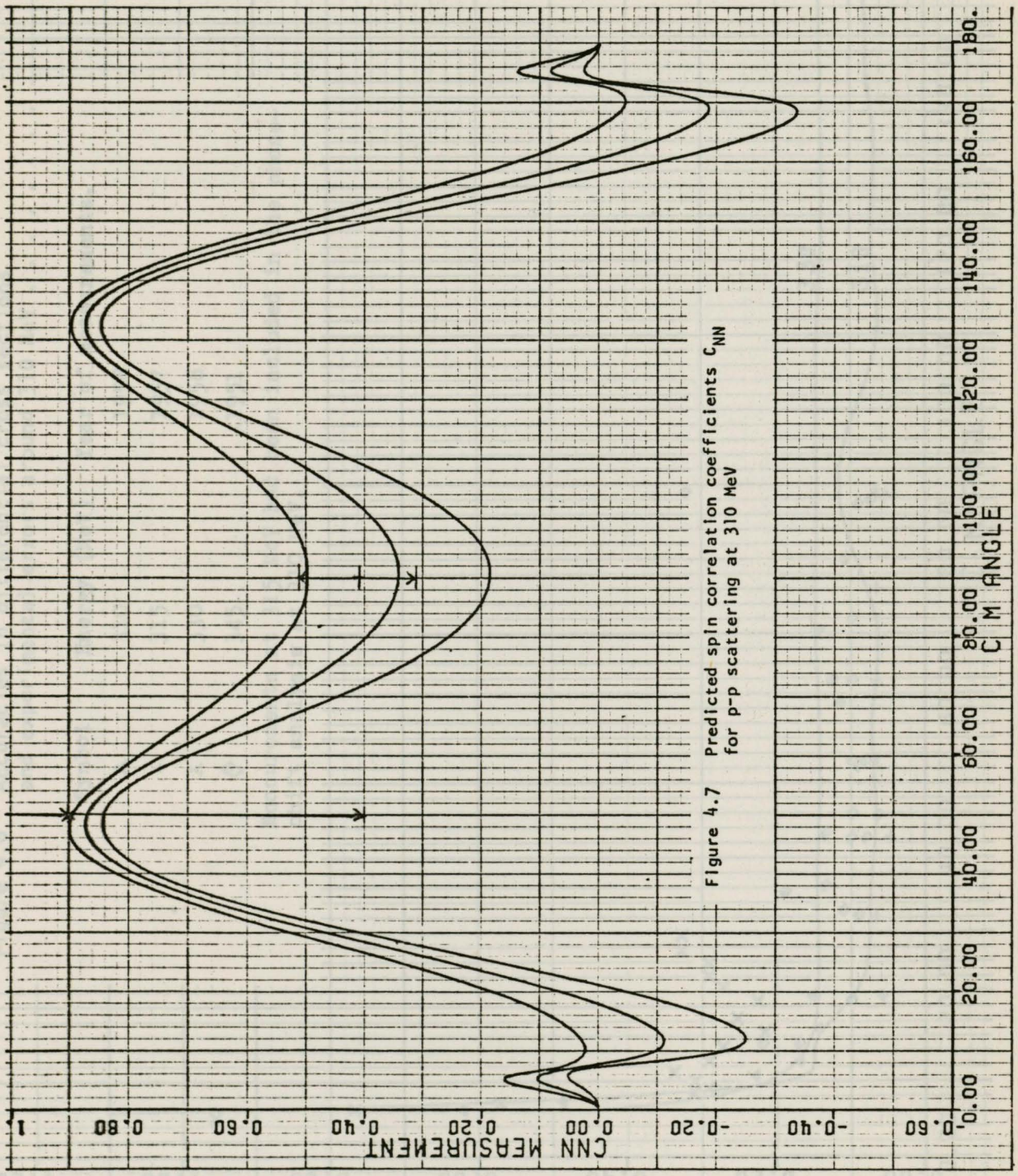

Figure 4.7 Predicted spin correlation coefficients C_{NN} for p-p scattering at 310 MeV

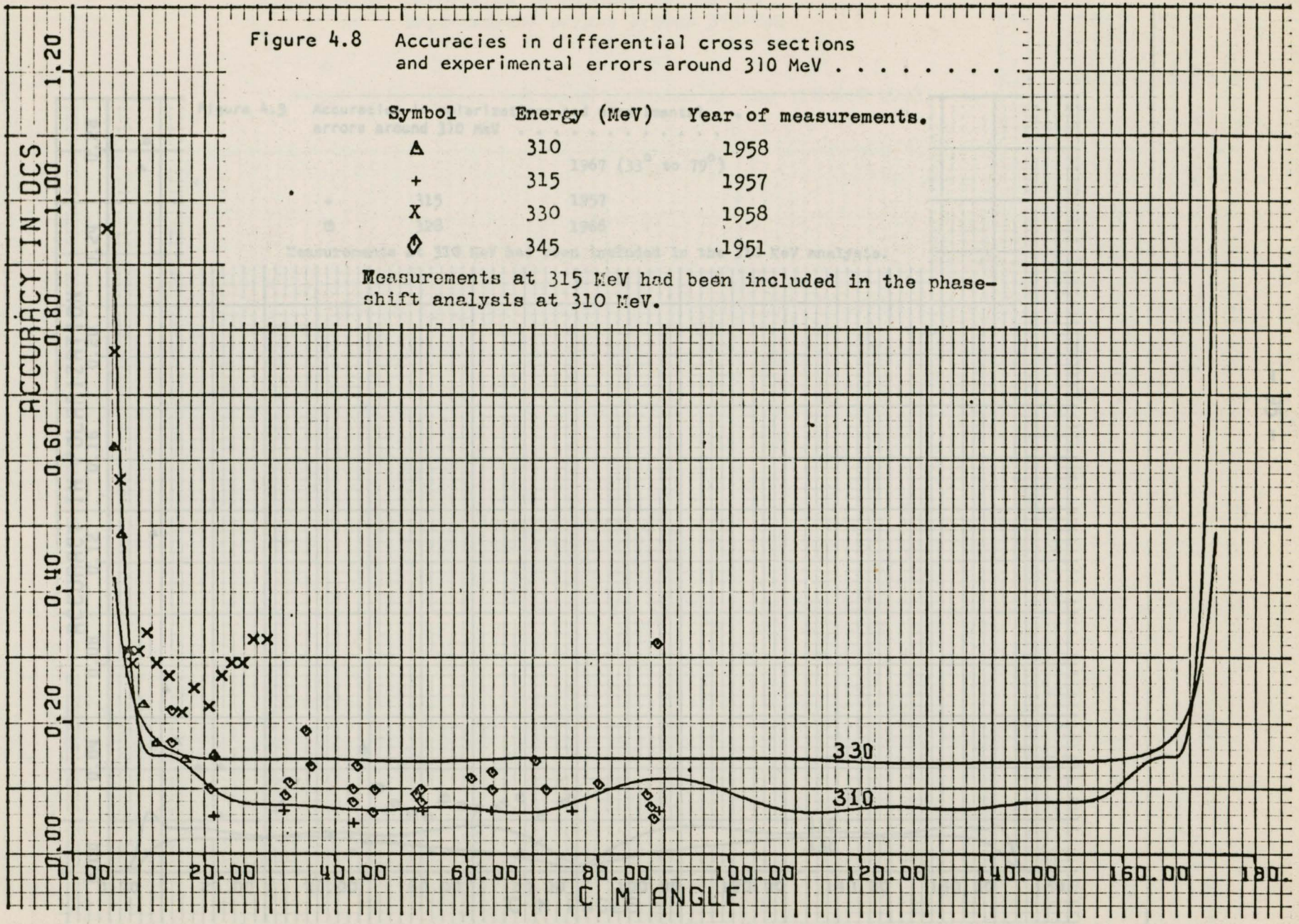

Figure 4.8 Accuracies in differential cross sections and experimental errors around 310 MeV . . . . . .

Symbol	Energy (MeV)	Year of measurements.
Δ	310	1958
+	315	1957
X	330	1958
◊	345	1951

Measurements at 315 MeV had been included in the phase-shift analysis at 310 MeV.

Figure 4.9 Accuracies in polarizations and experimental errors around 310 MeV . . . . . .

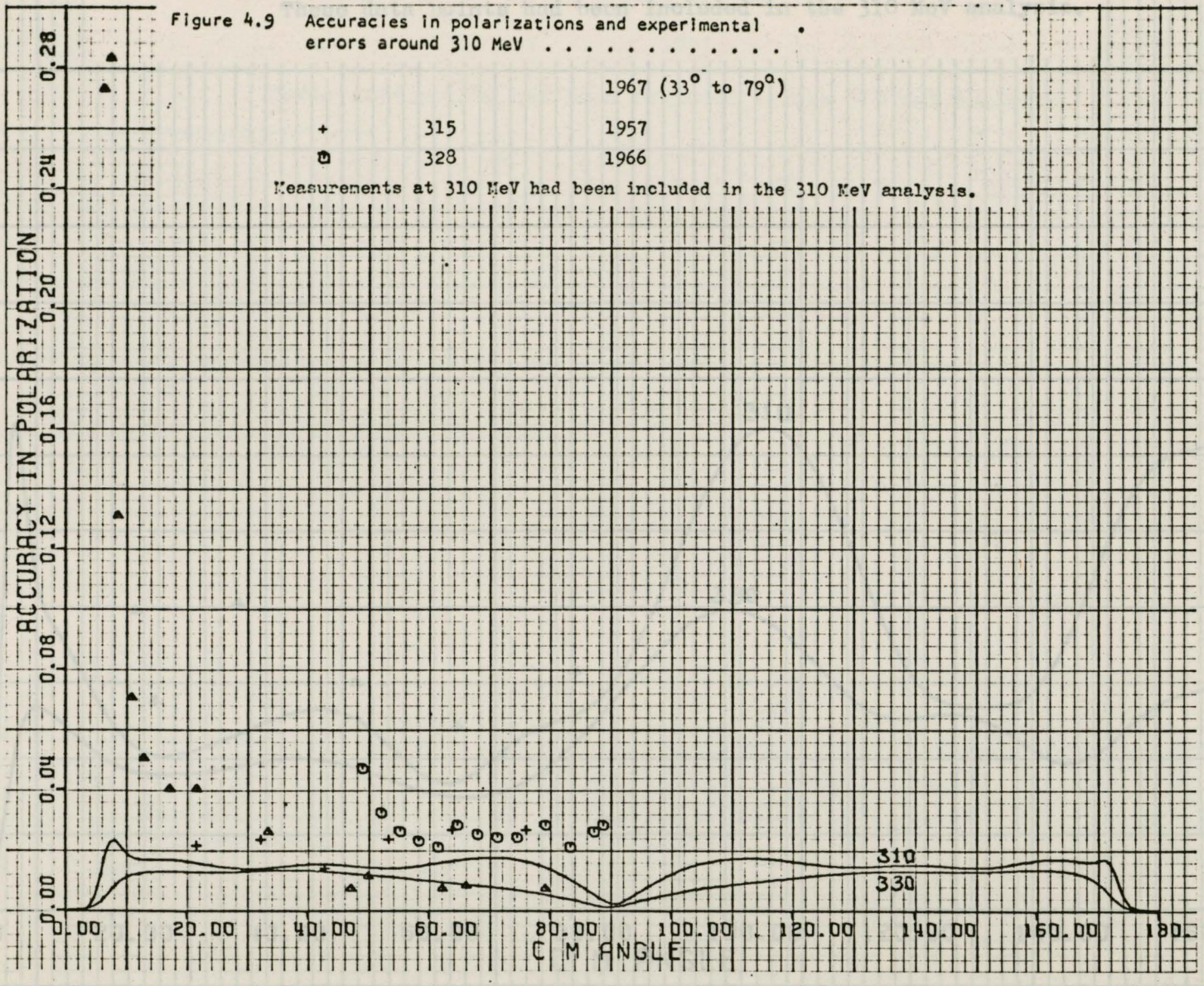

Figure 4.10 Accuracies in depolarization and experimental errors around 310 MeV .

▲ 310 1957

These data points had been included in the 310 MeV analysis.

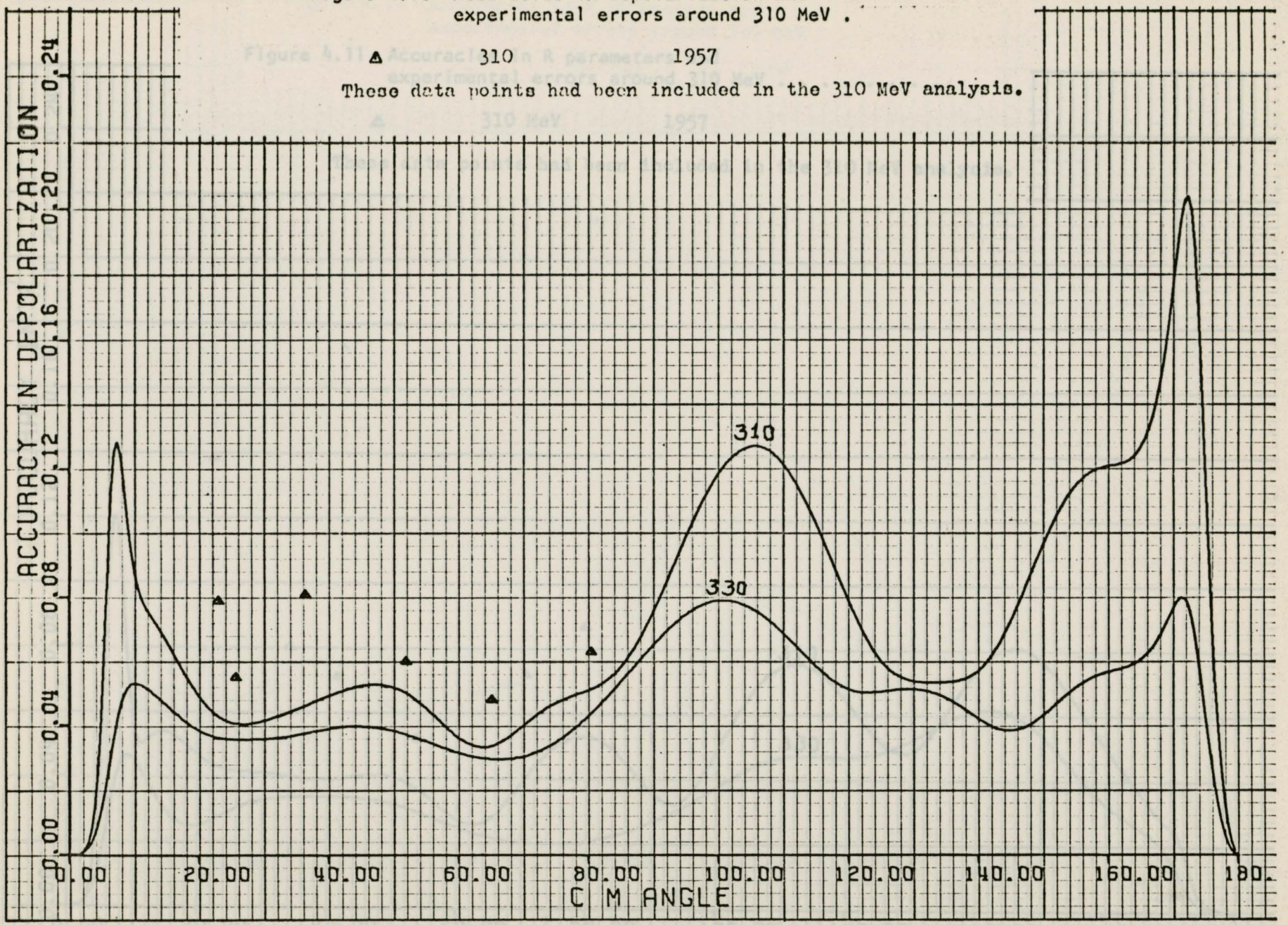

Figure 4.11 Accuracies in R parameters and
experimental errors around 310 MeV . . . . . .

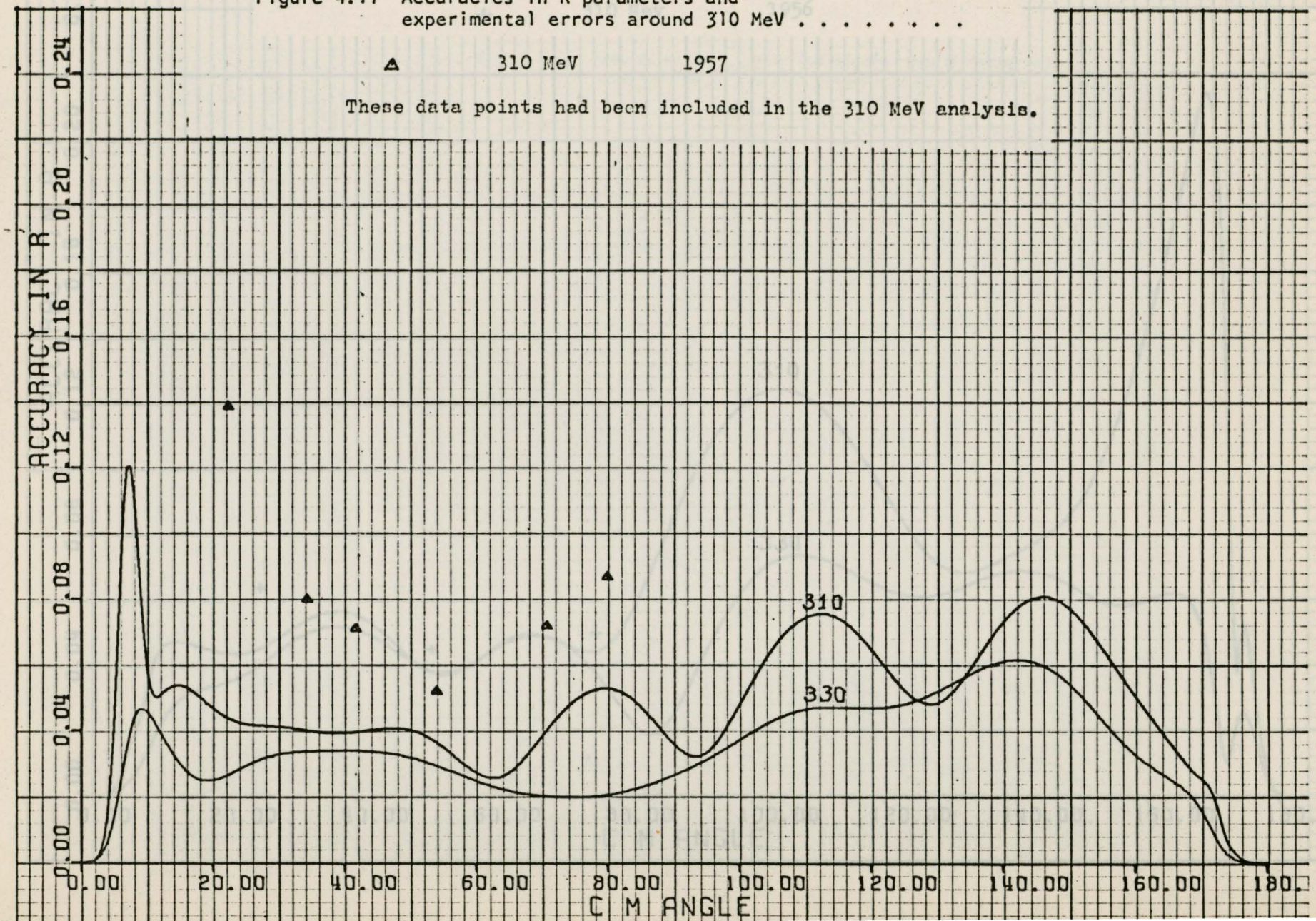

Figure 4.12 Accuracies in A parameters and experimental errors around 310 MeV . . . . . .

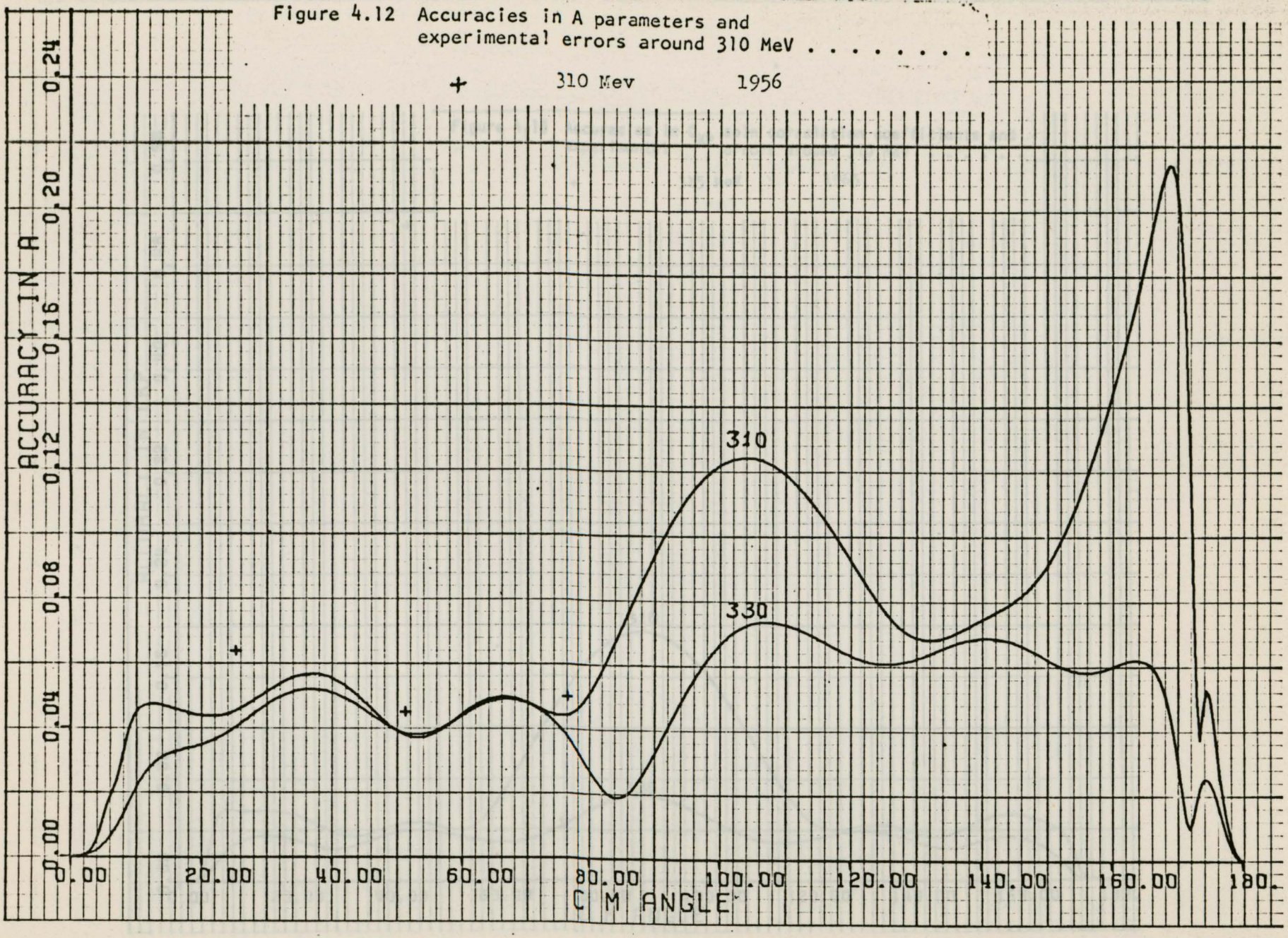

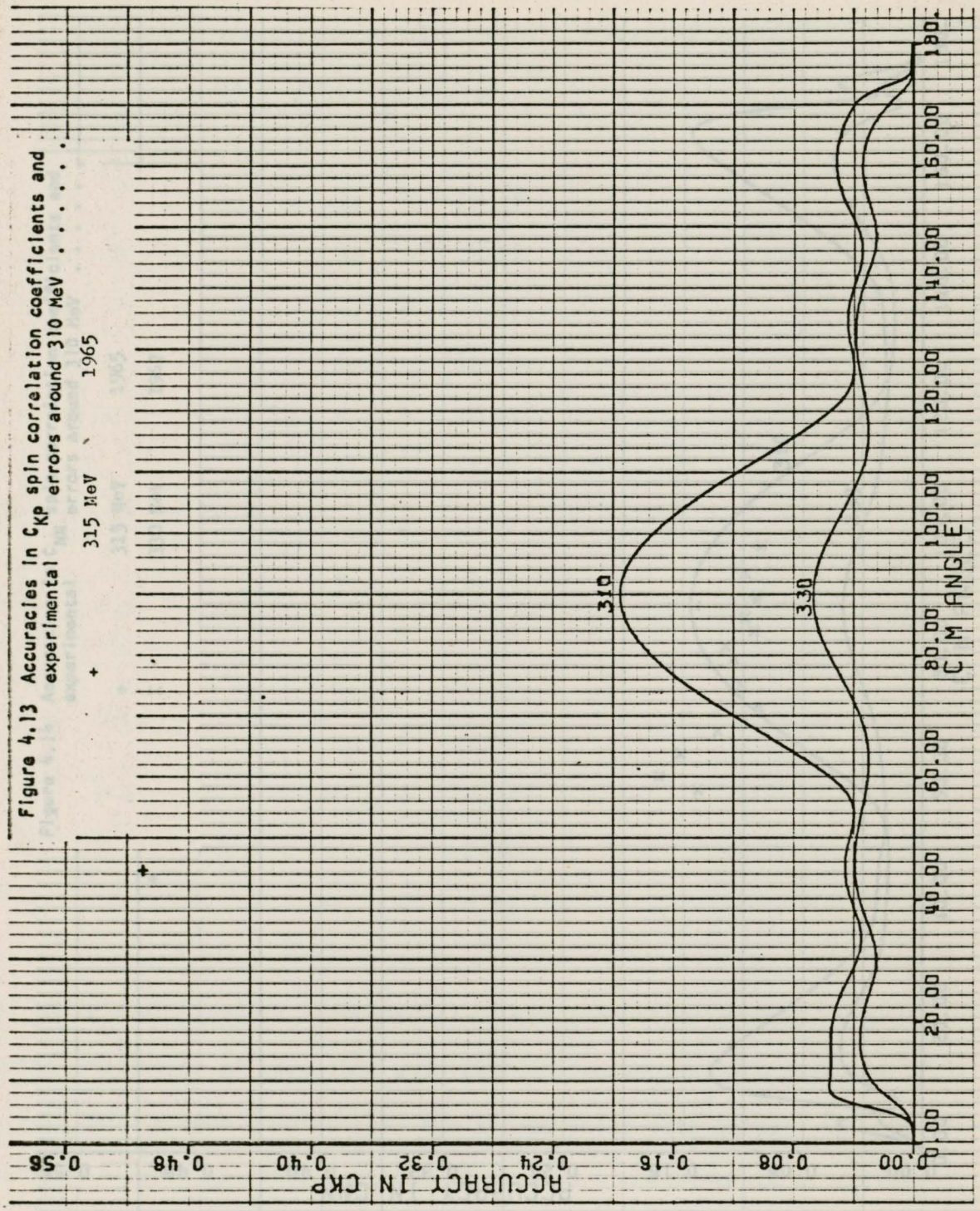

Figure 4.13 Accuracies in C_{KP} spin correlation coefficients and experimental C_{KP} errors around 310 MeV . . . . . .

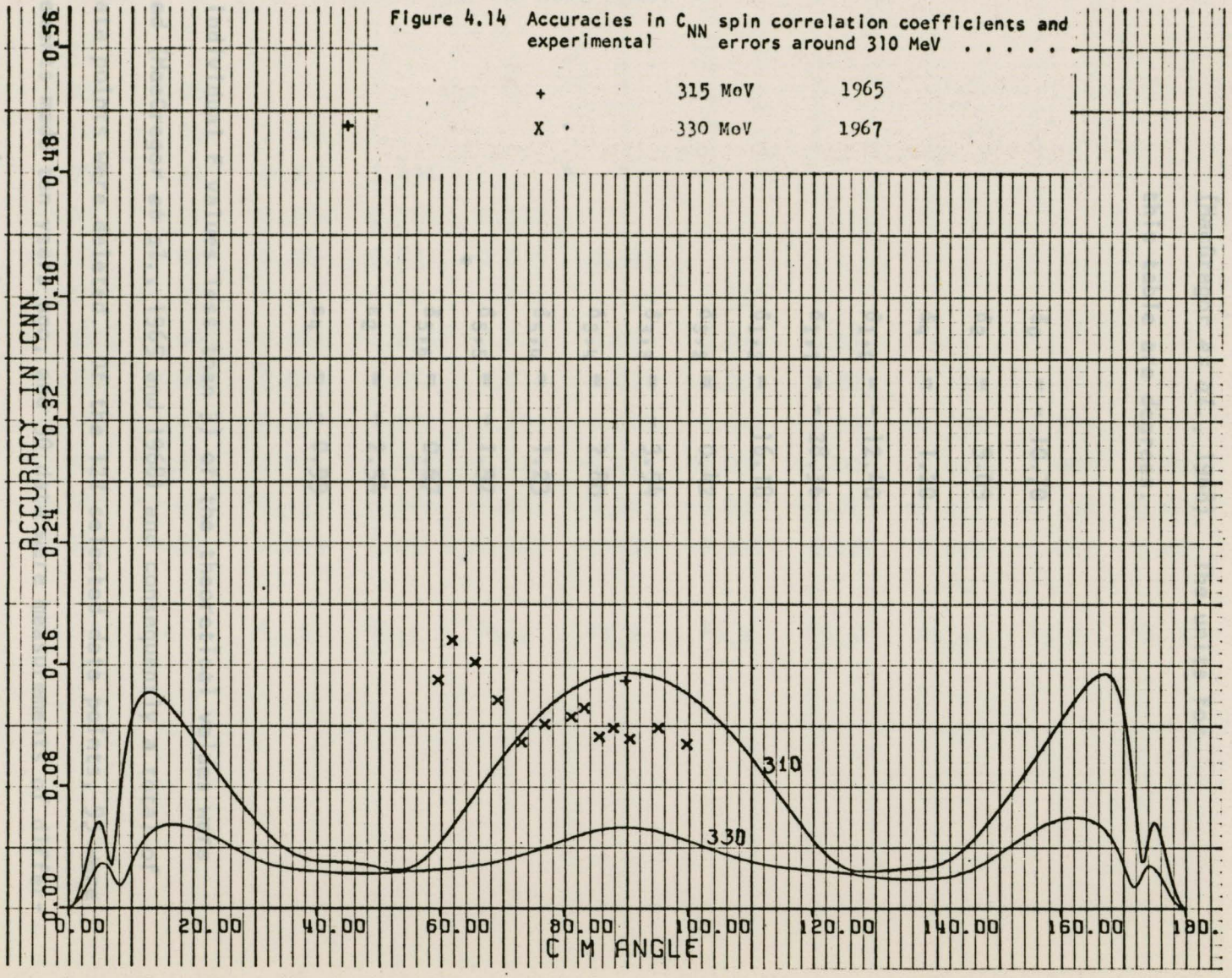

Figure 4.14 Accuracies in C_{NN} spin correlation coefficients and experimental errors around 310 MeV . . . . .

+	315 MeV	1965
X	330 MeV	1967

Table 4.1. Phase shifts for p-p scattering at 330 MeV (MacGregor *et al.*, 1968). The units for this table are degrees.

δ_0	- 10.70
δ_2	9.09
δ_4	1.20
$\delta_{1,0}$	- 12.40
$\delta_{1,1}$	- 28.36
$\delta_{1,2}$	16.18
$\delta_{3,2}$	0.42
$\delta_{3,3}$	- 3.54
$\delta_{3,4}$	2.80
$\delta_{5,4}$	1.23
$\delta_{5,5}$	- 1.92
$\delta_{5,6}$	0.67
ε_2	- 2.54
ε_4	- 0.99

(i.e. individual F values less than 3) of the theoretical values were selected (MacGregor *et al.*, 1965 and 1968) and consequently a total of nine data points were deleted. Of the 122 selected data points, 93 were measurements made ten years ago, and 90 data were measurements of differential cross section or polarization.

The accuracies calculated from the two different error matrices agree fairly well in shape. The accuracies of all physical quantities, except

Table 4.2. Error matrix in degree^2 for p-p scattering at 330 MeV (MacGregor *et al.*, 1968)

2.125													
-0.033	0.271												
-0.093	-0.034	0.061											
0.286	-0.128	-0.002	2.451										
-0.511	0.050	0.111	0.097	1.436									
-0.117	-0.009	0.024	0.310	0.164	0.317								
0.010	-0.032	0.013	-0.485	-0.033	-0.019	0.319							
0.447	-0.039	-0.020	0.534	-0.287	-0.036	-0.139	0.368						
-0.032	-0.032	-0.005	-0.084	-0.055	-0.024	0.073	0.011	0.059					
-0.159	-0.058	0.004	0.079	0.052	0.017	-0.024	-0.003	0.024	0.112				
0.085	0.125	-0.017	-0.301	0.032	-0.107	-0.009	-0.112	-0.053	-0.105	0.271			
-0.097	-0.024	0.016	-0.044	0.052	-0.017	-0.011	-0.030	-0.002	0.029	0.003	0.025		
-0.063	0.086	-0.017	-0.139	0.124	-0.047	0.003	-0.034	-0.029	-0.077	0.137	-0.013	0.192	
-0.125	-0.083	0.002	0.019	0.031	-0.001	-0.024	-0.028	0.025	0.070	-0.047	0.021	-0.046	0.085
δ_0	δ_2	δ_4	$\delta_{1,0}$	$\delta_{1,1}$	$\delta_{1,2}$	$\delta_{3,2}$	$\delta_{3,3}$	$\delta_{3,4}$	$\delta_{5,4}$	$\delta_{5,5}$	$\delta_{5,6}$	ε_2	ε_4

for differential cross section determined from MacGregor's error matrix, are relatively higher than those calculated from the error matrix described in Chapter 3. This is because, firstly, more measurements of differential cross section and polarization had been used in their analysis to reduce the uncertainties in phase shifts. Secondly, the introduction of the one-pion-exchange-contribution has reduced the uncertainties in certain phase shifts (MacGregor *et al.*, 1965). Thirdly, the error matrix provided for the solution at 330 MeV does not include elements corresponding to the pion-nucleon coupling constant. Neglect of the uncertainty in the normalization constant results in better calculated accuracies.

For the case of differential cross sections, the accuracies of measurements at 310 MeV are better than at 330 MeV. This is a reflection of the fact that the differential cross sections were more precisely measured at 310 MeV over the angular range from 20° to 90°.

The experimental errors in measurements other than differential cross section and polarization are relatively large in comparison with the calculated accuracies from the solution at 330 MeV. In other words, the uncertainties in the phase shifts are strongly dominated by the measurements of differential cross section and polarization rather than the other types of measurements. Using more measurements of differential cross section and polarization in the phase-shift analysis at 330 MeV reduces the weight of the other types of measurements in the determination of the error matrix.

The experimental errors of measurements made later than 1957 agree fairly well with the accuracies calculated from the error matrix for the solution at 310 MeV, except for the spin correlation C_{KP} which is very poor. The set of data points at 310 MeV used in the phase-shift analysis in Chapter 3 is not complete enough to determine a unique solution; however, we see from Fig. 4.8 to Fig. 4.15 that the curves for 310 MeV and 330 MeV agree well in shape; hence we believe that the type 1 solution and the corresponding error matrix make a very reasonable prediction of accuracies.

4.3 Summary

Estimation of the experimental accuracies in new data necessary to improve phase shift solutions at 310 MeV have been based on the accuracies for the various scattering parameters calculated from the present phase shift analysis.

For convenience, we define a standard accuracy for a quantity A in the angular range between θ_1 and θ_2 as

$$p(\theta_i, \theta_j) = \left[\frac{1}{N} \sum_{i=1}^{N} (\Delta A_i)^2_{calc.} \right]^{1/2} \qquad (4.2)$$

where $(\Delta A_i)_{calc.}$ is the calculated accuracy from equation (4.1) at the angle θ_i which is in the range defined by θ_1 and θ_2. The index i runs over all the data points in the angular range. In this case points are calculated every 0.5 degree.

Employing this definition we list the calculated standard accuracies for p-p scattering parameters at 310 MeV in several angular ranges as follows.

1) For the measurements of cross section the standard accuracy for the angular range between
   i) 6.5° and 10° is 0.5 mb/sr,
   ii) 10° and 20° is 0.14 mb/sr,
   iii) 20° and 90° is 0.08 mb/sr.
2) For polarization measurements the standard accuracy for the angular range between 2° and 90° is 0.015.
3) For the depolarization measurements, the standard accuracy for the angular range between
   i) 0.5° and 8° is 0.067,
   ii) 8° and 20° is 0.076,
   iii) 20° and 30° is 0.043,
   iv) 30° and 90° is 0.048,
   v) 90° and 120° is 0.109.
4) For the measurements of the R parameter the standard accuracy for the angular range between
   i) 10° and 20° is 0.052,
   ii) 20° and 50° is 0.041,
   iii) 50° and 90° is 0.041,
   iv) 90° and 120° is 0.060.
5) For the measurements of the A parameter the standard accuracy for the angular range between
   i) 10° and 20° is 0.046,
   ii) 20° and 40° is 0.051,
   iii) 40° and 60° is 0.044,
   iv) 60° and 80° is 0.047,
   v) 80° and 90° is 0.073,
   vi) 90° and 100° is 0.117.

6) For the measurements of the spin correlation coefficient C_{KP} the standard accuracy in the angular range between

   i) 2° and 10° is 0.037,

   ii) 10° and 30° is 0.051,

   iii) 30° and 70° is 0.0572,

   iv) 70° and 120° is 0.157.

7) For the measurements of the spin correlation coefficient C_{NN} the standard accuracy in the angular range between

   i) 0.5° and 10° is 0.058,

   ii) 10° and 30° is 0.110,

   iii) 30° and 70° is 0.048,

   iv) 70° and 110° is 0.137.

These sets of standard accuracies serve as a reference for the required precision in the measurements in order to have new measurements play the same important roles as differential cross section and polarization measurements in the determination of the errors of the phase shifts.

Chapter 5

DISCUSSION AND CONCLUSIONS

Due to the advancement of the technology of particle accelerators in the past few years, proton beams with less contamination, better energy resolution, and better focusing will be available in the near future. As a consequence, there will be less technical difficulty in carrying out measurements of differential cross section and polarization with required accuracies at facilities such as TRIUMF.

Because of the difficulties in carrying out higher spin measurements, their experimental accuracies are not at present high, and so they do not appear to contribute greatly toward reducing the errors in the phase shifts. However, the importance of such measurements must not be underestimated, especially in an energy region where there are still various possible sets of phase shifts which fit the experimental data.

The traditional experimental method for measuring the final polarization has been by means of a carbon analyzer with scintillation counters detecting the rescattered protons. Due to recent development of techniques in the detection of particles, such as spark chambers, and in addition the use of polarized targets in the experiments, a great improvement in higher spin measurements may be expected. As a consequence, a flood of new data will be produced using machines such as TRIUMF.

However, improvement in individual measurements may or may not achieve the precision required to improve the knowledge of the phase shifts.

Consequently, on the basis of the present analysis, required precision for some of the most desirable measurements, believed to be most helpful in better determination of phase shifts at 310 MeV, are listed below.

1) Measurements of differential cross section in the angular range
   i) between 6.5° and 10° with the required precision of 0.5 mb, and
   ii) between 10° and 20° with the required precision of 0.14 mb.
2) Measurements of polarization of the outgoing proton beam between 2° and 20° with the required precision of 0.015.
3) Measurements of depolarization at scattering angles between 90° and 120° with the required precision of 0.11.
4) Measurements of the R parameter in the angular range between 90° and 120° with a precision of 0.06.
5) Measurements of the A parameter throughout the angular range from 20° to 100°, specifically between 90° and 100°, with a required precision of 0.12.
6) Measurements of C_{KP} throughout the whole angular range from 20° to 120° are needed; however, measurements between 70° and 120° with a required precision of 0.16 are most preferable.
7) More recent measurements of C_{NN} at 305 MeV and at scattering angles between 70° and 100° have been made with very reasonable precision (Fig. 4.14). It seems likely that the extension of measurements of C_{NN} to scattering angles smaller than 30° and greater than 100° are quite possible.

Although we have considered only seven different kinds of measurements, in order to have a unique determination of the M matrix at a given energy,

at least 9 independent quantities must be measured over the complete range of angles (Wright *et al.*, 1968). The measurement of another 2 quantities, such as the Wolfenstein parameters R' and A' (Wolfenstein, 1956) is also strongly recommended since presently no data exist at 310 MeV.

Phase-shift analysis of elastic p-p scattering has also been carried out at several other fixed energies (e.g., MacGregor *et al.*, 1957 to 1968) in the last fourteen years. At some energies below 310 MeV, due to recent measurements, our knowledge of phase shifts is more unambiguous than the case at 310 MeV, while at other energies, the data points are less well measured. To find the most significant measurements at these energies, the extension of the present work to the data sets at energies other than 310 MeV is suggested.

The computer program which has been developed may be used to analyze all experimental p-p data in the energy range where inelastic scattering is unimportant. An extension to include the analysis of n-p scattering is also quite straightforward but is not included in the present work.

Appendix A

SOME RELATIVISTIC RELATIONS USED IN CALCULATIONS

Using the conservation of magnitude of a four-momentum under a Lorentz transformation (Landau and Lishifz), we find the following expression for the wave number in the center-of-mass of the p-He system,

$$k \equiv \frac{P}{\hbar} = \frac{m_p c (\gamma^2 - 1)^{1/2}}{\hbar (1 + 2R\gamma + R^2)^{1/2}} \tag{A.1}$$

where P is the momentum of an incident proton in the center-of-mass system, R is the ratio of masses in the two-body system; i.e.,

$$R = \frac{m_p}{m_{He}} ,$$

and

$$\gamma = 1 + \frac{T_{lab.}}{m_p c^2} .$$

Here $T_{lab.}$ is the kinetic energy of the incident proton in the laboratory frame;

m_p is the rest mass of the proton;

m_{He} is the rest mass of helium;

c is the speed of light in vacuum.

In the case of p-p scattering we have that

$$k = \frac{m_p c}{\hbar} \sqrt{\frac{\gamma - 1}{2}} \tag{A.2}$$

Also, the scattering angle $\theta_{lab.}$ in the laboratory frame is related to the scattering angle θ in the center-of-mass frame by

$$\tan(\theta/2) = \left[1 + \frac{T_{lab.}}{2m_pc^2}\right]^{1/2} \tan\theta_{lab} \tag{A.3}$$

The following relation between laboratory and center-of-mass cross sections, which holds for p-p scattering

$$\frac{d\sigma(\theta,\phi)}{d\Omega} = \frac{\left[1 + \frac{T_{lab.}}{2m_pc^2}\right]^{1/2}}{4\cos\theta_{lab.}\left[1+\frac{T_{lab.}}{2m_pc}\right]} \cdot \frac{d\sigma(\theta_{lab.},\phi_{lab})}{d\Omega} \tag{A.4}$$

is obtained by modification of the result in Goldstein (1962).

Appendix B

CLEBSCH-GORDON COEFFICIENTS AND THE PARTIAL WAVE EXPANSION OF PLANE WAVES

1. Some useful properties of the Clebsch-Gordon coefficients $C_{\ell s}(J, m_J, m_\ell, m_s)$ are

i) $$\mathcal{Y}_{J\ell s}^{m_J} \equiv \sum_{m_\ell} \sum_{m_s} C_{\ell s}(J, m_J; m_\ell, m_s)\, Y_\ell^{m_\ell}(\theta,\phi)\, \chi_s^{m_s} \qquad \text{(B.1)}$$

ii) $$Y_\ell^{m_\ell}(\theta,\phi)\, \chi_s^{m_s} = \sum_{J=\ell-s}^{\ell+s} C_{\ell s}(J, m_J; m_\ell, m_s)\, \mathcal{Y}_{J\ell s}^{m_J} \qquad \text{(B.2)}$$

iii) $$\sum_{m_\ell} \sum_{m_s} C_{\ell s}(J, m_J; m_\ell, m_s)\, C_{\ell s}(J', m_J'; m_\ell, m_s) = \delta_{JJ'} \times \delta_{m_J m_J'} \qquad \text{(B.3)}$$

iv) $$\sum_{\ell-s}^{\ell+s} \sum_{m_J} C_{\ell s}(J, m_J; m_\ell, m_s)\, C_{\ell s}(J, m_J; m_\ell', m_s') = \delta_{m_\ell m_\ell'} \times \delta_{m_s m_s'} \qquad \text{(B.4)}$$

2. Tabulated Clebsch-Gordon coefficients for $s = \frac{1}{2}$:

$C_{\ell s}(J, m_J; m_\ell, m_s)$

	$m_s = \frac{1}{2}$	$m_s = -\frac{1}{2}$
$J = \ell + \frac{1}{2}$	$\sqrt{\frac{\ell + m_J + \frac{1}{2}}{2\ell + 1}}$	$\sqrt{\frac{\ell - m_J + \frac{1}{2}}{2\ell + 1}}$
$J = \ell - \frac{1}{2}$	$\sqrt{\frac{\ell - m_J + \frac{1}{2}}{2\ell + 1}}$	$\sqrt{\frac{\ell + m_J + \frac{1}{2}}{2\ell + 1}}$

3. Tabulated Clebsch-Gordon coefficients for s = 1:

$C_{\ell s}(J, m_J; m_\ell, m_s)$

	$m_s = 1$	$m_s = 0$	$m_s = -1$
$J = \ell+1$	$\sqrt{\frac{(\ell+m_J+1)(\ell+m_J)}{(2\ell+1)(2\ell+2)}}$	$\sqrt{\frac{(\ell-m_J+1)(\ell+m_J+1)}{(2\ell+1)(\ell+1)}}$	$\sqrt{\frac{(\ell-m_J)(\ell-m_J+1)}{(2\ell+1)(2\ell+2)}}$
$J = \ell$	$-\sqrt{\frac{(\ell+m_J)(\ell-m_J+1)}{2\ell(\ell+1)}}$	$\sqrt{\frac{m_J}{\ell(\ell+1)}}$	$\sqrt{\frac{(\ell-m_J)(\ell+m_J+1)}{2\ell(\ell+1)}}$
$J = \ell-1$	$\sqrt{\frac{(\ell-m_J)(\ell-m_J+1)}{2\ell(\ell+1)}}$	$-\sqrt{\frac{(\ell-m_J)(\ell+m_J)}{\ell(2\ell+1)}}$	$\sqrt{\frac{(\ell+m_J+1)(\ell+m_J)}{2\ell(2\ell+1)}}$

4. The partial wave expansion of the function $e^{ikz}\chi_s^{m_s}$.

The expansion of a plane wave, e^{ikz}, may be written as

$$e^{ikz} = e^{ikr\cos\theta} = \sum_\ell (2\ell+1) i^\ell j_\ell(kr) P_\ell(\cos\theta)$$

where the spherical Bessel functions behave like standing waves at infinity

$$j_\ell(kr) \underset{\text{large } kr}{\longrightarrow} \frac{1}{kr}\sin(kr - \tfrac{\ell}{2}\pi) \qquad \text{(B.5)}$$

(Messiah). Thus, at infinity we have

$$\begin{aligned} e^{ikz}\chi_s^{m_s'} &= \sum_\ell i^\ell(2\ell+1) j_\ell(kr)\sqrt{\frac{4\pi}{2\ell+1}}\, Y_\ell^0(\theta,\phi)\chi_s^{m_s'} \\ &= \sum_\ell i^\ell(2\ell+1) j_\ell(kr)\sqrt{\frac{4\pi}{2\ell+1}} \\ &\quad \times \sum_J \sum_{m_J} C_{\ell s}(J, m_J; 0, m_s')\, \mathcal{Y}_{J\ell s}^{m_J} \end{aligned} \qquad \text{(B.6)}$$

where equation (B.3) has been used in the second equality.

Since $m_J = m_\ell + m_s'$ and $C_{\ell s}(J, m_J; m_\ell, m_s') = 0$ if $m_J = m_\ell + m_s'$, the right-hand side reduces to

$$\sum_\ell i^\ell (2\ell+1)\, j_\ell'(kr) \sqrt{\frac{4\pi}{2\ell+1}} \sum_J C_{\ell s}(J, m_s; 0, m_s')\, \mathcal{Y}_{J\ell s}^{m_s'} \tag{B.7}$$

By using equation (B.1) in equation (B.7), we obtain

$$e^{ikz}\, \chi_s^{m_s'} = \sum_\ell \sum_J \sum_{m_s} i^\ell (2\ell+1) \sqrt{4\pi(2\ell+1)}\, j_\ell'(kr)$$
$$\times C_{\ell s}(J, m_s'; 0, m_s')$$
$$\times C_{\ell s}(J, m_s'; m_\ell, m_s)\, Y_\ell^{m_\ell}(\theta, \phi)\, \chi_s^{m_s}$$

at large kr. This expansion is useful in treating the incident plane waves in section 2.4 and 2.5.2.

Appendix C

ASYMPTOTIC RADIAL WAVE FUNCTION OF THE TRIPLET STATES

In general, for the three triplet states of same total angular momentum J, we have

$$g_{\ell s}(r) \longrightarrow \frac{D_{\ell J}\, e^{i\eta_{\ell J}}}{kr} \sin\left(kr - \frac{\ell}{2}\pi + \eta_{\ell,J}\right) \qquad (C.1)$$

at large r. The asymptotic total wave function can then be written as

$$\psi_{m_s'} \xrightarrow[\text{large } r]{} \sum_{\ell,J} g_{\ell J}(r)\, \mathcal{Y}_{J\ell s}^{m_s'} = \sum_{\ell J} \frac{d_{\ell,J}}{2ikr} \left\{ e^{i\left[kr - \frac{\ell}{2}\pi + 2\eta_{\ell,J}\right.} - e^{-i\left[kr - \frac{\ell}{2}\pi\right]} \right\} \mathcal{Y}_{J\ell s}^{m_s'}$$

Comparing this result with the partial wave expansion of the incident plane waves shown in Appendix A, i.e.

$$e^{ikz}\chi_1^{m_s} \xrightarrow[\text{large } r]{} \sum_{\ell,J} \frac{i^\ell \sqrt{4\pi(2\ell+1)}}{kr} \sin\left[kr - \frac{\ell}{2}\pi\right] \times C_{\ell s}(J, m_s'; 0, m_s')\, \mathcal{Y}_{J\ell s}^{m_s'}$$

we obtain

$$d_{\ell,J} = i^\ell \; 4\pi(2\ell+1)\; C_{\ell s}(J, m_s'; 0, m_s') \qquad (C.2)$$

or

$$\frac{d_{J+1,J}}{d_{J-1,J}} = -\sqrt{\frac{2J+3}{2J-1}} \cdot \frac{C_{J+1,s}(J, m_s'; 0, m_s')}{C_{J-1,s}(J, m_s'; 0, m_s')} \qquad (C.3)$$

a result which is used in section 2.5.2 in treating the M-matrix for nucleon-nucleon scattering.

(1) Allaby, F.V., Ashmore, A., Diddens, A.N., Eades, J., Huxtable, G.B. and Skruag, K. 1961. *Proceedings of Physical Society.* (London) 77A, 234.

(2) Anderson, H.L., Davidon, W.C., Glicksman, M., Kruse, U.E. 1955. *Physical Review,* 100, 279.

(3) Breit, G. 1966. *Physical Review,* 145, 779.

(4) Bryan, R.A. 1970. *Nuclear Physics,* A146, 359.

(5) Foote, J.H. 1960. University of California Radiation Laboratory Report. UCRL-9191.

(6) Garren, A. 1956. *Physical Review,* 101, 419.

(7) Grashin, A.F. 1959. *Soviet Physics JETP,* 36, 1223.

(8) Goldstein, H. 1962. *Classical Mechanics,* 1st ed., (Addison-Wesley).

(9) Hoshizaki, N. 1968. *Supplement of the Progress of Theoretical Physics,* 42, 107.

(10) Kazarinov, Yu. M., Leyar, F., Peter, G., Pisarev, A.F., Vahlbruch, K.M. 1965. *Soviet Physics JETP,* 20, 565.

(11) Landau, L.D. and Lishitz, E.M. 1965. *The Classical Theory of Fields,* Revised 2nd Ed., (Addison-Wesley).

(12) Lawden, D.F. 1967. *Mathematical Theory of Quantum Mechanics,* 1st Ed., (Methuen).

(13) Lock, W.O. and Measday, D.F. 1970. *Intermediate Energy Nuclear Physics,* Chapter 7, (Methuen).

(14) MacGregor, M.H., Cziffra, P., Moravcsik, M.J., and Stapp, H.P. 1959. *Physical Review,* 114, 880.

(15) MacGregor, M.H., Moravcsik, M.J., and Stapp, H.P. 1959. *Physical Review,* 116, 1248.

(16) MacGregor, M.H., and Arndt, R.A. 1965. *Physical Review*, 139, B362.

(17) MacGregor, M.H. and Arndt, R.A. 1966. *Physical Review*, 141, 873.

(18) MacGregor, M.H., Arndt, R.A. and Wright, R.M. 1968. *Physical Review*, 169, 1128.

(19) Merzbacher, E. 1961. *Quantum Mechanics*, 1st Ed. (John Wiley and Sons)

(20) Messiah, A. 1962. *Quantum Mechanics, Vol. 1 and 2.* (North-Holland)

(21) Mott, N.F. and Massey, H.S.W. 1965. *The Theory of Atomic Collision* (Oxford Press)

(22) Plummer, D.J., Hodges, T.A., Ramavataram, K., Montague, D.G., Chant, N.S. 1968. *Nuclear Physics*, A115, 253.

(23) Plummer, D.J. 1968. "Proton-Helium-4 Interactions in the Energy Region 25 to 30 MeV." Ph.D. Thesis, University of London.

(24) Powell, M.J.D. 1964. *Computer Journal*, 7, 155.

(25) Schiff, L.I. 1968. *Quantum Mechanics*, 3rd Ed. (McGraw-Hill)

(26) Stapp, H.P., Ypsilantis, T.J., Metropolis, N. 1957. *Physical Review*, 105, 302.

(27) Stapp, H.P., Macgregor, M.H. and Moravcsik, M.J. 1960. *Annual Review of Nuclear Science*, 10, 291.

(28) Thorndike, E.H. 1965. *Physical Review*, 138, B586.

(29) Wolfenstein, L. 1956. *Annual Review of Nuclear Science*, 6, 43.

(30) Wright, S.C., Handler, R., Limon, P., Pondrom, L., Olsen, S., Kloeppel, P. 1968. *Physical Review*, 169, 1026.

VITA

Surname: LIM Given Names: Sim Too

Place of Birth: Singapore, Singapore

Date of Birth: September 7, 1946

Educational Institutions Attended, with Dates of Entering and Leaving:

Nanyang University	1965 - 1969
University of Victoria	1969 - 1972
University of British Columbia	1972 -

Degrees, Diplomas, etc. Awarded, with Dates and Names of Institutions:

B.Sc.	1969	Nanyang University

Honours and Awards:

University of Victoria Graduate Scholarship 1970-1971

Publications:

"An Introduction to Free Electron Theory of Metals" Physics Digest, 1968.

THE UNIVERSITY OF VICTORIA LIBRARY

MANUSCRIPT DISSERTATION (or THESIS)

AUTHORITY TO DISTRIBUTE

AUTHOR: This dissertation may be lent or microfilm copies made available:

(a) Without restriction [redacted]

(b) With the restriction that, for a period of five years (until)the written approval of the following is required:

(1) The Chairman, School of Graduate Studies .....

(2) The Author .....

(3) both the Chairman, School of Graduate Studies, and the Author .....

BORROWERS: The borrower undertakes, by signing below, to give proper credit for any use made of the dissertation, and to obtain the consent of the author if it is proposed to make extensive quotations, or to reproduce the dissertation in whole or in part.

Signature of Borrower	Address	Date